Stony Brook University

The Regulation of Neutrophil Function by the Vitamin D Binding Protein (DBP).

A Dissertation Presented

by

David M. Habiel

to

The Graduate School

in Partial Fulfillment of the

Requirements

for the Degree of

Doctor of Philosophy

in

Molecular & Cellular Biology

(Immunology and Pathology)

Stony Brook University

May 2012

Stony Brook University

The Graduate School

David M. Habiel

We, the dissertation committee for the above candidate for the

Doctor of Philosophy degree, hereby recommend acceptance of this dissertation.

Richard R. Kew, Ph.D., Dissertation Advisor
Associate Professor, Department of Pathology,
Stony Brook University

Berhane Ghebrehiwet, DVM, DSc., Chairperson of Defense
Professor, Departments of Medicine and Pathology,
Stony Brook University

Kenneth B. Marcu, Ph.D.
Professor, Departments of Biochemistry and Cell Biology and Pathology,
Stony Brook University

Sanford R. Simon, Ph.D.
Professor, Departments of Biochemistry and Cell Biology and Pathology,
Stony Brook University

Edward A. Fisher, Ph.D., M.D., M.P.H.
Leon H. Charney Professor of Cardiovascular Medicine, Departments of Medicine, Pediatrics and Cell Biology, New York University

This dissertation is accepted by the Graduate School

Charles Taber
Interim Dean of the Graduate School

Abstract of the Dissertation

The Regulation of Neutrophil Function by the Vitamin D Binding Protein (DBP)

by

David M. Habiel

Doctor of Philosophy

in

Molecular & Cellular Biology

(Immunology and Pathology)

Stony Brook University

2012

Vitamin D binding protein (DBP), also called Gc globulin, is an abundant plasma protein belonging to the albumin gene family. DBP is primarily known for its role in the transport of vitamin D metabolites in the blood and extracellular fluids, and as an actin scavenger in the circulation. DBP also has been shown to be a chemotactic cofactor for the complement activation peptide C5a, and a deglycosylated form (DBP-MAF) has been shown to activate macrophages and osteoclasts *in vitro*. The *in vivo* relevance and the mechanism behind the chemotactic cofactor function of DBP are not known. In this report, a C5a induced alveolitis model was developed and the neutrophil migration into the lungs of DBP -/- and DBP +/+ mice was determined. There was a significant decrease in the number of neutrophils recruited into the lung at 4, 6, and 24 hours after instillation of C5a in DBP -/- mice as compared to DBP +/+ animals. *Ex vivo* analysis of DBP -/- bone marrow neutrophils revealed decreased surface expression of CD88 (C5a receptor), CD44 (DBP receptor), CD11b (cell adhesion molecule) and

decreased side scatter (less internal granularity). Functional analysis of DBP -/- bone marrow neutrophils revealed an intrinsic defect in migration, polarization and superoxide anion generation suggesting a role for DBP in neutrophil differentiation *in vivo*. This was confirmed using the promyelocytic cell line HL-60, where higher surface expression of CD88, CD44 and higher side scatter was observed when cells were differentiated in the presence of DBP. Finally, a mechanism by which DBP functions during chemotaxis and differentiation is proposed. Using a proteomic approach, it was observed that DBP treated neutrophils generate DBP-actin complexes which in turn induce secretion of the inflammatory amplifier S100A8/A9. This molecule has been implicated in neutrophil chemotaxis, polarization, superoxide anion generation and differentiation. *In vitro* analysis of human neutrophils confirmed that DBP treatment induced the generation of DBP-actin complexes and the formation of intracellular S100A8/A9 complexes. Furthermore, DBP-actin complexes were found to be potent inducers of S100A8/A9 release from neutrophils.

Table of Contents

List of Figures

List of Tables

List of Abbreviations

α1AGP – Alpha 1 acid glycoprotein
APC – antigen presenting cells
ARDS – Acute respiratory distress syndrome
BALF – Bronco-alveolar lavage fluid
BCR – B cell receptor
BSA – Bovine serum albumin
BSL2 – Biological safety level 2
C5aR – C5a receptor
CD44-ICD – CD44 intracellular domain
CLR – C-type lectin receptor
COPD – Chronic obstructive pulmonary disease
CR3 – Complement receptor 3
CSPG – Chondroitin sulfate proteoglycan
CVF – Cobra venom factor
DAF – Decay accelerating factor
DAMPs – Dangerous associated molecular pattern
DBP – Vitamin D binding protein
DBP-maf – Vitamin D binding protein-macrophage activating factor
DMSO – Dimethyl sulfoxide
DPBS – Dulbecco's phosphate buffered saline
EDC/NHS – N-ethyl-N-(dimethylaminopropyl) carbodiimide / N-hydroxysuccinimide
EDTA – Ethylenediaminetetraacetic acid
ELISA – Enzyme-linked immunosorbent assay
ERM – ezrin, radixin and moesin proteins
ESL-1 – E-selectin ligand-1
FACS – Fluorescence activated cell sorting
FBS – Fetal bovine serum
HBSS – Hanks buffered saline solution
HMGB1 – High-mobility group B1
HRGP – Histidine rich glycoprotein
HRP – Horseradish peroxidase
HSP – Heat shock protein
HSPG – Heparin sulfate proteoglycan
ICAM – Intracellular adhesion molecule
iE-DAP – g-D-glutamyl-mesodiaminopimelic acid
IL-8 – Interleukin 8

IL-8R – Interleukin 8 receptor
IκB – Inhibitor of Nf-κB
LPS – Lipopolysaccharide
LTB_4 – Leukotriene B_4
MAC – Membrane attack complex
MAPK – Mitogen activated protein kinase
MASP – Mannan-binding lectin serine protease
MBL – Mannan-binding lectin
MCP-1 – Monocyte chemotactic protein-1
MDP – muramyl dipeptide
MHC – Major histocompatibility complex
MMP – Matrix metallo-protease
MT- MMP – Membrane type-matrix metallo-protease
MyD88 – Myeloid differentiation primary response gene (88)
NBF – Neutral buffered formalin solution
NFDM – non-fat dry milk
NGAL – Neutrophil gelatinase-associated lipocalin
NLR – NOD-like receptors
PAF – Platelet-activating factor
PAMPs – Pathogen associated molecular patterns
PBS-T – Phosphate buffered saline-tween 20
PI3K – Phosphoinositide 3 kinase
PKC – Protein kinase C
PLD – Phospholipase D
PMA – phorbol 12-myristate 13-acetate
PRR – Pattern recognition receptor
PSGL-1 – P-selectin glycoprotein ligand-1
RAGE – Receptor for advanced glycation end products
RBC – Red blood cell
RLR – Retinoic acid inducible gene (RIG)-I-like receptors.
SLE – systemic lupus erythematous
SNAP – synaptosome-associated protein
SPR – Surface plasmon resonance
STAT – Signal transducer and activator of transcription
TCR – T Cell receptor
TEM – Trans-endothelial migration
TIR domain – Toll/IL-1 receptor domain
TLR – Toll like receptor
TNF – Tumor necrosis factor
TPA – 12-O-Tetradecanoylphorbol-13-acetate
TRAM – TRIF related adaptor molecule
TRIF – TIR-domain-containing adapter-inducing interferon-ß
VAMPs – vesicle associated membrane proteins

VCAM – Vascular cell adhesion molecule
VEGF – Vascular endothelial growth factor

Acknowledgments

I would like to thank Dr. Glenda Trujillo from the Pathology Department in Stony Brook University for developing the alveolitis model in the Kew laboratory, for performing all the alveolitis instillations and lavages and for her help in the data analysis. I thank Stephanie Burk from Dr. Ken Shroyer's laboratory in the Pathology Department of Stony Brook University for paraffin embedding all of the lung tissues and for teaching me how to section and stain paraffin blocks. I thank Antonius Koller from the proteomics center at Stony Brook University for performing the mass spectrometric analysis and NIH/NCRR 1 S10 RR023680-1 shared equipment grant (for the Thermo LTQ). I thank the flow cytometry core facility at Stony Brook University for teaching me how to use the flow cytometer and analyze flow cytometric data. I also thank Laurie Levine from Stony Brook's DLAR for maintaining the DBP -/- and DBP +/+ mice. I thank Dr. Jianhua Zhang for showing me how to genotype the DBP -/- mice. Additionally, I thank Lingyin Ge and Mahalakshmi Ramadass for their help with the alveolitis experiments and with the bone marrow cellular purifications. I would also like to thank my committee members, Dr. Sanford Simon, Dr. Ken Marcu, Dr. Berhane Ghebrehiwet, Dr. Edward Fisher and my thesis advisor Dr. Richard Kew for their helpful suggestions and support. And finally, I am thankful for MCB program NIH training grant support (T32-GM008468).

1. Introduction

1.1. Inflammation: an overview

Inflammation is a complex biological response involving many immune and non-immune cells all acting together to contain and eliminate harmful stimuli. There are five cardinal signs of inflammation: pain, heat, redness, swelling and loss of function of the affected organ. There are two major response elements to inflammation, a humoral (fluid-borne) response, which is composed of plasma proteins from the innate (complement) and adaptive (immunoglobulins) immune systems, and a cellular response, mainly driven by innate immune cells. Inflammation is classified into two major categories each with distinct properties, acute and chronic . Briefly, acute inflammation is fast onset and short lived and the primary cellular component is neutrophils. Chronic inflammation can follow persistent acute inflammation or develop without an acute event. It can last from weeks to years and its primary cellular components are macrophages and B and T lymphocytes of the adaptive immune system.

Innate immune cells are cells of a hematopoetic origin, including neutrophils, monocytes, macrophages, dendritic cells, mast cells, natural killer cells, basophils and eosinophils. These cells are responsible for mounting an early immune response against an infection by utilizing germ line encoded pattern recognition receptors (PRR). PRRs recognize a class of molecules called pathogen associated molecular patterns (PAMPs), which include bacterial and viral proteins, nucleotides and lipids. Additionally, PRRs also recognize a class of endogenous molecules collectively called danger associated molecular patterns (DAMPs) or alarmins. Non-immune cells, such as epithelial and endothelial cells, also express the same PRRs, as immune cells. PRR ligation and activation by PAMPs and/or DAMPs induces a rapid upregulation of cell

surface adhesion molecules and secretion of cytokines, this in turn leads to the recruitment of immune cells and amplification of inflammation. Neutrophils are rapidly recruited to the site of inflammation with peak recruitment at 3-5 hours after the initiation of inflammation. Following neutrophil recruitment, monocytes start to arrive to the site of inflammation within 24 hours, where they respond to several inflammatory stimuli and differentiate into macrophages. In most inflammatory reactions, after 48 hours, monocytes and macrophages become the major population at the site of inflammation.

1.2. Complement System

The humoral arm of the innate immune system is composed of a system of soluble proteins, called the complement system. The complement system is usually the first line of defense that pathogens encounter when they breach the epithelial barrier and enter into a host. It is composed of a collection of zymogens and non zymogens that are proteolytically activated on microbial surfaces by an enzymatic cascade ultimately leading to products that destroy the microbe as well as recruit and activate innate immune cells. There are three major activation pathways for complement: the classical pathway, the lectin pathway and the alternative pathway. The classical pathway is primarily activated by IgM and IgG immune complexes after binding to the C1q portion of C1 and inducing a conformational activation of the pro-enzymes C1r and C1s. The lectin pathway is activated when mannans (mannose residues) on the surface of infecting microbes, but not on self-cells, interact with the mannose binding lectin (MBL) and ficolins. This binding induces a conformational change, which leads to the activation of the enzymes MASP-1 and MASP-2. Both pathways form enzyme complexes that cleave C3 to C3a and C3b, then are modified by the addition of C3b to cleave C5 to C5a and C5b. Cleavage products of C3 and C5 have numerous biological functions and are the primary complement activation products.

The C3 cleavage product C3b (generated from classical or lectin pathways) activates the alternative pathway. However, C3 has a unique auto activation mechanism involving the highly reactive thiolester bond in C3. Hydrolysis of the thiolester converts C3 into an activated form with proteolytic cleavage, in this way C3 is always searching for microbial targets that will activate the alternative pathway. Once the pathway is initiated, more C3 will be cleaved to C3b and amplify the pathway.

C3b covalently binds to microbial surfaces through a reactive thiolester bond, and surface bound C3b acts as an opsonin, by binding to the complement receptor 3 (CR3, also called Mac-1 or CD11b/CD18) on phagocytes and facilitates microbial phagocytosis. The C5 convertase cleaves C5 to generate C5a, a very potent chemoattractant and anaphylatoxin, and C5b. C5b then binds to a microbial surface and subsequently binds to C6, C7, C8 and many molecules of C9. This complex, comprising of C5b-9 and called the membrane attack complex (MAC), forms a pore on microbial membranes, which leads to the lysis of the microbe. C5a is considered the most potent of the complement activation products.

1.3. PRRs, PAMPs and DAMPs

The cellular arm of the innate immune system recognizes invading microorganisms through germ line-encoded receptors called PRRs (reviewed in [1,2]). PRRs bind to conserved pathogenic proteins, nucleotides or lipids, which are generally referred to as PAMPs. PRRs can be classified as secreted, transmembrane, or cytosolic proteins. Secreted PRRs include collectins, ficolins and pentraxins, which bind to microbial cell surfaces and activate the complement system. This leads to the opsonization of these microbes and subsequent phagocytosis and clearance by neutrophils, monocytes and macrophages. Transmembrane PRRs

include complement receptors, which recognize complement opsonized microorganisms, C-type lectin receptors (CLRs) such as Dectin 1 & 2 which recognize ß-glucans and mannans respectively on the surface of microorganisms and toll like receptors (TLRs) which recognize different bacterial or viral membrane lipids, lipoproteins, RNA and DNA (see below). Cytosolic PRRs include retinoic acid inducible gene (RIG)-I-like receptors (RLRs), such as RIG-1 and MDA5 which detect viral RNAs, and NOD like receptors (NLRs), such as NOD1 & 2 which recognize structures of bacterial peptidoglycans such as g-D-glutamyl-mesodiaminopimelic acid (iE-DAP) and muramyl dipeptide (MDP). In addition to recognizing PAMPs, some PRRs, such as TLRs, recognize a class of endogenous proteins, which are released or secreted during inflammation, called DAMPs.

Some of the most studied and best-characterized PRRs are the TLRs (reviewed in [2]). Currently, 10 TLRs have been identified in human (TLR 1-10), and 12 (TLR 1-9 and 11-13) in mice with TLR 1-9 being the best characterized. TLR1, 2, 4, 5, and 6 are expressed on the plasma membrane and TLR 3, 7, 8 and 9 are expressed on endosomal membranes where they bind to microbial RNA and DNA upon cellular activation. Most TLR ligands induce the homodimerization (TLR 3, 4, 5, 6, 7 (in mouse) and 9) or heterodimerization (TLR1/ 2, TLR6/2 & TLR7/8 in human) of TLRs to induce a cellular response. The activation of TLRs leads to cellular responses such as priming and degranulation in neutrophils or cytokine and chemokine synthesis and secretion in neutrophils, monocytes and macrophages.

There are two major signaling mechanisms used by TLRs to induce cellular activation and gene transcription: the MyD88 dependent signaling pathway and the TRIF-dependent signaling pathway [3,4]. All TLRs utilize the MyD88 dependent signaling pathway with the exception of TLR3. In the MyD88 signaling pathway, MyD88 is recruited, either directly or

indirectly via an adaptor protein, to an intracellular Toll/IL-1 receptor domain (TIR) of TLRs, where it induces the activation of a signaling cascade, ultimately leading to the activation Nf-κB and MAPK. The TRIF-dependent signaling pathway, also called the MyD88 independent signaling pathway, is utilized only by TLR3 and TLR4. In this pathway, TRIF directly binds to activated TLR3 or indirectly to activated TLR4 via an adaptor protein called TRAM. TRIF then initiates a signaling cascade, which eventually leads to the activation of Nf-κB and subsequently the expression of cytokines and chemokines.

In addition to PAMPs, TLRs bind to and are activated by DAMPs, which are endogenous molecules secreted by activated inflammatory cells or passively released by necrotic cells. For example, HMGB1, a nuclear protein which is released by dead cells or actively secreted by activated macrophages [5],cleaved fibronectin [6], fibrinogen [7], the extracellular matrix glycoprotein Tenascin-C [8], Surfactant protein A and D [9,10], ß-defensin-2 [11], HSP60 [12], 70 [13], 72 [14], and 22 [15], GP96 [16 17], hyaluronic acid fragments [18], neutrophil elastase [19], lactoferrin [20], HSPG fragments [21] and S100A8/A9 [22,23] have all been shown to bind to and activate TLR4. These endogenous DAMPs are thought to play a major role in inflammatory amplification and thus their extracellular levels are highly regulated. However in some diseases, excessive secretion of DAMPs can lead to severe pathologies.

1.4. Cytokines and Chemotactic Factors

When PAMPs and DAMPs bind to and activate PRRs, they induce the expression and secretion of cytokines. Cytokines, formerly called lymphokines or monokines, are protein mediators secreted at different stages of inflammation to either enhance or terminate the inflammatory response [24,25 26]. Cytokines were initially thought to be secreted from leukocytes,

hence the terms lymphokines and monokines. However, it is clear now that many cytokines are also secreted from other cell types, such as epithelial and endothelial cells, and thus a more general term, cytokines, was established. Cytokines exist as proteins, lipids, or nucleotides and are released from cells of the innate and adaptive immune system and non-immune cells such as epithelial and endothelial cells. Cytokines are grouped into several families: 1. Colony stimulating factor family, 2. Interferon family, 3. Interleukin family, 4. TNF family and 5. unassigned family.

Chemoattractants or chemotactic factors are proteins, nucleotides and lipids, which induce cellular migration. The largest family of chemotactic factors is known as chemokines, which are a family of cytokines that can induce cell migration (chemotactic cytokines) [27]. Chemokines are grouped in four structurally similar families based on conserved cysteine (C) residues: C, CC, CXC, and CXXXC. Most chemotactic factors act by binding to and signaling through 7-transmembrane G-protein coupled receptors to initiate a series of biochemical signals that affect cellular polarization and motility. The response to chemotactic factors is not ubiquitous; specificity is achieved by differential expression of different chemoattractant receptors on different effector cells. Thus, the expression of chemoattractant receptors and the generation of chemotactic factors at different stages of inflammation determine which effector cells are attracted to the site of inflammation.

Neutrophils are the fastest migrating cells and thus are heavily used to study chemotactic factors. Neutrophil chemotactic factors are classified into two major groups: 1. End target and 2. Intermediary. Several immune and non-immune cells secrete intermediary chemotactic factors during an inflammatory reaction. The best characterized intermediary chemotactic factor is the chemokine IL-8 (CXCL8) [28], which is a potent neutrophil chemoattractant that is primarily

secreted by neutrophils, endothelial cells and macrophages during inflammation. Other neutrophil intermediary chemotactic factors include LTB_4 [29], PAF [30,31], MCP-1 [32], and CXCL2 [33]. End target chemotactic factors are generated during inflammation and infection. There are two members of this chemokine family, formylated methionine containing peptides (fMLP) and the complement activation peptide C5a.

1.5. C5a and C5a Receptors

C5a is a 74 amino acid fragment of the complement protein C5, which is generated during the activation of the complement system. It is a very potent anaphylatoxin due to its high capacity to induce histamine release from mast cells. The activity of C5a is tightly regulated in circulation by the action of carboxypeptidase N, which removes its carboxyl terminal arginine to generate C5a des Arg. C5a des Arg is approximately 100 fold less potent than C5a, a property that is due to its 200 fold reduced affinity to its receptor, C5aR, as compared to C5a [34]. Neutrophils respond differentially to C5a depending on its concentration. At lower concentrations (pico molar to approximately 10 nano molar), C5a induces neutrophil degranulation, expression of adhesion molecules and chemotaxis [35]. However, at higher concentrations (10 nM or higher) of C5a, there is a significant reduction in motility, but an increase in phagocytosis, superoxide anion and HOCl production [36-39]. A "paralyzed" neutrophil phenotype is often observed in sepsis patients, where the plasma C5a levels are between 10 nM and 100 nM, making C5a a double edge sword. C5a has been shown to be a major mediator in many diseases and pathological conditions other than sepsis such as asthma, rheumatoid arthritis, acute respiratory distress syndrome, systemic lupus erythematous, atherosclerosis, myocardial infarction and reperfusion injury. C5a acts by binding to its cell surface receptors C5aR (CD88) and C5L2, potentially a C5a decoy receptor.

C5aR is a 7-transmembrane spanning G-protein coupled receptor, which is coupled to pertussis toxin sensitive $G_{i\alpha 2,}$ and $G_{i\alpha 3}$ and insensitive $G_{\alpha 16}$ G-proteins. Once activated by C5a, C5aR signals by inducing a calcium influx into the cytosol, activating phosphatidyl-inositol-bisphosphate 3 kinase (PI3K), Akt, p38 MAPK, Ras, B-Raf, phospholipase D (PLD), protein kinase C (PKC), p21 activated kinases, signal transducers and activators of transcription (STATs), sphingosine kinase and NF-κB. C5aR was initially thought to be exclusively expressed in immune cells, however, C5aR has been observed to be expressed on non-immune cells such as vascular endothelial cells, bronchial epithelial cells, keratinocytes, synoviocytes, cardiomyocytes, astrocytes, microglia, neutral stem cells, and oligodendrocytes. In neutrophils, C5aR activation leads to the activation of PI3K, Akt, p38 MAPK, PKC and PLD, leading to the inhibition of apoptosis, degranulation, superoxide anion generation, and chemotaxis [40] [41-43]. Interestingly, C5aR activation has been observed to induce increased cytosolic IκBα, which correlated with the inhibition of NF-κB in neutrophils [43]{Guo:2004dr}.

C5L2 is a 7-transmembrane spanning receptor, which is expressed in immune and non-immune cells at much lower levels as compared to C5aR [42]. Unlike C5aR, C5L2 is predominantly an intracellular C5a receptor and is not G-protein coupled due to a change in the highly conserved DRY (Asp-Arg-Tyr) motif to DLC (Asp-Leu-Cys) in C5L2 [34]. Recently, C5L2 has been shown to be a negative regulator of C5a-C5aR signaling by disrupting the C5aR dependent activation of ERK1/2 through the ß-arrestin pathway [44].

1.6. Neutrophil Development

Neutrophils are the fastest migrating and the first responders to C5a. In humans, neutrophils are the most abundant leukocytes in circulation and in the bone marrow. Daily, 100

billion neutrophils are produced from the bone marrow and cleared from the blood. They make up approximately 60% of all leukocytes in the blood and their average life span in circulation is approximately 5 days [45]. Neutrophils are granular cells, with 4 major granular populations, secretory vesicles, gelatinase, specific, and azurophilc granules.

Neutrophil granules are categorized as primary or peroxidase positive (azurophilic) and secondary or peroxidase negative (gelatinase and specific) granules [46,47]. Granules differ by the protein content in their matrix and membranes. Granular proteins are thought to be targeted to granules by timed expression during the development of a granule subtype in developing neutrophils, a model that is called "targeting by timing" [48]. Granulopoesis is initiated in the early promyelocytic stage of differentiation, when immature transport vesicles bud off from the golgi, aggregate and fuse together to form peroxidase-positive (azurophil) granules, named due to their high content of myeloperoxidase [49 50 51]. The azurophil granules contain CD63 and CD68, which are usually used as markers for these granules, and a range of bactericidal enzymes and proteins such as azurocidin, BPI, defensins, elastase, lysozyme, proteinase-3, N-acetyl-ß-glucoasminidase and sialidase. Azurophil granules are usually the most difficult granules to exocytose, but when exocytosed, they are thought to fuse with phagolysosomes to aid in the killing of phagocytosed microorganisms [52]. Specific granules are thought to form in the myelocyte to metamyelocyte stages. At these stages, antibiotic rich substances such as lactoferrin, lysozyme, h-CAP-18, NGAL, and sialidase are expressed and thus incorporated into these granules. Additionally, specific granules contain many proteins and receptors, which play a role in neutrophil migration and inflammatory response such as the matrix proteases MMP-8 (collagenase), MMP-9 (gelatinase), MMP-25 (leukolysin) and the membrane proteins CD11b/CD18 (Mac-1), fMLP-R, fibronectin-R, Laminin-R, TNR-R, and uPA-R. The membrane of specific granules also

contains the NADPH oxidase subunit cytochrome b_{558} that plays a major role in the activation of NADPH oxidase, generation of reactive oxygen species and subsequent microbial killing. As cells leave the metamyelocyte stage and become banded cells (pre-neutrophils) gelatinase granules start to develop. Gelatinase granules, as their name suggests, contain a large amount of the matrix protease gelatinase, which is usually used as a marker for these granules. Like specific granules, gelatinase granules contain many proteins, which play a role in neutrophil migration and inflammatory response such as CD11b/CD18, fMLP-R, uPA-R, the matrix protease gelatinase, bactericidal proteins lysozyme and the NADPH oxidase subunit cytochrome b_{558}. The fourth and the outermost granular population are the secretory vesicles. They primarily contain many plasma proteins such as albumin and are thus thought to be endocytic vesicles. In addition, they contain membrane proteins which are required for the earliest neutrophil inflammatory response such as CD11b/CD18, fMLP-R, C1q-R, CR-1, the complement regulatory protein decay accelerating factor (DAF), the LPS receptor CD14, the low affinity Fc receptor FcγIII (CD16), alkaline phosphatase and the membrane metalloprotease leukolysin.

1.7. Cell Culture Model for Neutrophils: HL-60 Cells

Human neutrophils are short-lived terminally differentiated cells, which cannot be genetically manipulated. To study neutrophil development and function, often the HL-60 cell line is employed. HL-60 is a human leukemic cell line that was derived from the blood of a cancer patient with acute promyelocytic leukemia [53]. HL-60 cells do not require any hematopoetic growth factors for their survival and proliferation; they have been shown to proliferate in serum free medium containing transferrin and insulin [54]. The majority of HL-60 cells are present in culture as promyelocytes (90%) and with a small population (10%) of

spontaneously differentiated cells at multiple stages beyond the promyelocytic stage [53]. HL-60 cells can be induced to differentiate into neutrophil-like cells by culturing them in the presence of DMSO [55,56] or retinoic acid [57], monocyte-like cell by culturing them in the presence of 1, 25 $(OH)_2$ D_3 for 15 days [58-61] or macrophage-like cells by culturing them in the presence of the phorbol ester 12-O-Tetradecanoylphorbol-13-acetate (TPA) [62,63].

Undifferentiated HL-60 cells were observed to express myeloperoxidase and contain azurophil granules. Terminal DMSO or retinoic acid differentiation of HL-60 cells is thought to be incomplete. Based on cell surface receptor expression markers and functional characteristics, DMSO or retinoic acid differentiation of HL-60 cells have been observed to stop at the myelocyte, metamyelocyte and banded neutrophil stage [55,56,58]. Additionally, when HL-60 cells are induced to differentiate into neutrophil like cells, HL-60 cells do not develop any secondary granules, due to a combination of a lack of expression or mistargeting of secondary granule proteins to the plasma membrane or for extracellular secretion [48,64-66]. Other reported differences between DMSO or retinoic acid differentiated HL-60 cells and human neutrophils includes lower surface expression of CD16, CD17 and CD66b [58] and a lower chemotactic response to the chemokine IL-8 due to reduced expression of the IL-8 receptor, IL8Rß by differentiated HL-60 cells [67]. Despite these differences, HL-60 cells have been shown to behave like mature human neutrophils in many functional aspects and thus still remain as the best available cell culture model to study neutrophil development and function [67,68].

1.8. Neutrophil Migration During Inflammation

Endothelial cells activated by C5a, cytokines, chemokines or PRRs immediately up-regulate surface expression of P-selectin by exocytosis of Weibel-Palade bodies. Sustained

activation of endothelial cells leads to de novo transcription and surface expression of other adhesion molecules such as E-selectin, hyaluronan, P-selectin glycoprotein ligand-1 (PSGL-1), ICAM-1, ICAM-2 and VCAM-1[69,70]. In addition, activated endothelial cells initiate cell surface expression of neutrophil chemotactic factors such as IL-8 and PAF [71-73]. Transient interaction of endothelial P-selectin, E-selectin, PSGL-1 and hyaluronan with the neutrophil adhesion molecules PSGL-1, E-selectin ligand-1 (ESL-1), P-selectin and CD44 respectively results in neutrophil adhesion and subsequently rolling on endothelial surface.

High concentrations of cytokines and chemotactic factors induce endothelial cell retraction and vascular leakage near the site of inflammation. As rolling neutrophils encounter endothelial cells close to the inflammatory site, they bind to cell surface expressed chemotactic factors. The immobilized chemotactic factors then activate rolling neutrophil and induces L-selectin shedding, the fusion of most of the secretory vesicles and some secondary granules leading to the up-regulation and activation of cell surface CD11b/CD18, CD11a/CD18, chemoattractant receptors and matrix degrading enzymes [74-76]. This leads to firm adhesion of neutrophils to ICAM-1, ICAM-2 and VCAM-1 on endothelial cells and subsequent trans endothelial migration (TEM). TEM is aided by the exocytosis of specific and gelatinase granules, which leads to the secretion of collagenase and gelatinase and subsequent degradation of the vascular basement membrane [77]. After transmigration, neutrophils follow the gradient of chemotactic factor(s) toward the site of infection, where the chemotactic factor concentration is very high. High concentration of chemotactic factors inhibit neutrophil migration at the site of infection [78,79].

1.9. Neutrophil Polarization and Chemotaxis

Cellular migration is a complex biological response to environmental cues. Cellular migration can be classified as chemokinesis or chemotaxis. Chemokinesis is the non-directional locomotion of cells, however chemotaxis is the directional movement of cells towards a gradient of soluble molecules called chemoattractants or chemotactic factors. As previously mentioned, during inflammation, cells are recruited to the inflammatory site by chemotaxis toward a gradient of chemotactic factors released during inflammation. Neutrophils are the fastest migrating cells, the first cellular responders during inflammation and are thus often utilized to study chemotaxis. Chemotaxis is initiated when a cell senses the presence of a gradient of chemotactic factors. Once the chemotactic factors stimulate their receptors, different mediators are activated such as PLD, PI3K, PKC, p38 MAPK and/or Nf-κB. In neutrophils cellular polarization has been recently shown to be controlled by PI3K and the phosphatases PTEN and SHIP1, which spatially localize PI(3, 4, 5)P3 to the leading edge [80,81]. PI(3, 4, 5)P3 is known to recruit actin-nucleating proteins and thus induce actin polymerization in the leading edge of a polarized neutrophil [82]. Polarized actin polymerization plays a major role in cellular polarization by inhibiting tubulin polymerization at the leading edge [83], and by inducing polarized granular exocytosis toward the leading edge, thus supplying new adhesion molecules and chemokine receptors toward the chemoattractant gradient [84]. Polarization is maintained during chemotaxis by maintaining polarized actin polymerization, which is induced by the adhesion of integrins at the leading edge to endothelial cells or matrix proteins in response to the stimulation of receptors by chemotactic factors [85,86].

1.10. Chemotactic Cofactors: DBP

Neutrophils have a high capacity to generate oxidative radicals and their granules contain many destructive enzymes. Poorly controlled neutrophil activation and/or recruitment to an inflammatory site has been shown to cause tissue damage in several diseases such as sepsis, glomerulonephritis, autoimmunity, acute respiratory distress syndrome (ARDS), and chronic obstructive pulmonary disease (COPD). However, reduced neutrophil function has been shown to increase the susceptibility of the host to bacterial infections. For example, individuals with a mutation which leads to a defect in the activity of the integrins CD11b/CD18 and CD11a/CD18 and thus leukocyte adhesion and trans endothelial migration were observed to be susceptible for recurrent bacterial infections suggesting an important role of neutrophil migration in host defense [87]. Fortunately, neutrophil activation, migration and anti-microbial functions are tightly regulated and are confined to inflammatory sites and subsequently cleared. There are many factors that have been shown to augment neutrophil migration, such as α-1-anti-trypsin [88], heparin sulfate [89], ß endorphin [90], prostaglandin E2 [91] and the vitamin D binding protein (DBP) [92,93].

DBP, also called Gc globulin, is an abundant plasma protein with a mean concentration of 4 to 6 μM. It is predominantly synthesized as a 56 kDa protein by hepatocytes and has a half like of 2.5 days in the circulation [94]. DBP belongs to the albumin gene family, which includes albumin, alpha-fetoprotein and afamin, sharing a series of conserved cysteine residues and a tri-globular structure with albumin, except that DBP has a 124 amino acid truncation of the third domain [95]. DBP has been shown to bind monounsaturated and saturated free fatty acids [96]. There are three major alleles of DBP (e.g., Gc1f, Gc1s and Gc2) and approximately 120 rare variants. Gc1f differs from Gc1s at amino acid position 416, which is aspartic acid in Gc1f and glutamic

acid in Gc1s. Gc1f differs from Gc2 by a single amino acid substitution at position 420 where threonine is substituted with a lysine. Gc1s differs from Gc2 by two amino acids substitution at 416 and 420 where glutamic acid and threonine are substituted with aspartic acid and lysine respectively. Another notable difference between Gc1 and Gc2 is that Gc1 has been observed to be glycosylated on a threonine residue at position 420 [97].

Functionally, DBP is the major carrier of vitamin D and its metabolites in circulation [98] with a higher affinity for 25OH D_3 ($K_a = 5 \times 10^{-8}$ M) than 1, 25$(OH)_2$ D_3 ($K_a = 4 \times 10^{-7}$ M) [99]. Recently, in a mouse model of DBP deficiency (DBP -/- mouse) it was shown that DBP controls the plasma levels of vitamin D but not the tissue concentration of these metabolites, suggesting that this carrier protein is not required for tissue delivery of vitamin D [100]. However, it was suggested that DBP acts as a buffer for vitamin D in circulation by sequestering it and preventing its clearance in the glomerulus in the kidney. This is achieved by megalin and cubulin dependent re-absorption of vitamin D bound DBP by proximal tubular cells in the kidney [101,102]. The functional relevancy of this re-absorption mechanism was demonstrated when it was shown that DBP null mice were protected from vitamin D toxicity due to the loss of excess vitamin D in the urine [103].

DBP is considered to be the central protein in the extracellular actin scavenger system [104-106]. Actin is a cytoskeletal protein, which is present in two forms, monomeric actin (G-actin) and filamentous actin (F-actin). Upon cell injury or tissue damage, intracellular actin is released into the circulation. The ionic strength, pH and temperature in the extracellular environment promote spontaneous actin polymerization to F-actin. F-actin polymers can cause vascular obstruction especially in capillary beds of the lung and thus cause organ dysfunction and failure. This is prevented by the extracellular actin scavenger system, which is composed of DBP, gelsolin and

DNase I. Plasma gelsolin is an 82-kDa protein that is largely produced by skeletal, cardiac and smooth muscle cells [107]. Its concentration is plasma ranges from 200 to 300 µg/ml. Gelsolin binds to F-actin polymers, severs them into F-actin dimers and caps the dimers [108]. Due to the low concentration of actin in the blood, the dimers spontaneously depolymerize into monomers, where DBP binds to and sequesters the monomers [105,106,109]. In some instances, DNase I released from dying cells also binds to actin monomers, in addition to DBP, forming a DNase I-actin-DBP trimer and thus preventing actin polymerization [110].

DBP has also been shown to play a role in inflammation. As previously mentioned, the allelic form Gc1 of DBP has been reported to be glycosylated on a threonine residue at position 420. Yamamoto et al have previously shown that deglycosylation of DBP by the action of membrane bound ß-galactosidase on B-cells and sialidase on T-cells produce a form of DBP which has macrophage activating function, called DBP-macrophage activating factor or DBP-MAF [111]. Later it was discovered that DBP-MAF can also inhibit angiogenesis in a CD36 dependent manner [112] through the inhibition of endothelial cell proliferation and VEGF signaling [113]. Furthermore, the anti-angiogenic function of DBP-MAF has been shown to induce growth inhibition and regression of human pancreatic cancer in immune compromised mice [114].

DBP has been shown to act as a chemotactic cofactor to the complement activation peptide C5a and C5a des Arg in neutrophils [92,93,115-119], in monocytes [120]and to C5a in fibroblasts [121]. However, DBP did not enhance any other C5a derived neutrophil functions such as degranulation and oxidant generation. This chemotactic cofactor activity of DBP was shown to be specific for C5a and C5a des Arg and not other chemoattractants such as formylated peptides, IL-8, LTB_4 and platelet activating factor (PAF). Migration of neutrophils to C5a in physiological fluids such as complement activated serum and in bronchoalveolar lavage fluid of

ARDS patients has been shown to be largely dependent on the presence of DBP [122,123], suggesting that DBP is a physiologically relevant chemotactic cofactor to C5a and C5a des Arg. DBP has been observed to bind to the cell surface of neutrophils in a calcium and temperature dependent manner [118,124-126], and subsequently shed from the plasma membrane by the serine protease elastase [118,126]. Interestingly, both the binding and subsequent shedding of DBP by neutrophils is required for DBP's chemotactic cofactor function. Initial characterization of the DBP binding site on neutrophils indicated the presence of a chondroitin sulfate proteoglycan (CSPG) and the localization in detergent insoluble fractions of the plasma membrane [125,127]. The DBP binding CSPG was later identified to be CD44 (see below) [122,127]. In addition to CD44, there is evidence that cell surface actin may also be required for the binding of DBP to the surface of neutrophils (McVoy et al, manuscript in preparation). This is supported by Zhang et al, who observed that one of the two cell binding sequences in DBP is present within the actin-binding domain of DBP [128]. However, the mechanism and the *in vivo* relevance of DBP's chemotactic cofactor function to C5a and C5a des Arg is not known.

1.10.a. DBP Receptor: CD44

CD44 is a cell surface glycoprotein, which is ubiquitously expressed by most cells. There are 20 different isoforms of CD44, which are generated by alternative splicing and posttranslational modifications ranging in size from 85 to 200 kDa, with the 85-90 kDa CD44H (hematopoetic CD44) or CD44s (standard) being the most common form. CD44 is known to localize to lipid rafts in fibroblasts via an interaction of its transmembrane domain with lipid rich and Triton X-100 resistant plasma membrane domains [129,130]. CD44 is primarily known for its function as a hyaluronan receptor, a function that is thought to be dependent on the clustering of CD44 molecules on the cell surface [131]. In addition, CD44 has been implicated in several other

functions such as the regulation of fibroblast proliferation [132], survival of Th1 memory cells [133], and Th1 and Th2 T-cell differentiation [134], binding to E-selectin during neutrophil rolling on endothelial cells, the regulation of hematopoetic progenitor distribution [135], and suppression of TLR mediated inflammation [136].

CD44 has been implicated in cellular migration through its adhesion to hyaluronan and E-selectin on the surface of endothelial cells and through the indirect association of its cytoplasmic tail with the actin cytoskeleton in migrating neutrophils. When CD44 is activated, ankyrin mediates the contact of CD44 to the cytoskeletal component spectrin and the members of the band 4.1 superfamily ezrin, radixin and moesin (ERM) proteins, which are known to bind to F-actin through their carboxyl terminal [137]. This interaction cross links the actin cytoskeleton to the cytoplasmic domain of CD44 and is regulated by the phosphorylation of a serine residue in the cytoplasmic tail of CD44 by protein kinase C (PKC) and the phosphorylation of the ERM proteins by several growth factor receptors and PKCα. CD44 also has been hypothesized to play a role in cellular migration through basement membranes and extracellular matrices by acting as a specialized platform for the docking of matrix metalloproteases such as MMP7 and MMP9 [138,139].

CD44 has been shown to be shed from cells in response to PMA, ionomycin, cytokines and leukocyte derived proteases such as membrane type 1 and 3 metalloproteases (MT1-MMP and MT3-MMP) and ADAM10 [140,141] leaving behind its trans membrane and cytoplasmic domains. After shedding, cytoskeletal rearrangements are observed, implicating the shedding of CD44 in cellular motility. Soluble CD44 has been shown to act as an antagonist to hyaluronan binding to CD44 [142,143]. The transmembrane domain can be further cleaved by the presenilin dependent γ-secretase, a membrane aspartyl protease, at two sites, one close to the cytoplasmic

border and the other within the transmembrane region [144]. The cleavage of the transmembrane domain close to the cytoplasmic border leads to the release of CD44's intracellular domain (CD44-ICD), which translocates to the nucleus and promotes transcription through TPA-responsive elements [145].

1.11. Dysregulated Inflammation and Diseases

An inappropriate or exacerbated inflammatory response can be lethal. A well-characterized example of dysregulated systemic inflammation is sepsis. Sepsis, a condition that is usually caused by systemic dissemination of microorganisms or their associated PAMPs (LPS), is known to have a very high mortality rate. The systemic dissemination of PAMPs lead to massive generation and release of numerous inflammatory mediators. Elevated C5a levels are highly correlated with pathology and mortality of sepsis. The presence of large amounts of C5a leads to systemic vascular leakage, which causes hypovolemic shock in the host. Additionally, high concentrations of C5a cripples neutrophils and down regulates their anti-microbial properties, leading to immune-suppression, and subsequent multi organ failure and death.

Many proteins, lipids and nucleotides mediate inflammation through the amplification of the inflammatory response. If left unregulated, these mediators can be detrimental to the host as previously discussed. For example, TNFα is known to be significantly up regulated in rheumatoid arthritis and a current treatment for this disease neutralizes this cytokine. In sepsis, many therapeutic approaches are underway to block the action of C5a (reviewed in [42,146]).

1.12. Neutrophil Inflammatory Amplifier: S100A8/A9

S100A8/A9, an inflammatory amplifier that exacerbates the pathology of several diseases, exists as a large pool in neutrophils. These two proteins exist as calcium-dependent heterodimers which are members of a superfamily of calcium binding proteins and are also called calprotectin, L1 antigen, calgranulin A & B or MRP8/14. S100A8/A9 is predominantly expressed in neutrophils, where it makes up approximately 40% of all cytosolic proteins, and to a lesser extent in monocytes, where it makes up approximately 1% of all cytosolic proteins [147,148]. S100A8 and S100A9 are known to heterodimerize through a hydrophobic domain found on the C-terminus of both monomers [149,150]. Upon the elevation of cytosolic calcium, S100A8/A9 has been shown to form a calcium bound heterotetramer [151,152] and then translocate to the plasma membrane. In addition, calcium induced heterotetramers have been observed to translocate to the intermediate filament tubulin, where they can induce microtubule polymerization and turnover [153-155]. S100A8/A9 has been observed to be secreted from neutrophils in response to the chemoattractants C5a and fMLP [156] and from monocytes after adhesion to extracellular matrix proteins and endothelial cells [157]. Once secreted, S100A8/A9 has been shown to play a role in the endothelial cell activation and retraction, adhesion of neutrophils and monocytes to endothelial cells, and subsequent trans endothelial migration [155,158-162].

At low concentrations (10^{-12} - 10^{-10} M), S100A8/A9 has been shown to be chemotactic to neutrophils [163]. However, at higher concentrations (10^{-7} M and higher) S100A8/A9 was not chemotactic to neutrophils, but was observed to induce cellular adhesion to fibrinogen in a CD18 dependent manner [163], degranulation of secondary granules [164], and subsequent increase the surface expression and the activation of CD11b/CD18 [165]. S100A8/A9 has been shown to exert

most of its extracellular functions by binding to the receptor for advanced glycation end products (RAGE) [166,167] and TLR4 [22,23,168,169].

In addition to its extracellular functions, S100A8/A9 has been implicated in several intracellular processes in neutrophils. For example, S100A8/A9 has been shown to play a major role in the assembly of NADPH oxidase, the generation of superoxide anions [170-175] and arachidonic acid metabolism [176,177]. The heterotetramer is thought to bind to and stabilize several neutrophil lipids such as arachidonic acid and LTB_4 [172,176,178,179]. Once secreted, S100A8/A9 delivers arachidonic acid to endothelial cells by interacting with the fatty acid transporter CD36 [161].

A null mutation of S100A8 caused early resorption of mouse embryos suggesting a vital role in embryogenesis [180]; but the S100A9 knockout mouse was viable with no obvious defect(s) [158]. Interestingly, the protein expression of S100A8 in the S100A9 knockout mouse was significantly reduced in bone marrow granulocytes and completely absent in blood and tissue neutrophils. However the mRNA level of S100A8 in S100A9 -/- bone marrow and blood neutrophils was comparable to that found in wild type bone marrow and blood neutrophils, suggesting that the S100A9 is required for the stability of S100A8 in the cytosol of neutrophils [158]. To this end, it has been shown that the heterodimeric and heterotetrameric forms of S100A8 and S100A9 were significantly more resistant to trypsin and proteinase K degradation as compared to the homodimeric forms [181], suggesting that the physiological form of S100A8 and S100A9 is predominantly the heterodimeric and heterotetrameric forms. Neutrophils from S100A9 knockout mice failed to up-regulate surface CD11b in response to IL-8, had a defect in polarized actin polymerization, diminished trans endothelial migration and recruitment to the site

of inflammation in a wound healing model as compared to neutrophils from wild type mice [155,158].

1.13. S100A8/A9 and Disease

Excessive secretion of S100A8/A9 can amplify inflammation and exacerbate diseases. For example, S100A8/A9 has been shown to be significantly increased in the serum and synovial fluids of rheumatoid arthritis [157,182] and Kawasaki disease patients [162]. In addition to an increase in serum concentration of S100A8/A9 in Kawasaki disease patients, Viemann et al showed immuno-histochemical evidence that endothelial cells lining the blood vessels in these patients were almost completely coated with the heterodimer [162]. As previously mentioned, TNF-α over production has been observed in the plasma and synovial fluids of rheumatoid arthritis patients and is thought to significantly contribute to the symptoms and pathology of the disease. Sunahori et al have shown that the heterodimer might lead to the over production of TNF-α in these patients by its induction of TNF-α expression and secretion by monocytes and macrophages ex vivo [182]. Loser et al have shown that local S100A8/A9 production was essential for the development of auto-reactive CD8+ T-cells, a process that was dependent on TLR4 activation by S100A8/A9 [23]. S100A8/A9 have also been implicated in other diseases such as coronary artery diseases [162,168,183-186], inflammatory bowl diseases [187,188], neurological diseases [189-191] and cancer [167,192-195].

In this dissertation, a mechanism by which DBP functions in neutrophil chemotaxis and differentiation will be proposed. Using a proteomic approach and *in vitro* analysis, it was observed that DBP treated neutrophils generate DBP-actin complexes which in turn induce secretion the inflammatory amplifier S100A8/A9. Furthermore, DBP-actin complexes were

found to be potent inducers of S100A8/A9 release from neutrophils. The *in vivo* relevance for the chemotactic cofactor function for DBP was determined using a C5a induced alveolitis model to measure neutrophil migration into the lungs of DBP -/- and DBP +/+ mice. There was a significant decrease in the number of neutrophils recruited into the lung at 4, 6, and 24 hours after instillation of C5a in DBP -/- mice as compared to DBP +/+ mice. *Ex vivo* analysis of DBP -/- bone marrow neutrophils revealed decreased surface expression of CD88 (C5a receptor), CD44 (DBP receptor), CD11b (cell adhesion molecule) and decreased side scatter (less internal granularity). Functional analysis of DBP -/- bone marrow neutrophils revealed an intrinsic defect in migration, polarization and superoxide anion generation suggesting a role for DBP in neutrophil differentiation *in vivo*. In accord with the latter observation, HL60 cells differentiated in the presence of DBP had increased surface expression of CD88 and CD44 along with enhanced side scatter.

2. Materials and Methods

2.1. Reagents.

Recombinant purified mouse C5a was purchased from R&D systems (Minneapolis, MN). HBSS with calcium and magnesium, DPBS, penicillin/streptomycin and RPMI 1640 were purchased from Cellgro/Mediatech (Manassas, VA). EDTA was purchased from Gibco-Life Technologies (Grand Island, NY). Fetal bovine serum (FBS) and bovine serum albumin (BSA) were purchased from Gemini Bio (West Sacramento, CA). Gills hematoxylin III was purchased from Poly Scientific R&D Corp (Bay Shore, NY) and eosin Y was purchased from Anatech Ltd. (Battle Creek, MI). Anti-DBP antibody was purchased from Gallus Immunotech Inc. (Cary, NC). All flow cytometric antibodies were purchased from Biolegend (San Diego, CA) unless otherwise noted. Collagenase A and DNase I were purchased from Roche (Indianapolis, IN). HL-60 cells were acquired from ATCC (Manassas, VA). 25-OH Vitamin D was purchased from Enzo Life Sciences (Farmingdale, NY). Purified DBP, HRGP and α1AGP were purchased from Athens Research and Technology (Athens, GA). LPS was purchased from Sigma (St. Louis, MO). Actin was purchased from Cytoskeleton Inc. (Denver, CO).

2.2. DBP -/- Mice.

DBP-/- mouse line was reconstituted by in vitro fertilization of wild-type C57BL/6 female with DBP-/- sperm (from males fully backcrossed onto a C57BL/6 background). The founder heterozygotes (DBP+/-) were bred to generate DBP -/- and DBP +/+ homozygotes. The mice were genotyped as previously described [103]. The genotype of the DBP -/- and DBP +/+ mice was confirmed by PCR of tail tissue and phenotype by western blot analysis of serum using

anti-DBP antibody (Gallus Immunotech Inc.). In some experiments, wild-type DBP +/+ C57BL6 mice were purchased from Jackson labs.

2.3. C5a-induced Alveolitis.

Purified recombinant mouse C5a (R&D systems) was instilled into the lungs of eight to ten week old anesthetized DBP +/+ or DBP -/- mice at a concentrations of 0.25 μg or 1.0 μg per 24 grams of body weight via oropharyngeal aspiration (O.A.) as previously described [196,197]. As a control, the same volume of PBS was instilled into the lungs. The mice were sacrificed at 2.5, 4, 6, 24 or 48 hours after C5a instillation. Their lungs lavaged using sterile HBSS + 5 mM EDTA solution, four 1ml aliquots. The bronchoalveolar lavage fluid (BALF) was then spun down to pellet the cells. The red blood cells (RBCs) were lysed using AFCS solution (155 mM NH_4Cl, 10 mM $KHCO_3$, 0.1 mM EDTA and adjusted to pH 7.2 with 1N HCl). The cells were washed, centrifuged, resuspended in 110 μl of flow cytometry staining buffer (1% BSA in DBPS + 0.05% NaN_3), counted and stained for flow cytometric analysis.

2.4. Flow Cytometry of BALF Cells.

The cells were prepared as described in the alveolitis methods section. The cells were then counted using an automated cell counter (Bio-Rad, Hercules, CA), and resuspended in 110 μl of flow cytometry staining buffer. The cells were then blocked using TruStain fcX (Biolegend) for 15 minutes on ice and then stained with 80 ng of PE conjugated anti-Gr-1 (Biolegend), 400 ng of FITC-conjugated anti-F4/80 (Biolegend), 160 ng of PE/Cy7 conjugated anti-CD11c (Biolegend), and 80 ng of APC conjugated anti-CD11b (Biolegend) for 15 minutes on ice. The cells were then washed twice with flow cytometry staining buffer and then fixed in 2 % paraformaldehyde. Flow cytometric data were then collected using a BD FACS Calibur II flow cytometer and the

data was analyzed using FlowJo (Tree Star Inc., Ashland, OR). Neutrophils were defined as Gr-1 high staining cells and macrophages were defined as F4/80 positive staining cells. The total number of neutrophils and macrophages was determined by multiplying the total number of cells by the percentage of Gr-1 high cells and F4/80 positive cells respectively.

2.5. Preparation of Cobra Venom Factor (CVF) Activated Serum.

DBP +/+ and DBP -/- mice were sacrificed, and blood was collected by cardiac puncture. The collected blood was transferred into coagulation activating tubes (Terumo medical corporation, Somerset, NJ) and incubated at room temperature for 15-30 minutes or until the clot has begun retracting. Then the tubes were spun down at 8400 rpm (6500 xg) for 10 minutes at 4 ºC. 300 µl of DBP -/- or DBP +/+ serum was transferred into a new tube containing $MgCl_2$ (2 mM final concentration) and 10.5 µl of CVF (Complement Tech, Tyler, Texas). To activate complement, the serum was incubated at 37°C for 60 minutes with gentle mixing every 15 minutes. After complement activation the amount of C5a and C5a des Arg generated was quantified using a sandwich ELISA and the samples were then aliquoted and stored at -80°C until further use.

2.6. Mouse C5a ELISA.

Maxi-Sorb 96 well plates were coated with rat anti mouse C5a monoclonal capture antibody (BD-Biosciences, San Diego, CA), diluted to 5 µg/ml in coating buffer (35 mM $NaHCO_3$, 15 mM Na_2CO_3, pH 9.6) overnight at 4°C. The next morning, each well was blocked with 300 µl of blocking buffer (3% non fat dry milk (NFDM) in PBS-T (PBS + 0.05% Tween-20)) for 1 hour at room temperature. After 1 hour, each well was washed three times with wash buffer (PBS-T). The standards (0.1, 1, 2.5, 5, 10 and 50 ng/ml of purified mouse C5a) and serum samples (diluted 1:500-1:1000) were added to the appropriate wells and incubated at room temperature in an

orbital shaker for 90 minutes. After 90 minutes, all samples were aspirated and the wells were washed 4 times with wash buffer. After washing, the captured C5a was detected by adding 100 µl of 0.5 µg/ml of biotin conjugated rat anti mouse C5a detection antibody (BD-Biosciences) to each well and incubated at room temperature for 1 hour with shaking. After 1 hour, the samples were aspirated, the wells were washed 4 times with wash buffer and 16 ng of HRP conjugated streptavidin (KPL, Gaithersburg, Maryland) was added to each well and incubated for 30 minutes at room temperature with shaking. After 30 minutes, the samples were aspirated and the wells were washed 5 times with wash buffer. After washing, 100 µl of substrate solution (KPL) was added to each well, and the plate was incubated for 10 minutes or until ready judging by the blue color in the wells. Once ready, 100 µl of stop solution (KPL) was added to each well and the plate was read in a plate reader (Spectramax M2, Molecular Devices, Sunnyvale, CA) at 450 nm. The data were analyzed using Softmax Pro version 5.0 (Molecular Devices).

2.7. Preparation of Lung Homogenates.

Mice were instilled with purified mouse C5a (1 µg/24 grams of mouse) by O.A. as previously described. Four hours after instillation, the mice were sacrificed and divided into two groups; in one group the lungs were lavaged and in the other group the lungs were not lavaged. The lungs were subsequently isolated and placed into a well in a 24 well plate containing 1 ml of complete culture medium (RPMI 1640 + 10% FBS). The lungs were then minced using a small surgical scissor. The minced lungs were then transferred into a 15 ml conical tube containing 5 ml of fresh collagenase solution (1 mg/ml type IV collagenase, 25 U/ml DNase, 5% FBS and the volume was brought up to 5 ml with RPMI). The samples were then incubated at 37°C for 45 minutes with shaking every 10 minutes. After the incubation, the tissue was broken up into cellular suspension by passing it through an 18-gauge needle 20 times. Then the samples were

then spun down at 1600 rpm (~515 x g) for 5 minutes. The supernatants were aspirated and the pellets were resuspended in AFCS solution to lyse RBCs. The samples were mixed with the AFCS solution and immediately spun at 100 rpm for 5 minutes. The supernatants were saved and the pellets, containing large tissue aggregates, were discarded. The supernatants were subsequently spun down at 1600 rpm for 5 minutes. The supernatants were aspirated and the cells were resuspended in 500 µl of flow cytometry staining buffer. The samples were then counted using an automatic cell counter (Bio-Rad), stained and analyzed by flow cytometry as previously described.

2.8. Lung Histology.

Purified mouse C5a (1 µg/24 grams of mouse) was instilled into the lungs of DBP +/+ or DBP -/- mice as previously described. As a control, the same volume of saline was instilled into the lungs of DBP +/+ or DBP -/- mice. Four hours after instillation, the mice were sacrificed, their lungs were lavaged, inflated with 10% neutral buffered formalin (NBF, Fisher Scientific, Pittsburgh, PA), isolated and fixed in a 50 ml conical tube containing 10% NBF overnight at room temperature. The following day, the fixed lungs were embedded in paraffin and sectioned (5 µm thick sections) onto glass microscope slides (Fisher Scientific). The slides were then stained with hematoxylin and eosin and mounted as follows: the slides were deparaffinized by placing them in three changes of xylene for 5 minutes each. The deparaffinized slides were then hydrated by dipping them ten times in two changes of 100% ethanol, then 10 times in two changes of 95% ethanol, then dipped 3 times in tap water and subsequently dipped twice in deionized water. The slides were then stained with Mayer's hematoxylin for 4 minutes after which they were washed by dipping them 3 times in tap water. The slides were then destained by dipping them 8 to 10 times in 1% acid alcohol (1% HCl in 70% EtOH). After destaining, the

slides were washed by dipping them 15 times in tap water, then blued by dipping them 5 times in 1% ammonium hydroxide and then washed again by dipping them 3 times in tap water. The slides were then equilibrated in 95% ethanol for 1 minute and stained in alcoholic eosin Y by dipping them 3 times in the eosin Y solution. Following eosin Y staining, the slides were washed by dipping them 10 times in two changes of 95% ethanol, followed by dipping them 10 times in three changes of 100% ethanol and finally by dipping them 10 times in three changes of xylene. Coverslips were then mounted on the slides and left overnight to dry. The following day, pictures were taken at 400x magnification using a Nikon Eclipse Ti microscope.

2.9. Isolation of Mouse Bone Marrow Neutrophils.

Mouse bone marrow neutrophils were isolated as previously described [198]. Briefly, DBP +/+ or DBP -/- mice were euthanized and their femurs and tibias were isolated. In a BSL2 tissue culture hood, the extreme distal tip of both extremities were cut off and the bone marrow was washed out using a 26 gauge needle and 10 ml DPBS per mouse into a 15 ml conical tube. The bone marrow cells were then mixed and large pieces of tissue were allowed to settle down for 60 seconds after which the supernatant was carefully transferred into a new 15 ml conical tube. The cells were then centrifuged at 1000 rpm (200 x g) for 10 minutes at room temperature. The supernatant was aspirated and RBCs were lysed by resuspending the cells in 1 ml AFCS solution and incubating them at room temperature for 2 minutes. After 2 minutes, 10 ml of DPBS was added to the cells and the cells were spun down at 1000 rpm (200 x g) for 10 minutes at room temperature. The supernatant was then aspirated and whole bone marrow cells were resuspended in HBSS or chemotaxis buffer for migration analysis. For superoxide anion generation and phagocytosis assays, neutrophils were enriched by treating the whole bone marrow cells in DPBS with a three layer percoll gradient (GE, Piscataway, NJ). From the bottom to the top:

78% percoll, 69% percoll, and 52% percoll (where 100% percoll is equal to 45 ml of percoll + 5 ml of 10x HBSS). The bone marrow cells were layered on top. The gradient was centrifuged at 1500 rpm (450 x g) in a swinging bucket rotor for 30 minutes at room temperature without breaking. The enriched neutrophil population was collected from the 69%/78% interface and the pellet. Cells were washed 2x with DPBS prior to use in any of the assays. Neutrophil purity was assessed by staining the purified cells with PE conjugated anti Gr-1 antibody followed by flow cytometric analysis. Using this procedure, neutrophils were enriched to approximately 70-80% of all the cells (or enriched by approximately 2 fold; data not shown).

2.10. Isolation of Mouse Blood Cells.

To isolate blood leukocytes, DBP +/+ and DBP -/- mice were sacrificed and 550 µl of blood was collected by cardiac puncture and transferred into a tube containing EDTA (Terumo Medical Corporation). To lyse all RBCs, 5 ml of AFCS solution was added to the cells. Following a 2-minute incubation at room temperature, 10 ml of DPBS was added and the cells were spun down at 1000 rpm (200 x g). The supernatant was aspirated and the cells were washed once in DPBS resuspended in flow cytometry staining buffer. The cells where then stained and analyzed by flow cytometry as previously described.

2.11. Filter-Based Chemotaxis Assay.

The migration assay was performed as previously described [199] with some modifications. Briefly, bone marrow cells were purified from DBP +/+ and DBP -/- mice as previously described and resuspended at a concentration of 10 million cells per ml in chemotaxis buffer (HBSS plus 10 mM HEPES and 1% BSA). Purified mouse C5a or chemotaxis buffer control was loaded into the bottom chamber of a Neuroprobe 48-Well Micro Chemotaxis Chamber

(Neuroprobe, Gaithersburg, MD). A 3-µm or a 5-µm cellulose nitrate filter was placed in the middle between the top and the bottom chambers (Neuroprobe). Purified bone marrow cells were subsequently loaded into the top chamber and the cells were allowed to migrate for 30 minutes at 37 ºC and 5% CO_2. After migration, the filters were removed from the microchemotaxis chamber and fixed in 100% 2-propanol for 5 minutes. The filters were then stained by placing them in acid hematoxylin (filtered 100 ml of Harris type hematoxylin plus 4 ml of acetic acid) for 5-10 minutes. The filters were then rinsed in distilled deionized water (ddH_2O) and destained by transferring them in acid alcohol (0.2% 6 N HCl in 70% 2-propanol) for 2-4 minutes. The filters were then rinsed in ddH_2O and blued by transferring them in bluing agent (166.154 mM $MgSO_4$ plus 23.807 mM $NaHCO_3$ in ddH_2O) for 1-2 minutes. After bluing, the filters were rinsed in ddH_2O and dehydrated by placing them in 70% 2-propanol for 1 minute, 95% 2-propanol for 1 minute and finally in 3 changes of 100% 2-propanol for 3 minutes each. The filters were then cleared by transferring them in 100% xylenes and subsequently mounted on a double coverslip and left to dry overnight. The next day the filters were analyzed using a Nikon microscope by measuring the distance the cells migrated into the filter at 400x magnification in 5 different fields of view. The data was subsequently averaged and graphed using Prism (Graphpad Software, La Jolla, CA). The migration assay was performed using bone marrow from three different DBP +/+ and DBP -/- mice.

2.12. Under Agarose Migration Assay.

The under agarose migration assay was performed as previously described [200] with some modifications. All plates were prepared in a BSL2 tissue culture hood to maintain a sterile environment. A 22 x 22 mm cover slip (Fisher Scientific) was placed into a 35 mm dish (BD Biosciences) and was washed 3x with 100% methanol. After washing, the methanol was

allowed to evaporate for 30 minutes, the coverslips were coated with type I collagen (0.005% collagen solution in 1% acetic acid + ddH_2O, Elastin products Co. Inc., Owensville, Missouri) by adding 3 ml of 50 ng/ml collagen solution to each plate, and incubated at 4 ºC overnight. The next morning, the collagen solution was aspirated, and each plate was washed 3 times with DPBS. The agarose solution was prepared by mixing a preheated (70 ºC) solution of 1% BSA dissolved in 20 ml of RPMI and 10 ml of 2x HBSS (8 ml of ddH2O + 2 ml of 10x HBSS) with 5% agarose dissolved in 10 ml of ddH2O. Immediately after mixing, 3 ml of the agarose solution was added to each plate and the agarose was allowed to polymerize for 1 hour at room temperature. After one hour, 3 holes (2.3 mm apart) were punched in duplicates in the agarose plate using a custom-made hole punching apparatus. After the holes were punched, the agarose was cleaned out of each well carefully using an aspirator, the plates were incubated at 37 ºC and 5% CO_2 for 1 hour to equilibrate the pH. After one hour, any condensed liquid was aspirated from the wells, then the chemoattractants were loaded in the top wells, the buffer controls were loaded in the bottom wells and whole bone marrow cells or human neutrophils (20 million per ml) were loaded in the middle wells. Mouse bone marrow cells and human neutrophils were allowed to migrate for 4.5 and 3.25 hours respectively after which, the cells were aspirated and 1.3 ml of 2% paraformaldehyde was added to each plate to fix the cells. Pictures of migrating cells toward the chemoattractant well and the buffer well were taken using a Nikon Eclipse Ti microscope at 100x magnification. The pictures were analyzed using Macnification software (Interface Design Software) and ImageJ (NIH). The net distance migrated was determined by calibrating a measuring tool in Macnification to a picture of a stage micrometer and then measuring the distance migrated by the cells towards the chemoattractant well and subtracting the distance migrated towards the buffer well. The net number of migrating cells was

determined using ImageJ software by using the cell counter tool by subtracting the number of cells migrating towards the buffer from the number of cells migrating towards the chemoattractant. Each migratory condition was performed using bone marrow from 3 DBP +/+ or DBP -/- mice or human neutrophils from one donor.

2.13. Immunofluorescence of Migrating Neutrophils.

Under agarose migration assay on human blood leukocytes and mouse bone marrow cells was performed as previously described. After migration, the plates were fixed using 2% paraformaldehyde overnight at 4 ºC. The next morning, the agarose was removed and the plates containing the coverslips were washed 3 times with wash buffer (DPBS containing 1% BSA). The samples were blocked by adding 2 ml of blocking buffer (DPBS containing 1% BSA and 10% FBS) in each plate and subsequent incubation with shaking on an orbital shaker for 30 minutes at room temperature. The samples were then stained by adding 2 ml of blocking buffer containing 2 µg of chicken anti human DBP (Gallus Immunotech) and 0.4 µg of mouse anti human S100A8/A9 (Hycult Biotech, Plymouth Meeting, PA). The samples were incubated with the primary antibodies for 2 hours at room temperature with shaking. After 2 hours, the samples were washed 3 times with wash buffer and then stained with alexa flour 488 conjugated donkey anti chicken antibody and alexa flour 594 conjugated goat anti mouse antibody (Life Technologies) for 1 hour at room temperature with shaking. After 1 hour, the samples were washed 4 times with wash buffer, stained with DAPI (Life Technologies) diluted in wash buffer for 10 minutes and then mounted on a glass microscope slide (Fisher Scientific) and left to dry overnight. For mouse bone marrow cells, the cells were stained with 5 µl of alexa flour 594-conjugated phalloidin (200 U/ml, Life Technologies) for 2 hours at room temperature followed by washing 4 times with wash buffer and mounting on a glass microscope slide. The samples

were then analyzed using a Nikon Ti fluorescent microscope at 200x and 1000x. To measure the average fluorescence, gates were drawn around stained migrating cells and the average fluorescence was determined using the Macnification software. The average fluorescence was exported to and graphed using Prism (Graphpad Software).

2.14. Superoxide Anion Generation.

Superoxide anion generation was measured as previously described [201] with some modification. Briefly, bone marrow neutrophils from DBP +/+ or DBP -/- mice were enriched as previously described and resuspended at a concentration of 10 million cells/ml. Two million cells were transferred into a new microfuge tube, and incubated for 5 minutes at 37°C and 5% CO_2 in 600 µl HBSS containing 0.25% BSA. The cells were subsequently treated with 120 µM cytochrome C in PBS (Sigma) and 10% DBP +/+ or DBP -/- complement activated serum or 10 ng/ml PMA in a final volume of 1 ml of HBSS containing 0.25% BSA. The treated cells were incubated for 30 minutes at 37°C and 5% CO_2 with gentle shaking every 10 minutes. After 30 minutes, the reaction was stopped by placing the tubes in wet ice for 5 minutes and subsequently centrifuged at 1600 rpm (200 x g) for 10 minutes at 4°C. 200 µl of the supernatant was transferred into a clear 96 well plate in duplicates and the absorbance was measured at 550 nm using a Spectramax M2 plate reader (Molecular Devices). Nano-moles of cytochrome C reduced were obtained by multiplying the absorbance value at 550 nm by 71.4.

2.15. Phagocytosis Assay.

Alexa flour 594-conjugated zymosan (Life Technologies) was reconstituted at a concentration of 20 mg/ml (approximately 2 x 10^7 zymosan particles per mg). 0.5 mg (or 1 x 10^7 zymosan particles) was transferred to a microfuge tube and HBSS was added to obtain a final volume to 1

ml. The zymosan particles were spun down at 9000 rpm (7500 x g) for 5 minutes and resuspended in 0.5 ml of 12.5% DBP +/+ normal mouse serum and incubated for 30 minutes at 37°C with vortexing every 10 minutes to opsonize the particles with complement proteins. After opsonizing, the zymosan particles were then washed twice with HBSS and resuspended at a final concentration of 0.5 mg/ml (or 1 x 10^7 zymosan particles/ml) in 1 ml of HBSS. Bone marrow neutrophils were enriched from the bone marrow of DBP +/+ and DBP -/- mice and resuspended at a final concentration of 10 million cells per ml of HBSS. The enriched cells were then mixed with opsonized zymosan 1:1 and incubated at 37°C and 5% CO_2 for 1 hour. To control for non-phagocytosed, cell surface bound particles, certain aliquots were mixed with zymosan and incubated on wet ice (~1°C) for 1 hour. After 1 hour of incubation, all samples were placed on ice for 1 minute and then 100 µl of 2.5 mg/ml of trypan blue was added to quench extracellular fluorescence. Cells were washed once with HBSS, resuspended in 0.4 ml of 2% paraformaldehyde and flow cytometric data were collected using a BD FACS Calibur II and analyzed using FlowJo (Tree Star Inc). This experiment was performed using bone marrow from 4 DBP +/+ and DBP -/- mice.

2.16. Purification of Human Neutrophils.

Human neutrophils were purified from whole blood as previously described [202]. Briefly, blood was collected from donors into EDTA containing purple top vacutainer tubes (BD Biosciences). Blood was transferred into a 50 ml conical tube, mixed 1:1 with 3% dextran and incubated for 15 minutes at room temperature to sediment the RBCs. The leukocyte containing supernatant was transferred into a new 50 ml conical tube, washed twice with DPBS and resuspended in 4 ml of DPBS, layered on top of 3 ml of histopaque 1077 (Sigma). The gradient was spun down at 1300 rpm (340 x g) for 30 minutes at 15 °C without breaking. After 30 minutes, the supernatant was

aspirated and the neutrophil containing pellet was resuspended in 2 ml of DPBS. RBCs were lysed by adding 6 ml of sterile water to the resuspended pellet, incubating for 60 seconds and subsequently adding 2 ml of 0.6 M NaCl. The cells were spun down and washed once with DPBS then resuspended in HBSS.

2.17. DBP-Actin Complexes.

Lyophilized DBP and actin were resuspended in DPBS and mixed at 1:1 molar ratio in a microfuge tube. The mixture was incubated at room temperature for 1-2 hours to generate DBP-actin complexes prior to experimental use.

2.18. Neutrophil Treatment with Purified Proteins.

Purified human neutrophils were resuspended at a concentration of 5 million cells per ml in HBSS. One million neutrophils in a total volume of 225 µl of HBSS containing 1 µM DBP, α1 acid glycoprotein (α1AGP), histidine rich glycoprotein (HRGP), actin, or DBP-actin complexes were transferred into microfuge tubes and incubated at 37 °C and 5% CO_2 for 30 minutes. After 30 minutes, the cells were spun down at 1200 rpm (100 x g) for 5 minutes at 4 °C, the conditioned supernatant transferred into a new microfuge tube and the pellet was fixed using 2% paraformaldehyde for intracellular staining. The conditioned supernatants were spun down again at 8400 rpm (6500 x g) for 10 minutes, transferred into a new microfuge tube and frozen down at -80 °C for future analysis. To analyze conditioned supernatants for the presence of S100A8/A9 and actin, equal volume of conditioned supernatants were loaded into a native gel and a western blot was performed using a mouse monoclonal antibody which is specific for a conformational epitope which is only found in the heterodimer or heterotetramer of S100A8/A9 but not the monomers (Hycult Biotech) [203]. To detect DBP-actin complexes, a native gel western blot was

performed on conditioned supernatants using an anti-actin monoclonal antibody (Fisher Scientific).

2.19. Identifying Proteins in DBP-Treated Neutrophil Supernatants.

Neutrophils were purified from whole blood and treated with 1 μM DBP, 400 pM C5a or a combination of the two for 30 minutes at 37 ºC and 5% CO_2 as previously described. As a control, untreated neutrophils were incubated for 30 minutes at 37 ºC and 5% CO_2. After 30 minutes, the cells were spun down and conditioned supernatants were collected. To identify DBP-neutrophil proteins complexes, the conditioned supernatants were loaded into two identical 10% native gels and subjected to electrophoresis. To identify potential proteins released by neutrophils in response to DBP, the conditioned supernatants were loaded into two identical 10% SDS-PAGE gels and subjected to electrophoresis. Following electrophoresis, one of the two identical gels was transferred into a PVDF membrane and a western blot was performed using chicken anti-DBP (Gallus Immunotech) and an HRP conjugated donkey anti chicken secondary antibodies. The other two gels were silver stained using Pierce silver stain kit (Fisher Scientific). The western blot performed using the native gel was utilized to identify any DBP-neutrophil protein bands in the silver stained native gel. Silver stained protein bands which were present in the DBP-treated but weaker or absent in the untreated samples in the SDS-PAGE gel (figure 21) or which were potential DBP-neutrophil protein complex as assessed by the native gel were identified by mass spectrometry as previously described by [204]. Briefly, gel bands were cut out destained, reduced, alkylated and trypsin digested (Promega, mass spectrometry grade, Madison, WI) as previously described by [205]. The digested samples were subsequently diluted in 2% Acetonitrile (ACN), 0.1% Formic Acid (FA) solution (Buffer A) and analyzed by automated microcaplillary liquid chromatography-tandem mass spectrometry. Using a P-2000 CO_2 laser

puller (Sutter Instruments, Novato, CA), 100-µm i.d. fused silica was pulled to a 5-µm i.d. tip. Using a pressure bomb, the pulled capillaries were packed with 10 cm of 5 µm Magic C18 material (Agilent, Santa Clara, CA), placed in-line with a Dionex 3000 HPLC equipped with an auto sampler and subsequently equilibrated in buffer A. Using the auto sampler, the digested peptide samples were loaded into the column and separated in the HPLC using a flow rate of 300 nL/min in a gradient of buffer A and buffer B (98% acetonitrile, 0.1% formic acid). The HPLC was performed as follows: 100% buffer A for 5 min, 5% to 40% buffer B gradient over 30 minutes, 40% to 80% buffer B gradient over 5 minutes, 80% buffer B for 3 minutes and finally 80% buffer B to 100% buffer A over 1 minute. The eluted peptides were electrosprayed, via the application of a 1.8 kV distal voltage, directly into a Thermo LTQ ion trap mass spectrometer equipped with a custom nanoLC electrospray ionization source. Full mass spectra (MS) followed by five tandem mass events (MS/MS), which were sequentially generated from the five most intense ions at 35% collision energy, from peptides over a 400-2000 *m*/*z* range were recorded. Xcalibur data system (Thermo Finnigan, San Jose, CA) was utilized to control the mass spectrometer scan function and the HPLC solvent gradients. MzXML files containing all the data for all MS/MS spectra were obtained by extracting RAW file MS/MS spectra data using ReAdW.exe (http://sourceforge.net/projects/sashimi). The MS/MS data were searched using InsPecT [206] against a human proteome database (Version December 23, 2011). Common contaminants and +16 on Methionine, +57 on Cysteine modifications were added. Peptides with a minimum p-value of 0.01 were further analyzed.

2.20. Intracellular Staining for Flow Cytometry.

Treated neutrophils were fixed in 2% paraformaldehyde for 30 minutes at 4 ºC, then spun down and permabilized by washing twice with 1x BD perm/wash buffer (BD Biosciences). The cells

were then blocked with 1.2 µg of non-immune human IgG for 15 minutes on ice and stained with 600 ng of anti-S100A8/A9 (Hycult Biotech) for 30 minutes on ice. After 30 minutes, the cells were washed twice with 1x BD perm/wash buffer and stained with 40 ng of APC conjugated goat anti mouse IgG (Biolegend) for 30 minutes on ice. After 30 minutes, the cells were washed twice with 1x BD perm/wash buffer and then resuspended in 2% paraformaldehyde. Flow cytometric data were collected using a BD FACS calibur II flow cytometer and analyzed using FlowJo (Tree Star Inc.).

2.21. BIAcore SPR of U937 cells.

U937 cells were purchased from ATCC and cultured in RPMI containing 1x penicillin/streptomycin and 10% FBS at 37 ºC and 5% CO_2. They were passaged three times a week. The interactions between cells and DBP were evaluated as described in [128] using a BIAcore 2000 (BIAcore AB, Upsala, Sweden). Full-length native DBP was covalently coupled to a CM5 sensor chip using N-ethyl-N-(dimethylaminopropyl) carbodiimide / N-hydroxysuccinimide (EDC/NHS) according to the manufacturer's instructions. The surface of the CM5 sensor chip was activated with EDC/NHS for 20 min before adding either DBP (5 µM) 10 mM sodium carbonate buffer, pH 5.0. Excess NHS was deactivated for 20 min using 1 M ethanolamine, pH 8.5. The efficiency of DBP coupling was determined by injecting 5 µg/ml affinity-purified goat anti-human DBP into the flow cell at 10 µl/min at 22°C. U937 cells were pretreated with 10 µg of rabbit anti-actin polyclonal antibody (Sigma), 10 µg of rabbit IgG or buffer (untreated) for 30 minutes at 37 ºC. The cells were then spun down and re-suspended in HBSS prior to SPR analysis. Cell-DBP binding interactions were determined by injecting untreated, anti-actin or IgG pretreated cell suspensions at a flow rate of 5 µl/min at 22 °C in HBSS containing 0.005% Tween 20. The sensor chip was stripped and regenerated using 0.8 M

glycine (pH 2.0) containing 0.6 M NaCl. The regeneration conditions were adjusted to achieve a subsequent binding response that was within 10% of the initial (first injection) binding value. A blank sensor chip that was EDC/NHS-activated and ethanolamine blocked was used as a background reference in all experiments. Net resonance response units (RU) were determined by subtraction of the background values using BIAevaluation software version 4.1. Figure 28b in the chapter 2 section 1 shows a representative sensorgram of response units versus time. All experiments were performed twice to verify results.

2.22. HL-60 cells culture, treatments and differentiation.

HL-60 cells were cultured in RPMI containing 1x penicillin/streptomycin and 10% FBS at 37 ºC and 5% CO_2. They were passaged three times a week. To differentiate HL-60 cells, cells were plated at a concentration of 1 million per ml and treated with 1.3% DMSO (w/v) in the presence or absence of 1 μM DBP, 1 μM DBP-actin complexes, 100 ng/ml LPS, 1 μM 25-OH D_3 or 1 μM DBP + 1 μM 25-OH D_3 for 5 days at 37 ºC and 5% CO_2. After 5 days, the cells were split into two microfuge tubes, spun down, and one of the tubes was stained with PE conjugated anti CD88 and alexa flour 647 conjugated anti-CD44 and analyzed by flow cytometry. The other tube was flash frozen for future lysate analysis. To control for LPS contamination in the DBP stock, HL-60 cells were differentiated in the presence of 50 ng/ml of Polymyxin B (Sigma), treated with 1 μM DBP or 100 ng/ml LPS, or left untreated. To examine the functionality of bovine DBP in FBS, HL-60 cells were treated with 1 μM DBP, 1 μM 25 OH-D_3, 1 μM DBP + 1 μM 25-OH D_3 and then incubated for 5 days at 37 ºC and 5% CO_2. The cells were then stained with PE conjugated anti-CD88 and alexa flour 647 conjugated anti-CD44 and analyzed by flow cytometry.

2.23. Flow cytometry staining and analysis of HL-60 cells.

HL-60 cells were differentiated and treated as previously described. The cells were then spun down and resuspended in 100 µl of flow cytometry staining buffer, and blocked by incubating the cells with 1.2 µg of non-immune human IgG on ice for 15 minutes. After 15 minutes, the cells were stained with 10 µl of PE conjugated anti-human CD88 and 200 ng of alexa flour 647-conjugated anti-human CD44 in a total volume of 200 µl of flow cytometry buffer for 15 minutes on ice. To control for background non-specific staining, the cells were stained with PE conjugated mouse IgG and alexa flour 647-conjugated mouse IgG. After 15 minutes, the cells were washed twice with 1 ml of flow cytometry staining buffer and fixed in 2% paraformaldehyde. Flow cytometric data were acquired using a BD FACS calibur II and the data were analyzed using FlowJo.

2.24. Western blot analysis of HL-60 cell lysates.

HL-60 cells were differentiated and treated as previously described. The cells were spun down and lysed in 1.5 M Tris buffer containing 1% Triton X-100 and protease/phosphatase inhibitor cocktail (Cell Signaling, Danvers, MA) for 15 minutes on ice. The lysed cells were then spun down at 13, 000 rpm to pellet any non solubilized fragments and the cell lysate was transferred into a new microfuge tube. A Lowry protein assay was performed on all the lysates and the protein concentration was normalized to the lowest protein concentration detected by adding more lysis buffer. Equal volume and concentration of proteins was loaded into an SDS-PAGE gel, and a western blot was performed using anti phospho IKK α/ß (Cell Signaling). The membrane was subsequently re-blotted using anti phospho p38 MAPK (Cell Signaling) and anti GAPDH (Santa Cruz Biotechnology, Santa Cruz, CA).

3. Chapter 1: The role of DBP in neutrophil chemotaxis *in vivo*

3.1. The DBP -/- mouse

Several groups have shown that DBP functions as a chemotactic cofactor *in vitro* for the complement activation peptide C5a [92,93,115,117,118,126], but this role of DBP *in vivo* has not been determined. Therefore, to investigate the role of DBP in neutrophil chemotaxis *in vivo*, frozen sperm from DBP -/- mouse was acquired from Dr. Nancy Cooke from the University of Pennsylvania and the mouse line was re-derived by in vitro fertilization of a wild-type (DBP+/+) female C57BL/6 mouse. The DBP +/- heterozygotes were bred to generate DBP -/- and DBP +/+ homozygotes. As we were establishing the DBP -/- and DBP +/+ colonies, we noticed that the DBP -/- mice were leaner than both DBP +/+ littermates and DBP +/+ mice purchased from Jackson Labs. On average, DBP -/- mice weighed approximately 8% less than DBP +/+ mice as determined by weighing 34 DBP +/+ mice and 21 DBP -/- mice (figure 1). Otherwise, there was no other major phenotypic difference between DBP +/+ and DBP -/- mice.

3.2. DBP is required for the optimal migration of neutrophils to the site of inflammation in vivo.

DBP is an *in vitro* chemotactic cofactor for several cells types, but most notably neutrophils, migrating to complement activation peptides C5a and C5a des Arg (the stable circulating degradation product). However, its *in vivo* relevance in chemotaxis has never been studied. To this end, a C5a induced alveolitis model was developed (figure 1) and used to determine whether DBP is a chemotactic cofactor for neutrophil migration into the site of inflammation *in vivo*. To determine an optimal concentration of C5a that will induce alveolitis in mice without causing death, a pilot experiment was performed with different concentrations of C5a instilled into the lungs of the mice. Results showed that using 1 μg C5a per 24 gram mouse there was both 100% survival and a significant recruitment of neutrophils into the lung (data not shown). Thus, 1 μg of C5a or less was used for all of our subsequent experiments. To study the role of DBP in neutrophil recruitment in an alveolitis model, mice were instilled with 1 or 0.25 μg of purified C5a. Each mouse was weighed beforehand and the amount instilled into the lung was adjusted based on a 24-gram mouse. At different time points after instillation, mice were euthanized, and their lungs were lavaged. The cellular content in the bronchoalveolar lavage (BAL) was quantified using an automated cell counter. The BAL cells were then stained with PE-conjugated anti-Gr-1 (a neutrophil marker) and FITC-conjugated anti-F4/80 (a macrophage marker) and analyzed by flow cytometry to determine the total number of neutrophils and macrophages in the BAL (Figure 1).

To test for the presence of DBP in the inflamed lungs, equal volume of BAL fluid (BALF) was loaded into an SDS-PAGE gel and blotted with an anti-DBP antibody (figure 2). As predicted, DBP was only detected in BALF from DBP +/+ mice (figure 2 lanes 1-3). BALF

DBP was of a similar molecular weight as serum DBP from DBP +/+ mice (figure 2 lane 8) suggesting that the protein did not undergo any major modifications and was not degraded. This suggests that DBP is present at the site of inflammation where it can be in contact with inflammatory cells and that it does not undergo any major modifications or degradation in the alveolar spaces of the inflamed lungs.

The cellular content in the BAL from the DBP +/+ and DBP -/- mice was analyzed 2.5, 4, 6, 24 and 48 hours after instillation of 1 μg of purified mouse C5a or 4 hours after instillation of 0.25 μg of purified mouse C5a. As a control, DBP +/+ and DBP -/- mice were instilled with the same volume of PBS. Starting at 2.5 hours, we observed more BAL leukocytes in the BALF of DBP +/+ mice as compared to DBP -/- mice treated with 1 μg of C5a, but this difference did not reach statistical significance (figure 3A). However, at 4, 6, and 24 hours there was a significantly higher number of total BALF leukocytes observed in the BALF of DBP +/+ as compared to DBP -/- mice (figure 3A). PBS treated mice had very few cells in their BALF. The C5a-induced injury model was transient and reversible since we had 100% survival and 48 hours after C5a instillation the total number of BALF leukocytes was comparable to the PBS treated mice (figure 3A and data not shown). A similar trend was observed 4 hours after the instillation of a lower concentration of C5a (0.25 μg per 1 gram of mouse, figure 3B). These results indicate that DBP may play a role in leukocyte recruitment into an inflammatory site *in vivo*.

C5a is known to be chemotactic to both neutrophils and monocytes. Therefore, to determine the differential cellular types recovered from the BALF of mice instilled with 1 μg of C5a, total BALF leukocytes were stained with the neutrophil and monocyte marker, Gr-1, and the macrophage marker, F4/80. Neutrophils are known to express very high levels of Gr-1, while monocytes express intermediate to low levels of Gr-1. Thus, neutrophils were defined as

Gr-1 high cells, and monocytes were defined as Gr-1 medium to low cells. Macrophages were defined as F4/80 positive cells. There was a significant decrease in the number of neutrophils recovered from the BALF of DBP -/- mice as compared to DBP +/+ mice at 4, 6 and 24 hours after the instillation of C5a (figure 4a and data not shown). There was no significant monocyte recruitment at these time points as evident by the lack of Gr-1 medium to low population. A higher number macrophages was recovered from the BALF of DBP -/- mice as compared to DBP +/+ mice 4 and 6 hours after the instillation of C5a, however this increase did not reach statistical significance. This suggests that the decrease in the total BAL leukocytes observed in the DBP -/- mice was due to a decrease in the number of neutrophils recruited to the lungs.

To evaluate the morphology of the inflamed lungs, histological analysis of DBP +/+ and DBP -/- lungs 4 hours after the instillation of 1 μg of C5a was performed (Figure 5). The lungs of PBS treated DBP +/+ (top left) and DBP -/- (bottom left) were identical. However, C5a treated DBP +/+ lungs (top right) contained more leukocytes (as evident by the nuclear stain) and the alveolar lumen was thicker as compared to C5a treated DBP -/- lungs (bottom right), which contained slightly more cells than the PBS treated lungs with no significant difference in the alveolar lumen thickness. This supports the previous results and suggests that DBP may play a role in cellular recruitment to an inflammatory site.

The BALF cellular analysis (figures 3 & 4) clearly demonstrated that there were significantly fewer cells in the DBP-/- mice. However, since this data only measures cells recovered by lavage, it could have been possible that C5a induced similar numbers of neutrophils to the lungs of both mouse strains, but in the DBP-/- mice, cells were trapped in the lung interstitium. Histological analysis (figure 5) did not show this but this question was further addressed by homogenizing lungs both before and after lavage. Lungs from DBP +/+ and DBP -

/- mice were isolated 4 hours after instillation with 1 μg of C5a, digested and homogenized to generate a cellular suspension and cells were analyzed as previously described. As shown in figure 6, both DBP -/- lavaged (left panel) and non-lavaged (right panel) lungs contained significantly less neutrophils as compared to DBP +/+ lungs. PBS treated lungs from DBP +/+ mice contained slightly more neutrophils compared to saline treated lungs from DBP -/- mice, but this did not reach statistical significance (data not shown). These results clearly show that there is a recruitment defect in the DBP-/- mice, confirming the previous data and indicating that DBP is required for the optimal recruitment of neutrophils in a C5a induced alveolitis model of inflammation.

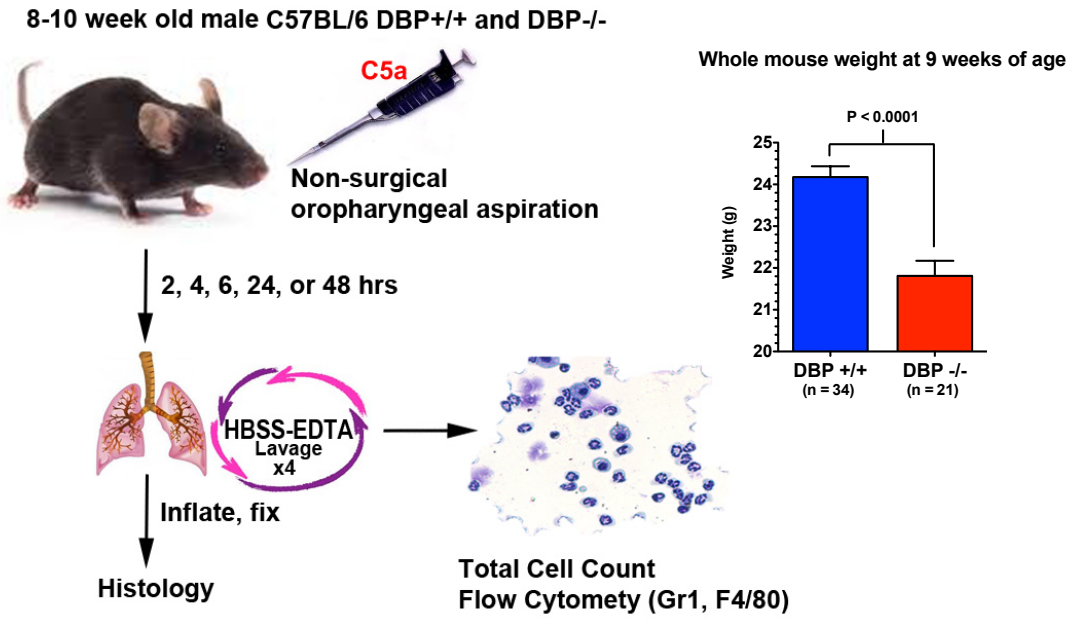

Figure 1 C5a induced alveolitis model.

8-10 week old DBP +/+ or DBP -/- mice were weighted and then instilled with C5a (1 µg or 0.25 µg per 24 g mouse) via the oropharyngeal aspiration method. The mice were then allowed to recover then sacrificed at 2.5, 4, 6, 24 and 48 hours and their lungs lavaged. In selected mice the lungs were inflated with 10% neutral buffered formalin (NBF) and prepared for histological analysis. Total cell number in the BAL was measured using an automatic cell counter and the cell types were determined by staining with anti Gr-1 and anti F4/80 to identify neutrophils and macrophages respectively. The weight shown above is the average weight of 34 DBP +/+ and 21 DBP -/- mice.

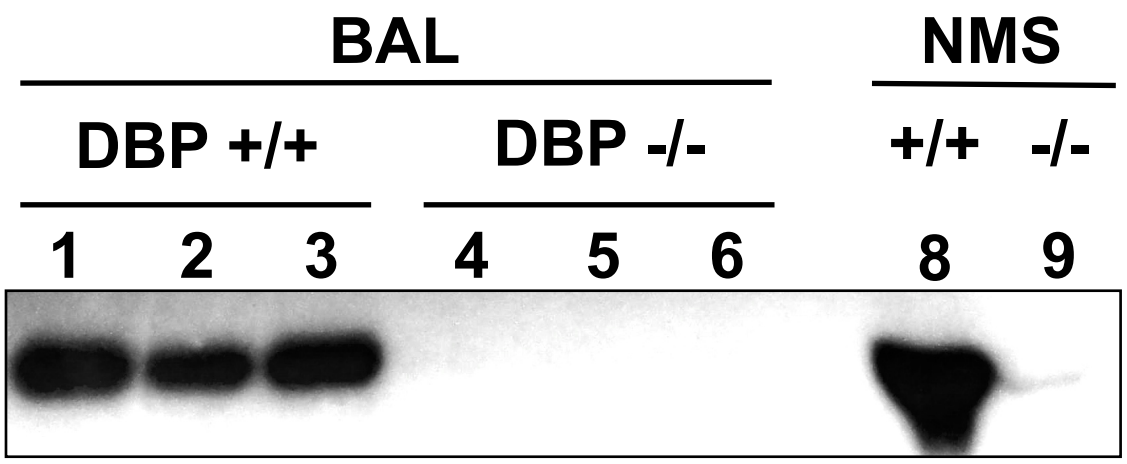

Figure 2 DBP was only detected in the BAL and serum of DBP +/+ mice.

To check for the presence of DBP in the BALF of DBP -/- or DBP +/+ mice, cell-free BALF recovered from the lungs of mice treated with 1 μg of C5a, was separated using SDS-PAGE and blotted with a chicken anti-DBP antibody (lanes 1-6). To test for the presence of DBP in blood, DBP +/+ and DBP -/- mice were euthanized, blood was collected by cardiac puncture and allowed to clot to generate serum. Serum was separated by SDS-PAGE and blotted with a chicken anti-DBP antibody (lanes 8 & 9).

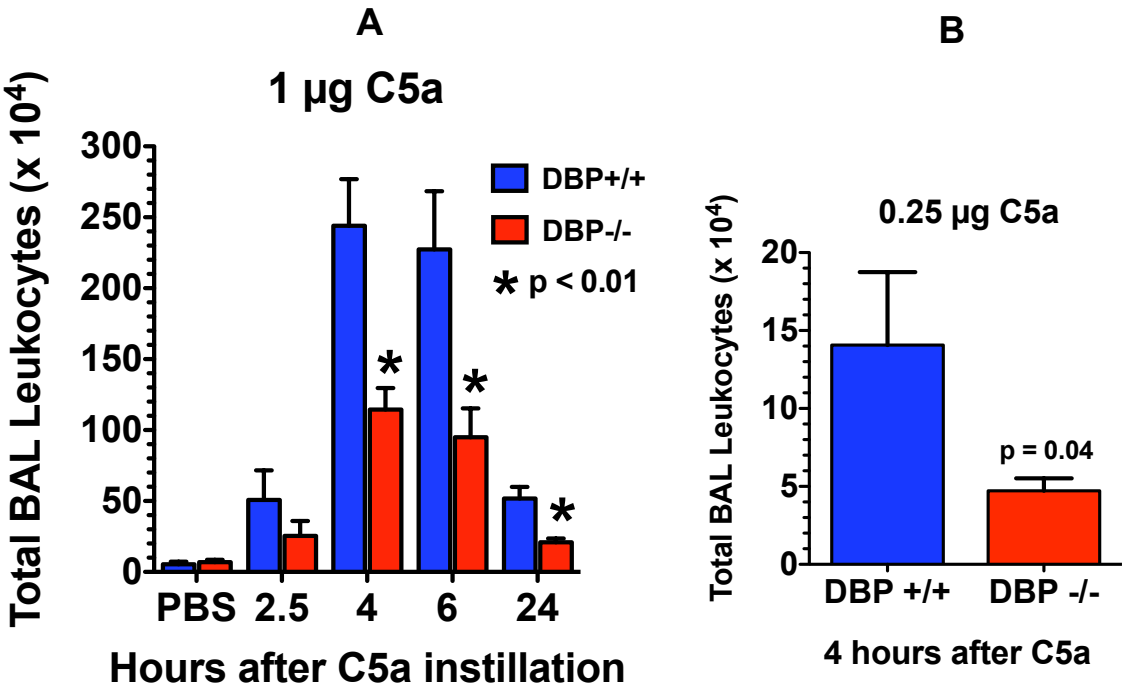

Figure 3 **Total number of BAL leukocytes in the BALF.**

BALF was recovered from the lungs DBP +/+ or DBP -/- mice instilled with 1 µg (A) or 0.25 µg (B) of C5a per 24-gram mouse. Red blood cells were lysed and BAL leukocytes in the BALF were counted using an automated cell counter. Shown above is the mean number of BAL leukocytes as determined from 4-5 DBP +/+ or DBP -/- mice from each time point. Statistical analysis was performed using ANOVA with a multiple comparisons post-test. * represents $p < 0.01$.

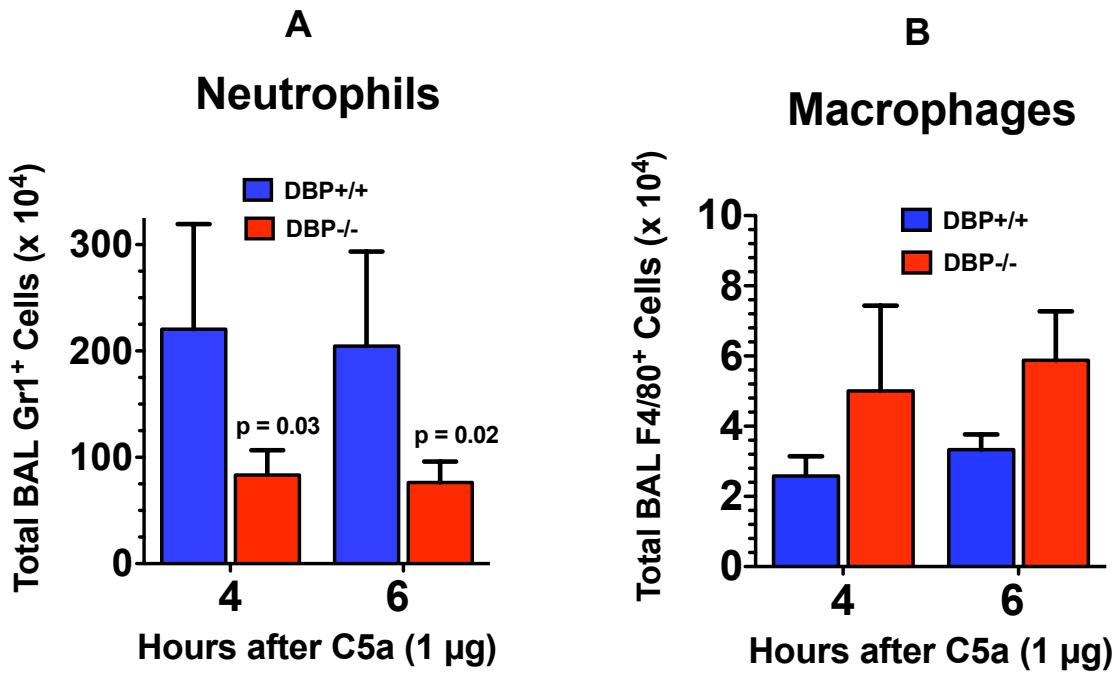

Figure 4 Differential BAL cell count.

Shown above is the average number of neutrophils and macrophages in the BAL of 4-5 DBP +/+ and DBP -/- mice instilled with 1 µg of C5a per 24-gram mouse. BAL leukocytes were stained with PE conjugated anti Gr-1 and FITC conjugated anti F4/80 and analyzed by flow cytometry. The total number of neutrophils (A) and macrophages (B) were calculated by multiplying the total number of BAL cells with the percent of cells that were Gr-1 and F4/80 positive respectively.

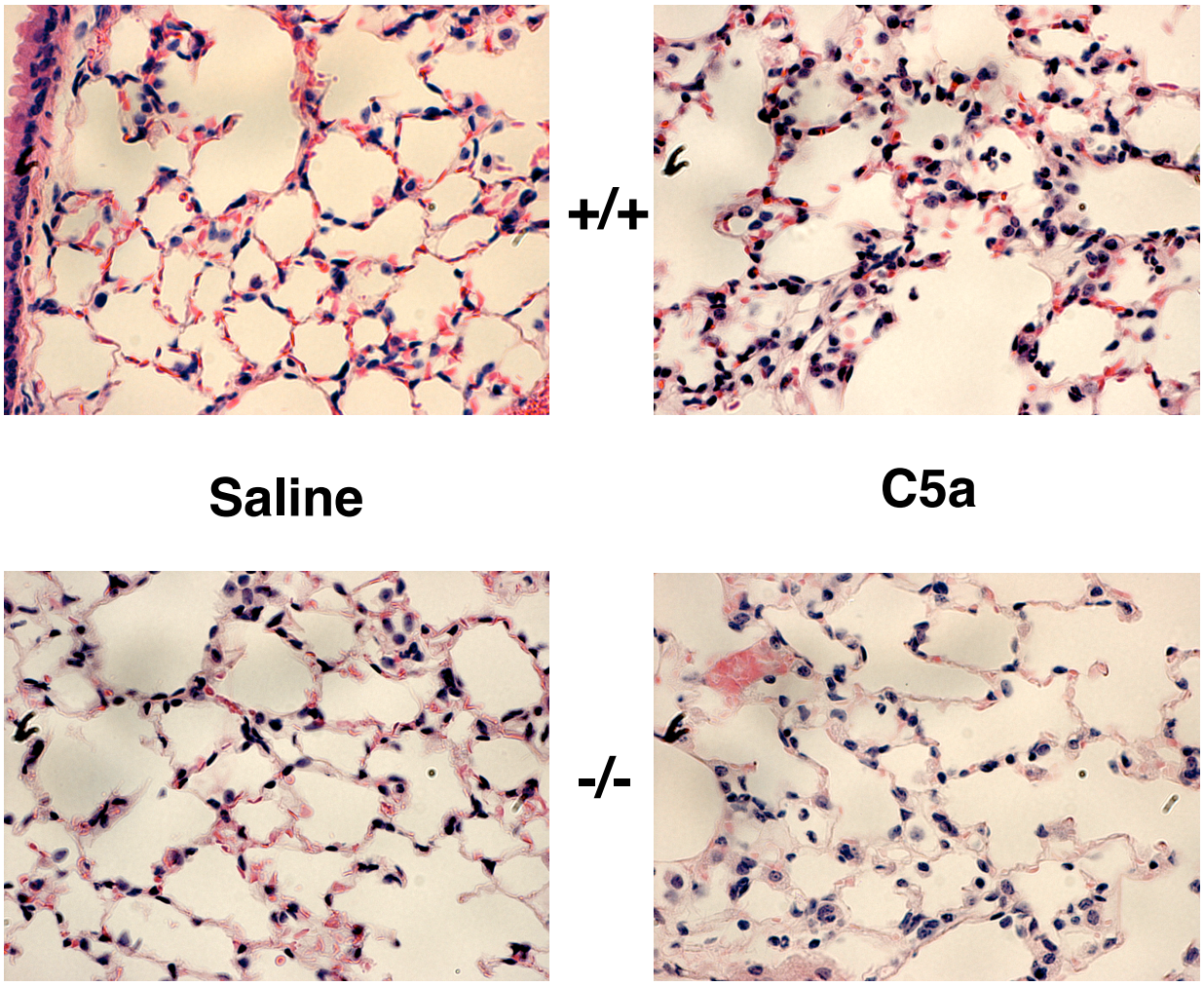

Figure 5 Histological analysis of lavaged lungs.

3 DBP +/+ or DBP -/- mice were instilled with 1 µg C5a. As a control, 2 mice were instilled with the same volume of PBS. Four hours later, the mice were sacrificed, their lungs were lavaged, inflated with 10% NBF, dissected out of the mouse, fixed and paraffin embedded. The lungs were then sectioned and H & E stained. Photos of the stained sections were taken using a Nikon Ti microscope at 400x magnification. The top two pictures are representative of lavaged lungs from a DBP +/+ mouse instilled with PBS (left) and C5a (right). The bottom two pictures are representative of lavaged lungs from a DBP -/- mouse instilled with PBS (left) and C5a (right).

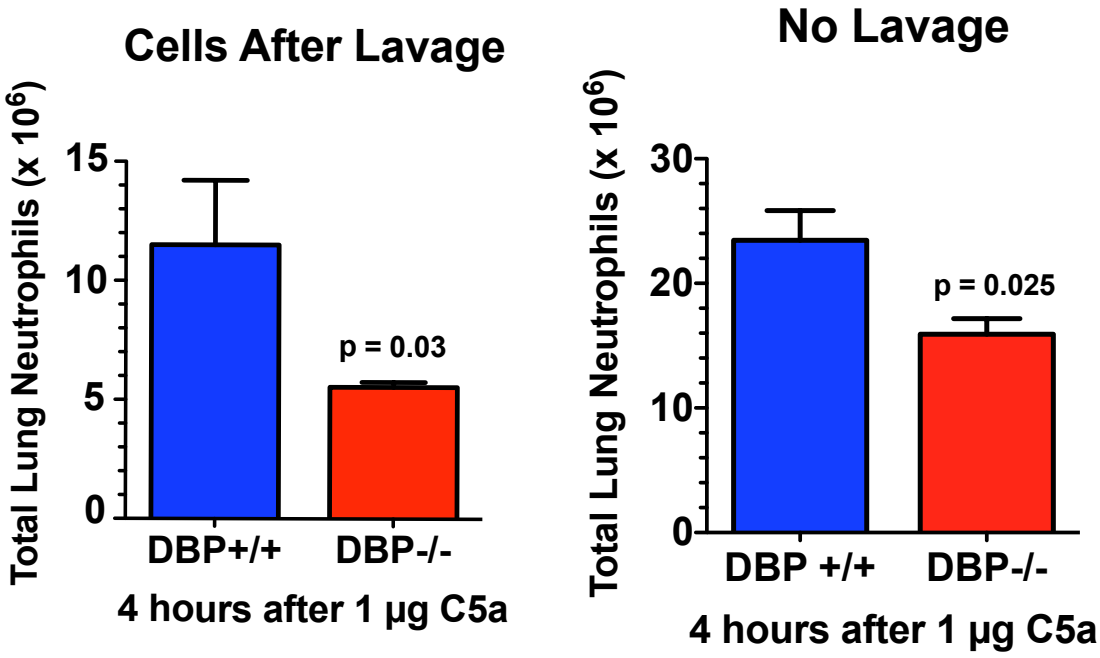

Figure 6 Total number of neutrophils in the lung.

Shown above is the average number of neutrophils in the lung of 5 DBP +/+ and DBP -/- before and after lavage. 1 µg of C5a was instilled into the lungs of DBP +/+ and DBP -/- mice. After 4 hours, the lungs were lavaged in half of the mice. All of the lungs were then isolated, minced and homogenized to create a single cell suspension. The cells were counted, stained with PE conjugated anti Gr-1 antibody and the percentage of Gr-1 high expressing cells was determined by flow cytometric analysis. The total number of neutrophils was calculated by multiplying the total number of lung cells by the percentage of Gr-1 high cells.

3.3. Exogenously added DBP can partially reverse the observed phenotype in DBP -/- mice.

If DBP is required extrinsically to augment neutrophil migration *in vivo*, one would hypothesize that adding DBP to the site of inflammation would induce more neutrophil recruitment into the lungs of DBP -/- mice after the instillation of C5a. Currently, purified mouse DBP is not available, so to test this hypothesis we utilized DBP containing (DBP +/+) or lacking (DBP -/-) serum. Complement activated serum (25%) from a DBP +/+ or DBP -/- mouse was instilled into the lungs of both DBP +/+ and DBP -/- animals. 4 hours after instillation, the mice were sacrificed, their lungs were lavaged, and the BAL cells were processed and analyzed as previously described. The level of C5a/C5a des Arg (measured by ELISA) generated in DBP +/+ and DBP -/- complement activated sera was essentially identical (figure 7b). There was no significant difference in the total number of BALF neutrophils detected in BALF from DBP +/+ mice treated with either DBP +/+ or DBP -/- complement activated serum. However, there was an increase in the total number of BALF neutrophils detected in the BALF of DBP -/- mice treated with DBP +/+ complement activated serum as compared to DBP -/- mice treated with DBP -/- complement activated serum (figure 7a). This suggests that adding DBP extrinsically to the site of inflammation can partially rescue the phenotype previously observed in the DBP -/- mice by inducing more neutrophil recruitment into the site of inflammation.

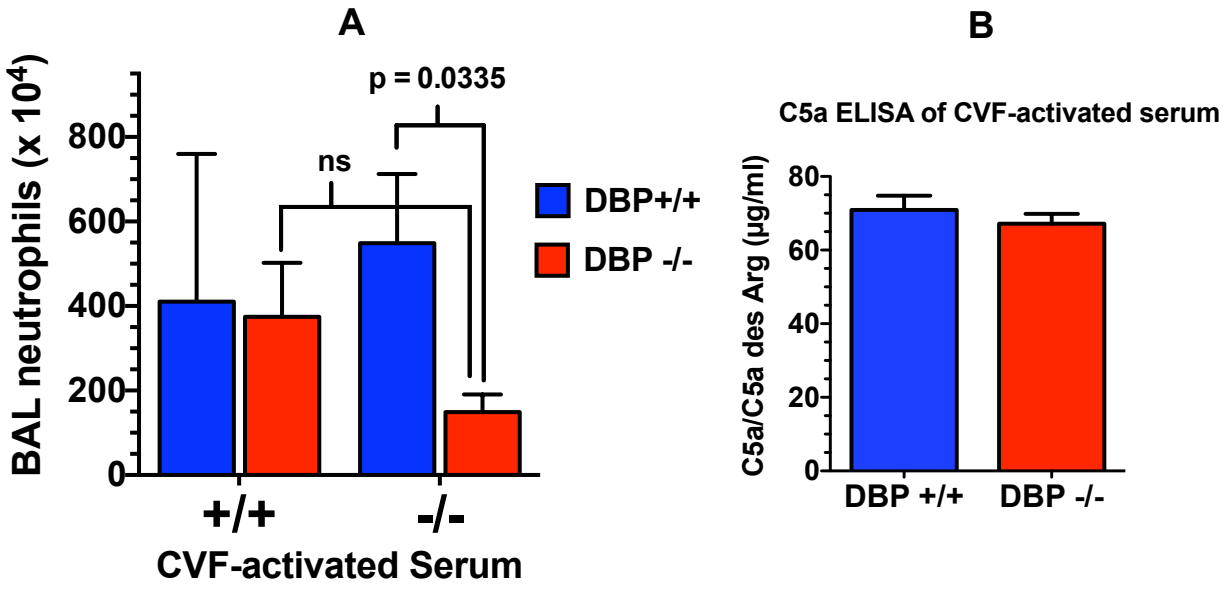

Figure 7 Exogenously adding DBP into the lungs of DBP -/- mice increase neutrophil recruitment into the lungs.

Complement activated serum from DBP +/+ and DBP -/- mice was diluted 1:4 in PBS and instilled into the lungs of DBP +/+ and DBP -/- mice. After 4 hours, the mice were sacrificed, the lungs were lavaged and the BAL cells were counted using an automated cell counter. To calculate the percentage of Gr-1 high neutrophils, BAL cells were stained with PE conjugated anti Gr-1 antibody and analyzed by flow cytometry. The total number of BAL neutrophils was calculated by multiplying the total number of BAL cells with the percent of cells that were Gr-1 high. Panel A shows the average number of BAL neutrophils from 4-6 DBP +/+ and DBP -/- mice. Panel B shows the concentration of C5a/C5a des Arg in the DBP +/+ and DBP -/- complement activated sera as determined by a C5a sandwich ELISA.

3.4. There is a significant increase in the surface expression of CD11b on DBP -/- BALF neutrophil 4 hours after the instillation of C5a.

There are several factors which can cause the reduction of neutrophil recruitment into the inflamed lung of DBP -/- mice, such as less neutrophils in the blood or bone marrow, reduced surface expression of the chemoattractant receptor, C5aR (CD88), or reduced surface expression of adhesion molecules required for cellular rolling, adhesion to endothelial cells or trans-endothelial migration through the vascular bed. To this end, the surface expression of several adhesion molecules (CD11b, CD11c, CD18 and CD44) was quantified by flow cytometry on BAL neutrophils (figure 8). Four hours after the instillation of 1 μg of C5a, the surface expression of CD11b and CD11c was significantly higher in BAL neutrophils from DBP -/- as compared to DBP +/+ neutrophils (figure 8a and 8b respectively). However, at all other time points, there was no significant difference in the surface expression of both integrins. There was also no significant difference in the surface expression of CD44 (a DBP receptor) and CD18 in BALF neutrophils collected 4 hours after the instillation of C5a (figure 8c and data not shown). It is known that the peak recruitment of neutrophils into tissues occurs 4-6 hours after the initial insult; a process that is highly dependent on the CD11b/CD18 induced trans-endothelial migration. It is estimated that in neutrophils approximately 95% of CD11b/CD18 is stored in intracellular granules, which are partially exocytosed upon the binding to immobilized chemoattractants on endothelial cells . This exocytosis, in addition to the shear force of blood circulation, then induces tight binding of rolling neutrophils to endothelial cells followed by trans-endothelial migration. The increased surface expression of CD11b on the surface of DBP -/- neutrophils in the BAL 4 hours after the initiation of inflammation, suggests that DBP -/- either have deregulated granule exocytosis, integrin endocytosis and/or integrin shedding.

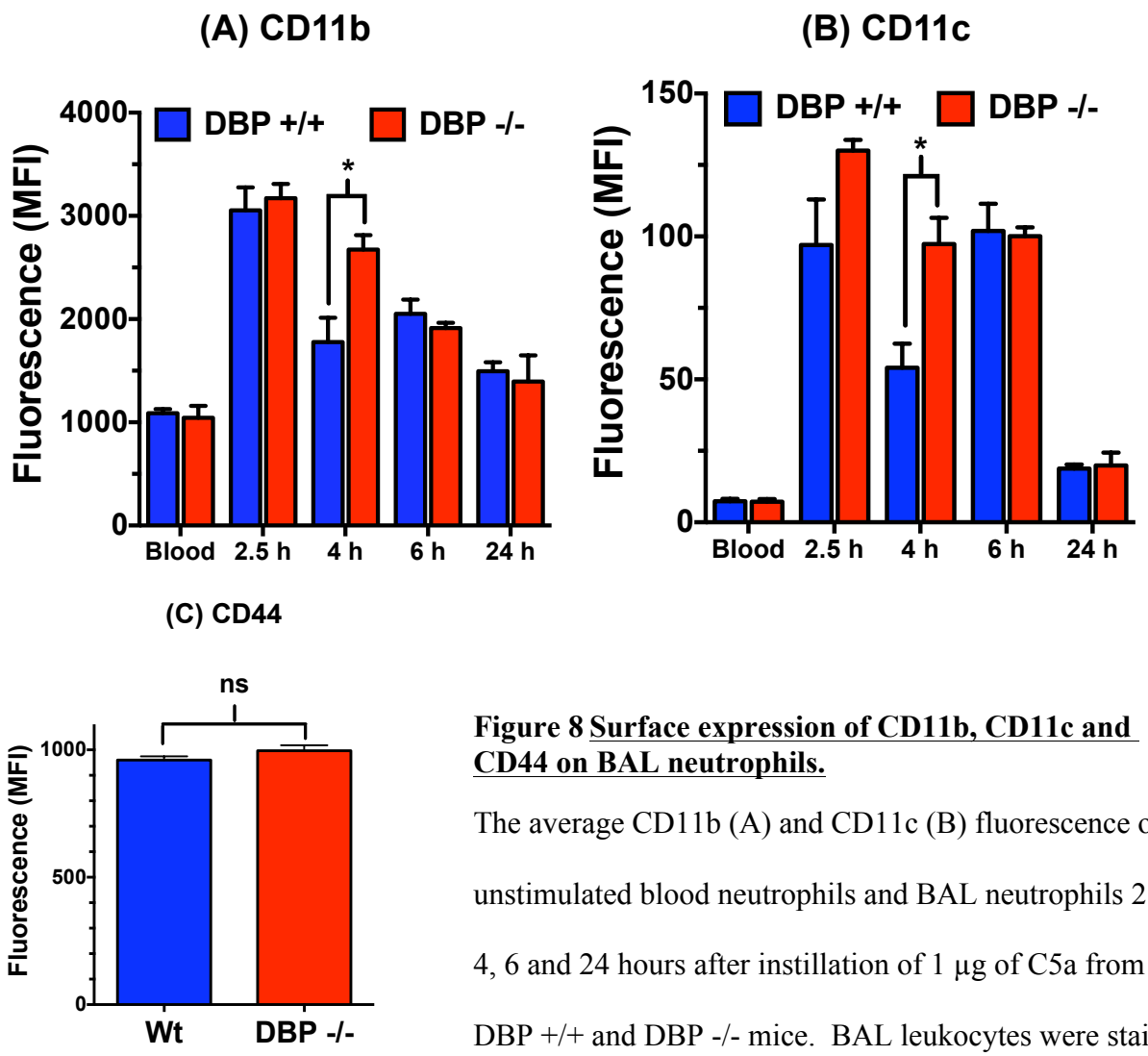

Figure 8 Surface expression of CD11b, CD11c and CD44 on BAL neutrophils.

The average CD11b (A) and CD11c (B) fluorescence on unstimulated blood neutrophils and BAL neutrophils 2.5, 4, 6 and 24 hours after instillation of 1 µg of C5a from 4-5 DBP +/+ and DBP -/- mice. BAL leukocytes were stained with PE conjugated anti Gr-1 to identify the neutrophil population, APC conjugated anti CD11b (A) and PE/Cy7 conjugated anti CD11c (B). In a separate experiment, at the 4-hour time point, BAL cells were stained with PE conjugated anti Gr-1 to identify the neutrophil population and APC conjugated anti CD44 (C). The cells were then analyzed by flow cytometry. Gr-1 high neutrophils were gated and their surface expression of CD11b (A), CD11c (B) and CD44 (C) was determined. * represents $p \leq 0.012$.

3.5. There is a significant decrease in the number of DBP -/- bone marrow neutrophils.

As previously mentioned, a decrease in the number of blood or bone marrow neutrophils in DBP -/- mice can lead to reduced neutrophil recruitment to a site of inflammation. Therefore, to compare the number of neutrophils in the blood, 5 DBP +/+ and DBP -/- mice were sacrificed, blood was collected by cardiac puncture and placed into a microfuge containing EDTA to prevent clotting. The red blood cells where then lysed using hypotonic buffer, the leukocytes were washed once with PBS, counted using an automated cell counter, then stained with anti-GR-1 and analyzed by flow cytometry. Blood neutrophils were defined as Gr-1 high expressing cells with a high side scatter (figure 9c, gated population). There was no significant difference in the number of total white blood cells (figure 9a) or the blood neutrophils (figure 9b) between DBP +/+ and DBP -/- mice.

To determine the number of neutrophils in the bone marrow, 5 DBP +/+ and DBP -/- mice were sacrificed, the femurs and tibias were isolated and bone marrow cells were flushed out of the isolated bones. Red blood cells were lysed using hypotonic buffer and whole bone marrow cells were washed once in PBS and stained with anti Gr-1. Due to the lack of a distinct Gr-1 high population, bone marrow neutrophils and pre-neutrophilic cells were defined as Gr-1 positive cells (figure 10c, gated population). There was no significant difference in the total number of bone marrow cells between DBP +/+ and DBP -/- mice (figure 10a). However, there was a significant decrease in the number of Gr-1 positive cells (figure 10b) and the surface expression of Gr-1 on DBP -/- bone marrow cells as compared to DBP +/+ bone marrow neutrophils suggesting that there is a significant decrease in the number of bone marrow neutrophils in DBP -/- mice relative to DBP +/+ mice (figure 11b).

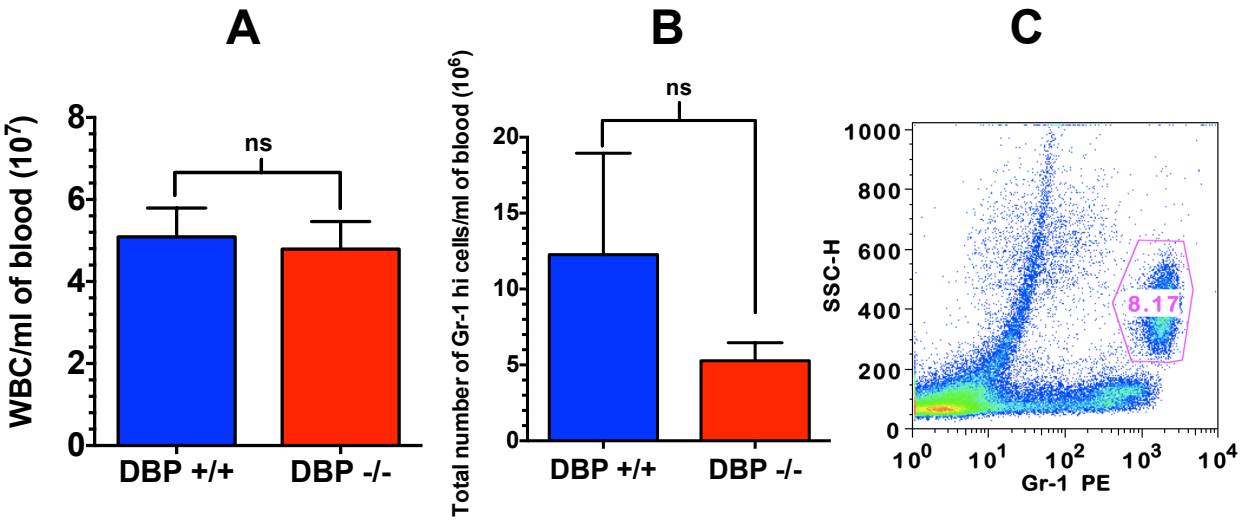

Figure 9 Analysis of blood leukocytes.

Shown above is the average number of blood leukocytes and neutrophils from 5 DBP +/+ and DBP -/- mice. Blood was obtained from DBP +/+ and DBP -/- mice by cardiac puncture. Red blood cells were lysed using hypotonic buffer and the number of blood leukocytes was determined using an automated cell counter (A). The cells were then stained with PE conjugated anti Gr-1 antibody. Neutrophils were identified by gating a population of cells that showed a high surface expression of Gr-1 and a high side scatter (C). The total number of neutrophils was calculated by multiplying the total number of blood leukocytes with the percentage of cells that were Gr-1 high and SSC high (Gated population in panel C) (B).

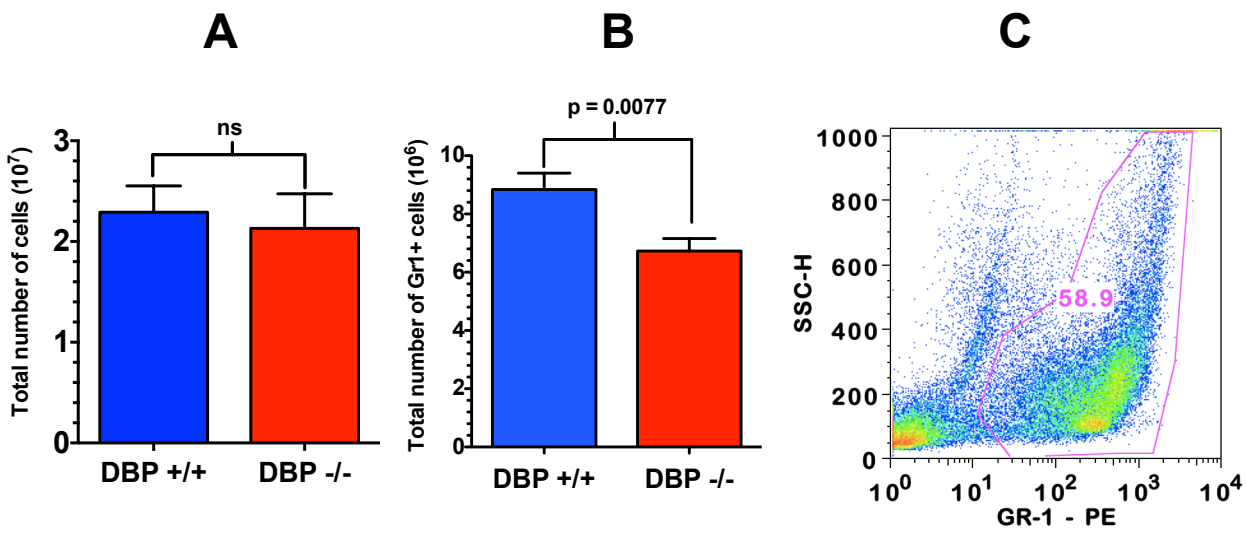

Figure 10 Analysis of bone marrow cells.

Shown above is the average number of whole bone marrow cells and bone marrow neutrophils from 5 DBP +/+ and DBP -/- mice. Bone marrow cells were isolated from femurs and tibias of DBP +/+ and DBP -/- mice. Red blood cells were lysed using hypotonic buffer and the number of bone marrow cells was determined using an automated cell counter (A). The cells were then stained with PE conjugated anti Gr-1 antibody and analyzed by flow cytometry. Neutrophils were identified by gating a population of cells that were positive for Gr-1 (C). The total number of neutrophils was calculated by multiplying the total number of bone marrow cells with the percentage of cells which were Gr-1 positive (gated population in panel C) (B).

3.6. There is a significant decrease in the side scatter, the surface expression of Gr-1, CD88 and CD44 on DBP -/- bone marrow neutrophils.

Blood and bone marrow neutrophils from DBP +/+ and DBP -/- mice were further characterized by staining them with anti Gr-1, anti CD11b, anti CD11c, anti CD18, and anti CD44. Flow cytometric analysis revealed that, in addition to the decrease in the number of Gr-1 positive cells, the average fluorescence of cell surface Gr-1 in DBP -/- bone marrow neutrophils was lower than the average fluorescence of DBP +/+ bone marrow neutrophils (figure 11a & 11b). Furthermore, we noticed that a granular population of Gr-1 high bone marrow cells was lost in 4 out of the 5 DBP -/- mice as judged by the decrease in the side scatter (figure 11a, mice 2-5, arrows).

Next, the surface expression of CD88 (C5a receptor) on bone marrow neutrophils was determined by staining purified whole bone marrow cells from 5 DBP +/+ and DBP -/- mice for Gr-1, to identify the bone marrow neutrophil population, and CD88 (figures 12). In the bone marrow of 4 out of 5 DBP -/- mice, there was an approximate 50% reduction in the percentage of Gr-1+ cells that stained positively for CD88 as compared to the bone marrow of DBP +/+ mice (figure 12a, mice 2-5). There was also a significant decrease in the surface expression of CD88, as determined by the decrease in the mean fluorescence staining of CD88, on DBP -/- bone marrow neutrophils as compared to DBP +/+ bone marrow neutrophils (figure 12b). This is in contrast to what was observed in the blood, where there was no difference in the surface expression of CD88 between DBP -/- and DBP +/+ blood neutrophils (figure 12c).

The surface expression of CD44 (a DBP receptor) on bone marrow and blood neutrophils was determined by staining DBP +/+ and DBP -/- bone marrow cells with anti Gr-1 and anti-

CD44. Bone marrow neutrophils of 4 out of 5 DBP -/- mice had diffuse CD44 staining as compared to DBP +/+ bone marrow neutrophils, which were uniformly stained for CD44 (figure 8a). This heterogeneity in CD44 staining observed in the bone marrow neutrophils from DBP -/- mice resulted from a decrease in the surface expression of CD44 on a subpopulation of Gr-1 + neutrophils (figure 8a). This heterogeneity in cell surface CD44 expression was also evident from the significant decrease in the mean fluorescence intensity of CD44 in bone marrow neutrophils from DBP -/- mice when compared to DBP +/+ mice (figure 13b). This is in contrast to what was observed in the blood, where there was no difference in the surface expression of CD44 between DBP -/- and DBP +/+ blood neutrophils (figure 13c).

Finally, the surface expression of CD11b, CD11c and CD18 on blood and bone marrow neutrophils was determined. The was a significant decrease in the surface expression of CD11b on bone marrow neutrophils from DBP -/- mice as compared to DBP +/+ mice, as evident by the decrease in the CD11b mean fluorescence intensity staining on DBP -/- bone marrow neutrophils relative to DBP +/+ bone marrow neutrophils (figure 14a). However, there was no significant difference in the surface expression of CD11c or CD18 on the bone marrow neutrophils from DBP -/- and DBP +/+ mice (figure 14b and 14c respectively). There was no significant difference in the surface expression of CD11b, CD11c and CD18 on blood neutrophils from DBP -/- and DBP +/+ mice (figure 14d, 14e and 14f respectively). Collectively, this data suggests that the DBP might play a role in the differentiation and maturation of neutrophils in the bone marrow, a function that might be compensated for upon the entry of bone marrow neutrophils into the blood.

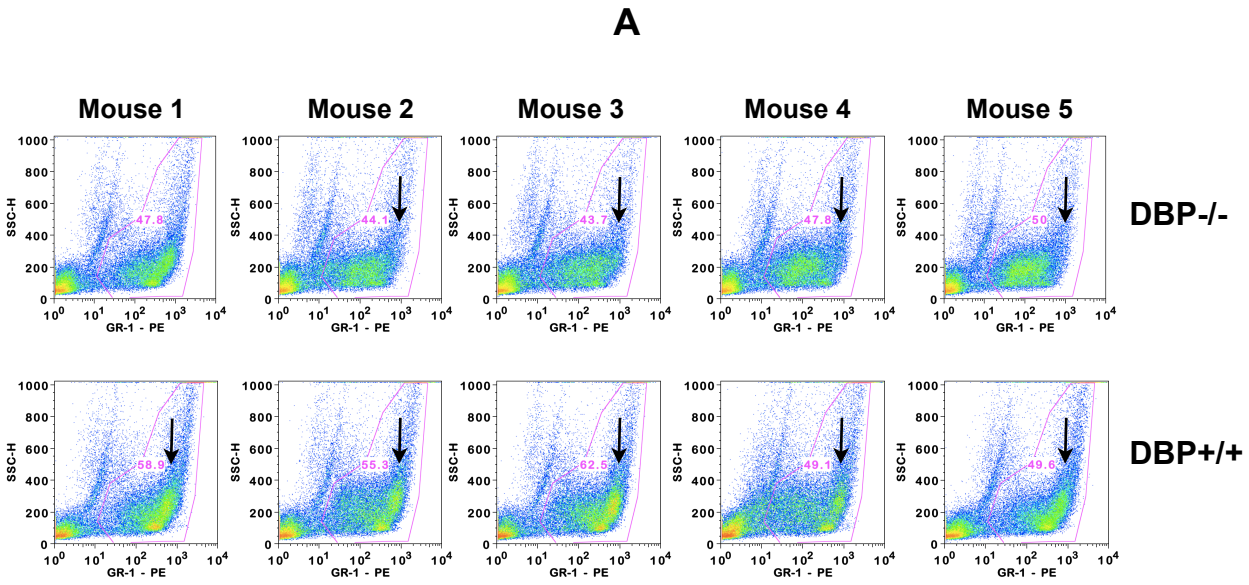

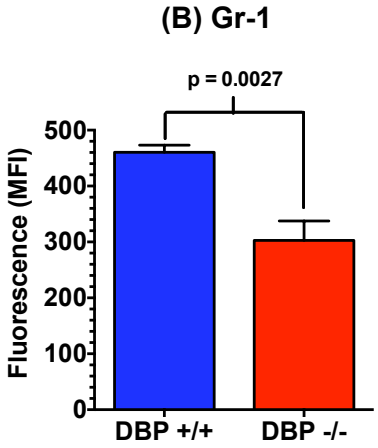

Figure 11 Analysis of the bone marrow cells by flow cytometry.

The Gr-1 staining distribution of Gr-1 positive (A) bone marrow cells from 5 DBP +/+ and DBP -/- mice against the side scatter. Bone marrow cells were isolated from femurs and tibias of DBP +/+ and DBP -/- mice. Red blood cells were lysed using hypotonic buffer and the cells were then stained with PE conjugated anti Gr-1 antibody. The cells were analyzed by flow cytometry. Panel B shows the average Gr-1 mean fluorescence intensity from 5 DBP +/+ and DBP -/- mice as determined using FlowJo (Tree Star Inc.).

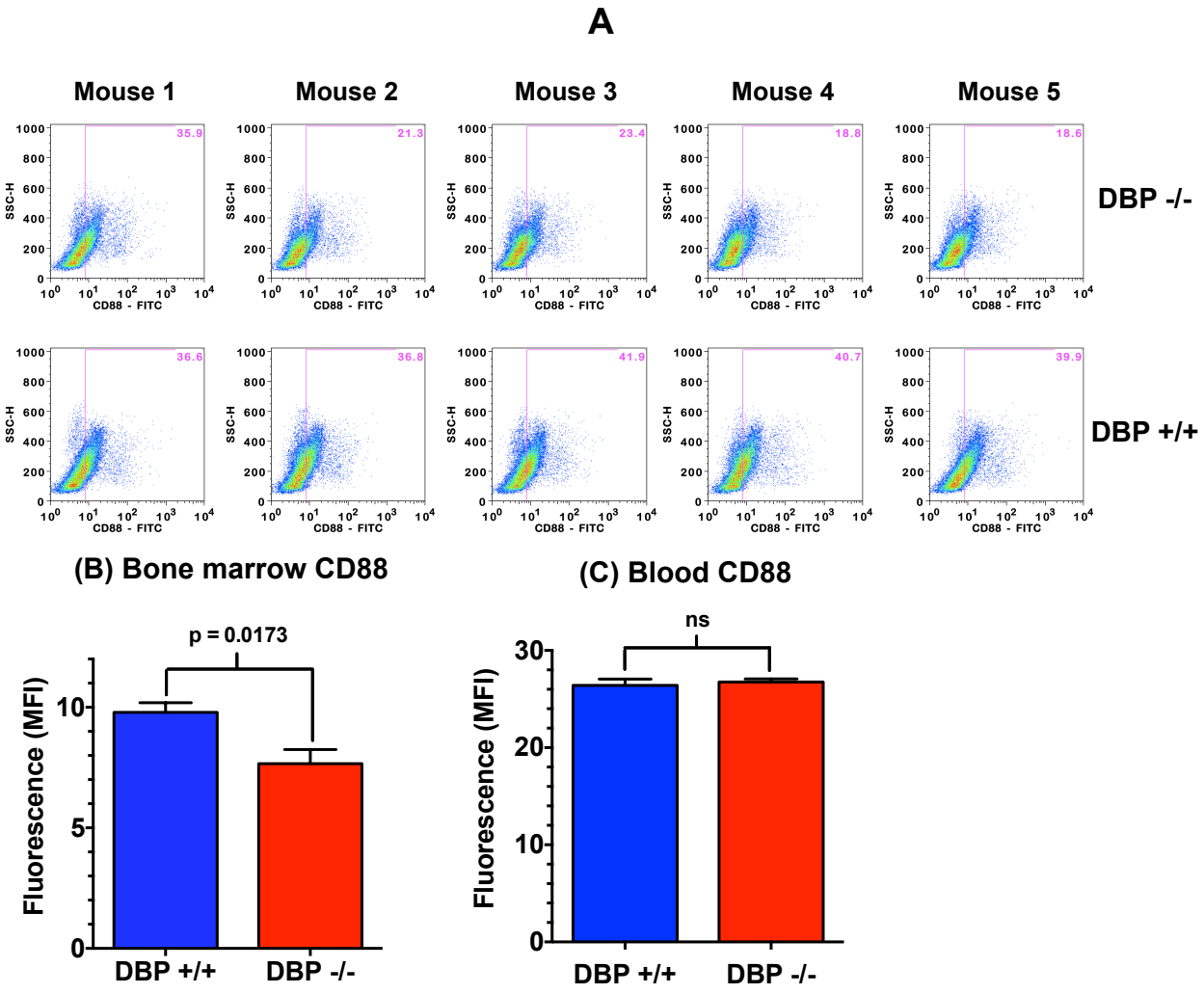

Figure 12 C5aR (CD88) expression on mouse neutrophils.

Bone marrow and blood cells were isolated from 5 DBP +/+ and DBP -/- mice. Red blood cells were lysed using hypotonic buffer and the remaining cells were stained with PE conjugated anti Gr-1, to identify the neutrophil population, and FITC conjugated anti CD88. The gates were drawn using the isotype control such that the isotype controls were negative for CD88 staining. The percent of bone marrow cells that stained positive for CD88 (A) was determined by plotting the Gr-1 positive cells in a dot plot for CD88 (x-axis) against the side scatter (y-axis). Panels B and C show the average mean fluorescence intensity for bone marrow CD88 and blood CD88 respectively from 5 DBP +/+ and DBP -/- as determined using FlowJo (Tree Star Inc.).

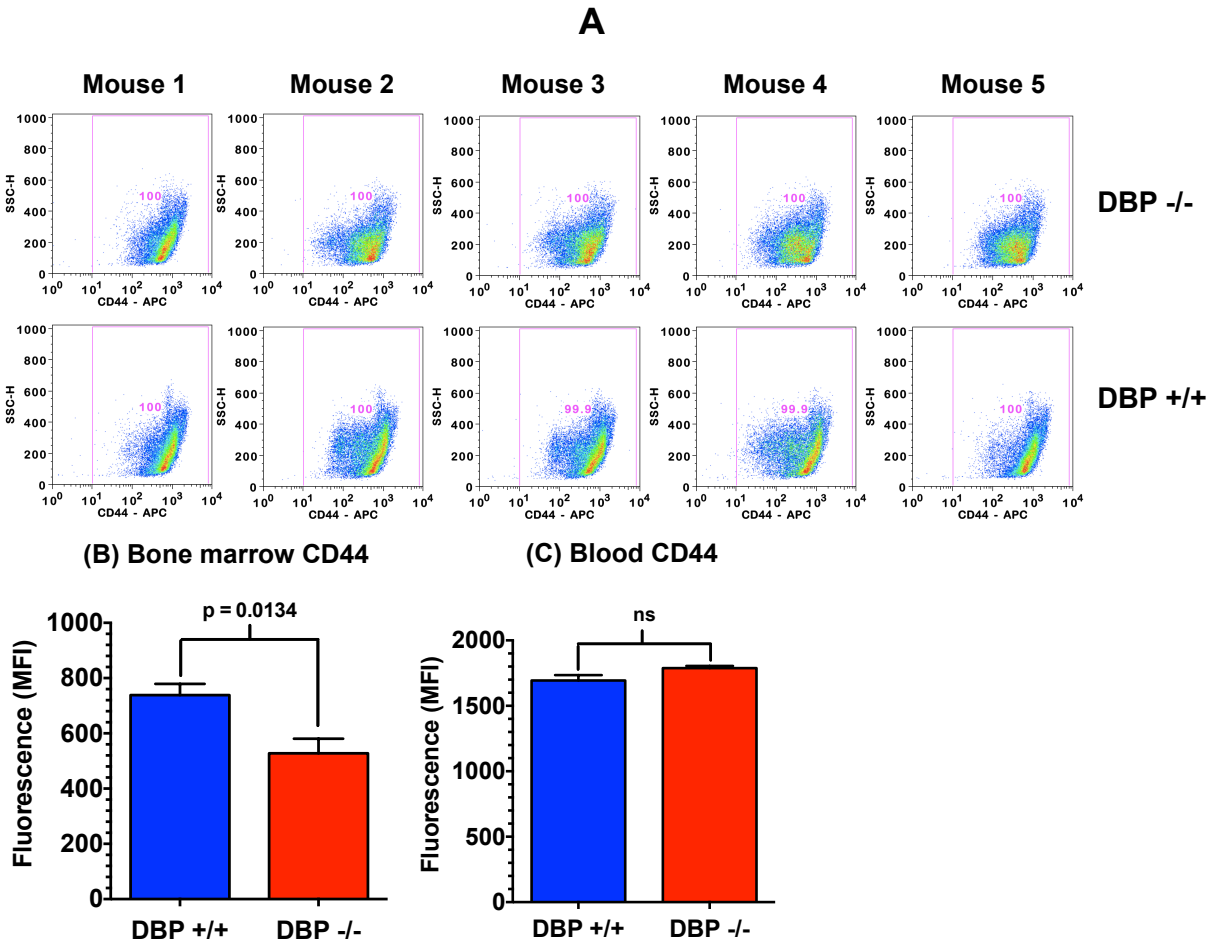

Figure 13 CD44 expression on mouse neutrophils.

Bone marrow and blood cells were isolated from 5 DBP +/+ and DBP -/- mice. Red blood cells were lysed using hypotonic buffer and the remaining cells were stained with PE conjugated anti Gr-1, to identify the neutrophil population, and APC conjugated anti CD44. The gates were drawn using the isotype control such that the isotype controls were negative for CD44 staining. The distribution of cell surface CD44 expression on Gr-1 positive bone marrow cells was determined by plotting the Gr-1 positive cells on a dot plot for CD44 (x-axis) against the side scatter (y-axis) (A). The average mean fluorescence intensity for bone marrow (B) and blood (C) neutrophil CD44 from 5 DBP +/+ and DBP -/- was determined using FlowJo (Tree Star Inc.).

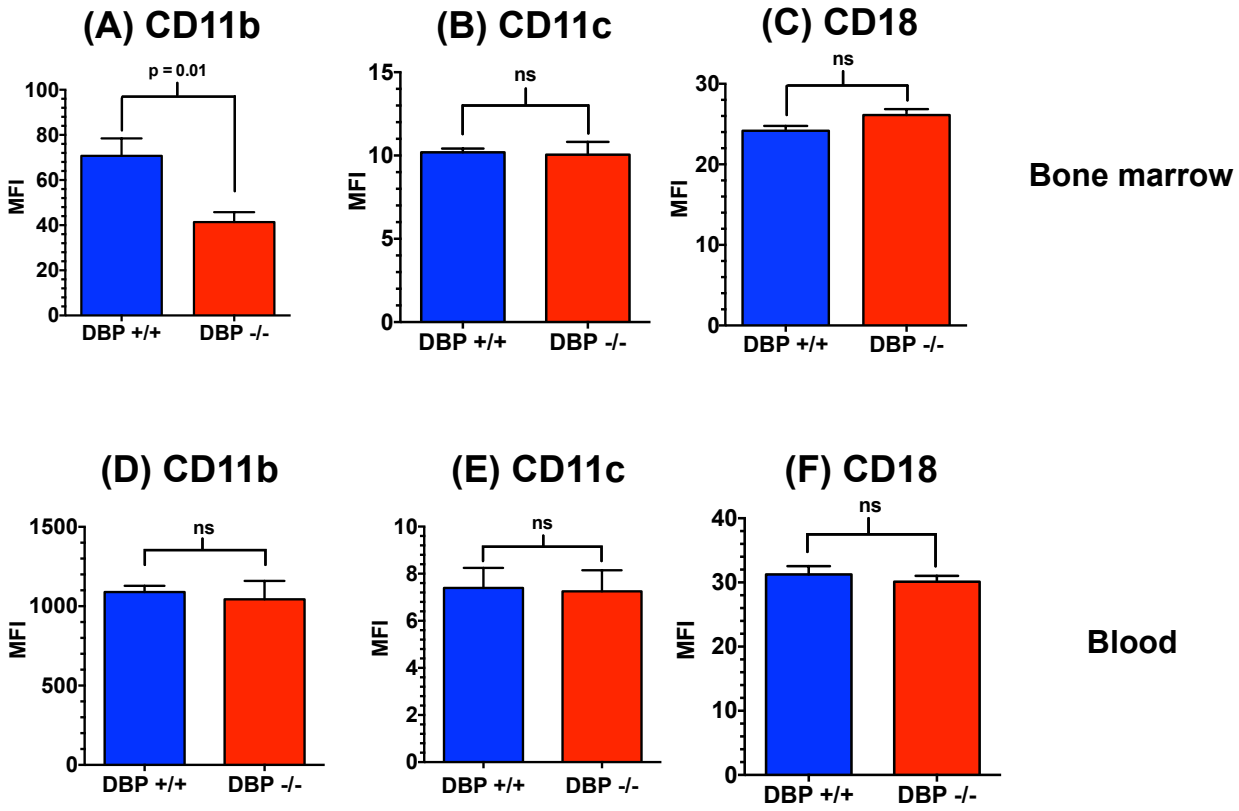

Figure 14 <u>The surface expression of integrins on bone marrow and blood neutrophils.</u>

Bone marrow (A-C) and blood cells (D-F) were isolated from 5 DBP +/+ and DBP -/- mice. Red blood cells were lysed using hypotonic buffer and the remaining cells were stained with PE conjugated anti Gr-1, to identify the neutrophil population, APC conjugated anti CD11b (A and D), PE/Cy7 conjugated anti CD11c (B and E) and FITC conjugated anti CD18 (C and F). The average mean fluorescence intensity for bone marrow neutrophil CD11b (A), CD11c (B) and CD18 (C) and blood neutrophil CD11b (D), CD11c (E) and CD18 (F) from 5 DBP +/+ and DBP-/- was determined using FlowJo (Tree Star Inc.).

3.7. There is an intrinsic migratory defect in the bone marrow neutrophils of DBP -/- mice.

The initial characterization of bone marrow cells suggests that there might be an intrinsic defect in the bone marrow neutrophil pool of DBP -/- mice. To determine whether this potential defect might lead to a functional defect in neutrophil chemotaxis, *ex vivo* chemotaxis assays were performed to purified C5a and to DBP +/+ and DBP -/- complement activated sera. Two different chemotaxis assays were utilized, a filter-based modified Boyden type chamber assay, and the under agarose chemotaxis assay on collagen coated coverslips. In the modified Boyden type chamber assay, cells migrate through a cellulose nitrate filter in three dimensions and the distance the cells migrate into the filter is measured using a microscope. In the under agarose chemotaxis assay, cells migrate on type I collagen under a layer of agarose in two dimensions toward a chemoattractant or a buffer control. The net distance and the net number of migrating cells can then be determined as described in the materials and methods. As shown in figure 15, there was no significant difference in the distance migrated by DBP +/+ and DBP -/- bone marrow neutrophils to purified mouse C5a in the modified Boyden type chamber assay. However, when bone marrow neutrophils were allowed to migrate on collagen coated coverslips in the under agarose chemotaxis assay, there was a significant increase in the net distance migrated by DBP +/+ and DBP -/- cells to DBP +/+ complement activated serum as compared to DBP -/- cells migrating to DBP -/- complement activated serum (figure 16c). There was no significant difference in the migration of DBP +/+ cells to either DBP +/+ or DBP -/- complement activated sera.

One of the strengths of the under agarose chemotaxis assay is the ability to determine the net number of migrating cells. As shown in figure 16a and 16b, there was a significant reduction

in the net number of migrating DBP -/- bone marrow neutrophils as compared to DBP +/+ bone marrow neutrophils to both DBP -/- and DBP +/+ complement activated sera. This suggests that DBP -/- bone marrow neutrophils might have an intrinsic defect in migration, which can be partially rescued by the addition of DBP, as shown in figure 16c.

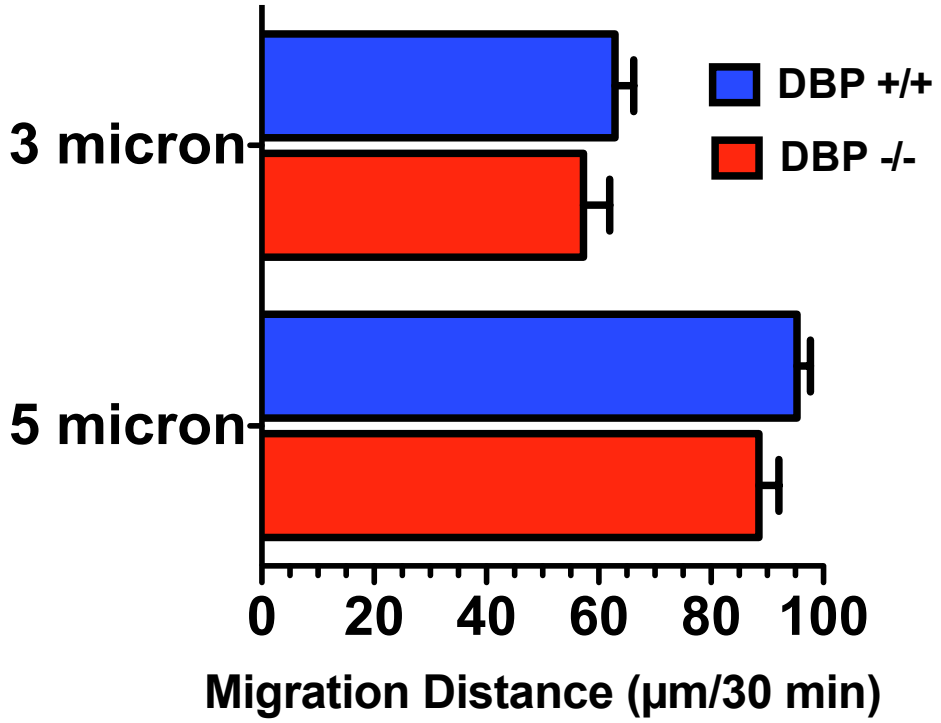

Figure 15 Modified Boyden type chamber migration of bone marrow neutrophils.

Bone marrow cells were isolated from femurs and tibias of 3 DBP +/+ and DBP -/- mice. The cells were then resuspended in HBSS containing 10 mM HEPES and 1% BSA at a concentration of 10 million cells per ml. The cells were then loaded into a 48 well micro chemotaxis chamber (Neuroprobe) and allowed to migrate into a cellulose nitrate filter containing 3 or 5 µm pores to 10 nM C5a for 30 minutes at 37 ºC. After 30 minutes, the filters were stained, mounted onto a double slide and the distance the neutrophils migrated into the filters was determined using a microscope at 400x magnification. The distance migrated was measured in 10 different fields at 400x magnification for each treatment and mouse. Shown above is the average distance migrated by bone marrow neutrophils from 3 DBP +/+ and DBP -/- mice.

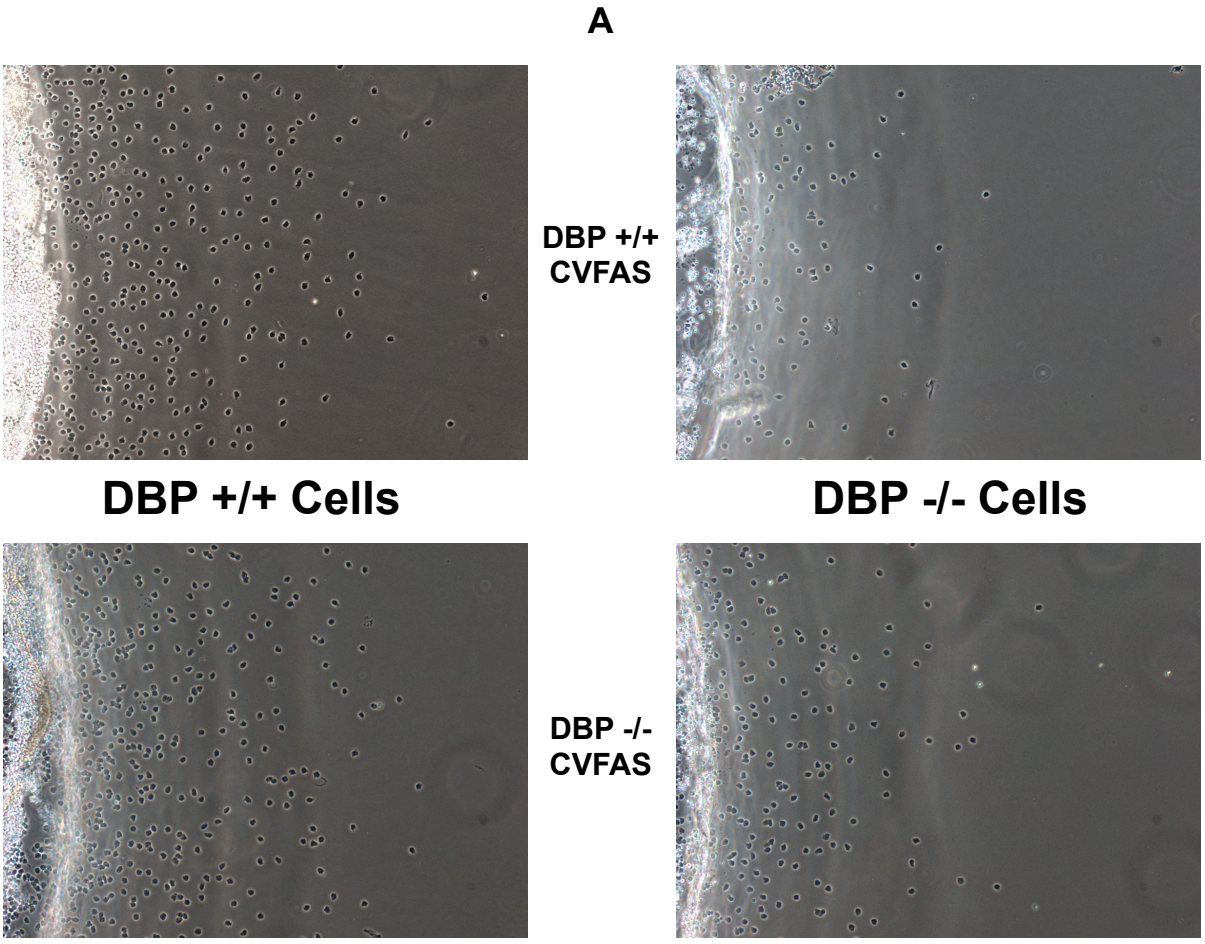
A
DBP +/+ CVFAS
DBP +/+ Cells
DBP -/- Cells
DBP -/- CVFAS
B
DBP +/+ PMN
DBP -/- PMN
Net number of migrating cells (4.5 h)
P = 0.0039
P = 0.0034
50
40
30
20
10
0
+/+ CVFAS
-/- CVFAS
C
DBP +/+ PMN
DBP -/- PMN
Net distance migrated (µm/4.5 h)
P = 0.0007
P ≤ 0.027
1500
1000
500
0
+/+ CVFAS
-/- CVFAS

Figure 16 Under agarose migration of bone marrow neutrophils.

Bone marrow cells were isolated from femurs and tibias of 3 DBP +/+ and DBP -/- mice. The cells were then resuspended in HBSS at a concentration of 20 million cells per ml, loaded into the middle well in an under agarose plate and allowed to migrate to 5% DBP +/+ or DBP -/- complement activated serum or HBSS (control) for 4.5 hours at 37 ºC. After 4.5 hours, the plates were fixed with 2% paraformaldehyde and pictures of neutrophils migrating towards the complement activated serum containing well (A) and HBSS were taken using a Nikon Ti microscope at 100x magnification. The distance migrated was measured by using the measurement tool in Macnification (Interface Design Software). The number of migrating cells was determined by using the cell counter tool in ImageJ (NIH). The net number of migrating cells was calculated by subtracting the number of migrating cells towards the buffer from the number of migrating cells towards the complement-activated serum (B). The net distance migrated was calculated by subtracting the distance migrated to the buffer from the distance migrated towards the complement activated serum (C). Shown above is the average net distance migrated and net number of migrating cells from bone marrow neutrophils of 3 DBP +/+ and DBP -/- mice.

3.8. There is a polarization defect in the bone marrow neutrophils of DBP -/- mice.

Polarization in the direction of a chemotactic gradient is the first step in the process of cell migration. To determine the polarization of migrating bone marrow neutrophils, the location of polymerized actin and the morphology of migrating cells was analyzed. DBP +/+ bone marrow neutrophils were allowed to migrate on collagen or BSA coated cover slips to DBP +/+ or DBP -/- complement activated serum for 4.5 hours. The cells where then fixed and the agarose was removed. The cells were permabilized and stained with Phalloidin to visualize F-actin and analyzed under a fluorescence microscope at 1000x magnification. There was no significant difference in phalloidin staining in DBP +/+ bone marrow neutrophils migrating on BSA coated coverslips to either DBP +/+ or DBP -/- complement activated sera (figure 17d). However, when cells were allowed to migrate on collagen coated coverslips, there was a significant increase in phalloidin staining, or F-actin polymerization, of DBP +/+ bone marrow neutrophils migrating to DBP -/- complement activated serum as compared to cells migrating to DBP +/+ complement activated serum (figure 17 a-c). In addition, the morphology of the cells migrating to DBP -/- complement activated serum showed more uniform and less polarized distribution of F-actin (fig. 17 b) as compared to cells migrating to DBP +/+ complement activated serum (fig 17a), which displayed a more polarized morphology. This suggests that DBP may play a role in neutrophil polarization during migration to complement activated serum.

A subsequent experiment was performed using both DBP +/+ and DBP -/- bone marrow neutrophils migrating to +/+ or -/- complement activated serum on collagen-coated coverslips. DBP -/- bone marrow neutrophils migrating to DBP -/- complement activated serum were unpolarized and many had regions of F-actin formation but with a uniform subcellular

distribution (figure 18a). Polarization in DBP -/- bone marrow neutrophils was partially restored when cells migrated to DBP +/+ complement activated serum (figure 18b). When DBP +/+ bone marrow neutrophils migrated to DBP -/- complement activated serum, they had a similar phenotype as DBP -/- bone marrow neutrophils migrating to DBP +/+ complement activated serum as evidenced by the partial polarization (figure 18c). However, when DBP +/+ migrated to DBP +/+ complement activated serum, most of the cells were polarized, with polarized F-actin formation only at protrusions extending out of the migrating neutrophils (figure 18d). This suggests that DBP might play a role in cellular polarization during chemotaxis to complement activated serum, and supports the alveolitis and under agarose chemotaxis results indicating that DBP -/- bone marrow neutrophils might have an intrinsic defect in chemotaxis which can be partially rescued by the exogenous addition of DBP during chemotaxis.

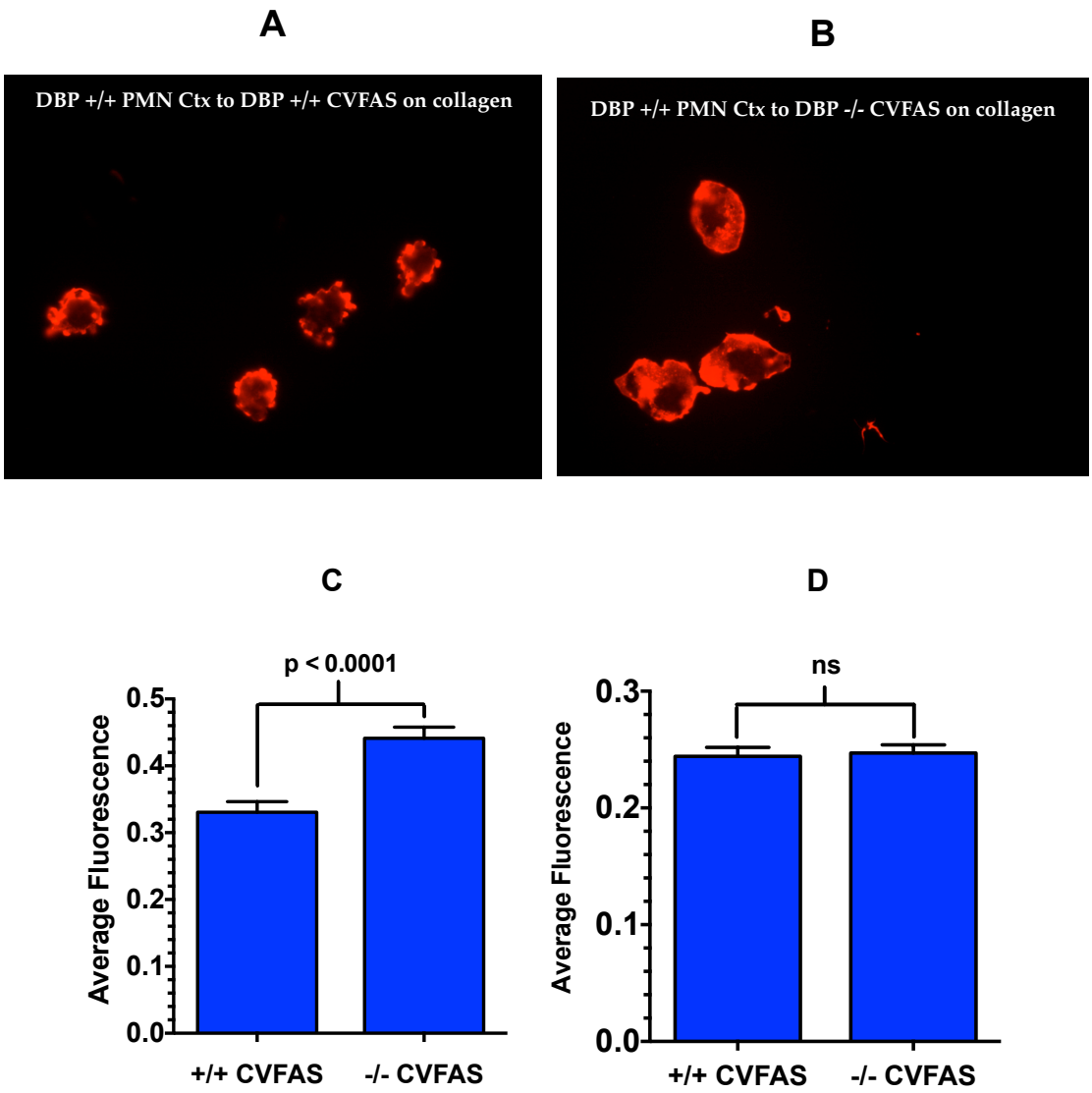
A
B
DBP +/+ PMN Ctx to DBP +/+ CVFAS on collagen
DBP +/+ PMN Ctx to DBP -/- CVFAS on collagen
C
D
p < 0.0001
ns
Average Fluorescence
0.5
0.4
0.3
0.2
0.1
0.0
+/+ CVFAS
-/- CVFAS

Figure 17 Neutrophils have a more polarized morphology when migrating in the presence of DBP.

Bone marrow neutrophils were purified from a DBP +/+ mouse and resuspended in HBSS at a concentration of 20 million cells per ml. 0.5 million cells were loaded into a collagen coated or BSA coated coverslip in an under agarose chemotaxis plate, and the cells were allowed to migrate to either DBP +/+ or DBP -/- complement activated serum or HBSS (control). After 4.5 hours, the cells were fixed in 2% paraformaldehyde overnight. The agarose was then discarded and the cells were permabilized and F-actin stained with alexa flour 594-conjugated phalloidin (Life Technologies). The coverslips were then mounted on to a microscope slide and analyzed using a Nikon Ti fluorescent microscope at 1000x magnification, shown above. (A) Shows a representative of DBP +/+ bone marrow neutrophils migrating to DBP +/+ complement activated serum. (B) Shows a representative of DBP +/+ bone marrow neutrophils migrating to DBP -/- complement activated serum. To quantify the average phalloidin fluorescence on neutrophils migrating on collagen (C) or BSA (D), 96 or more cells were individually highlighted and the average fluorescence was calculated using the Macnification software program. This experiment was performed twice using the bone marrow from 2 DBP +/+ mice.

(A) DBP -/- PMN ctx to DBP -/- CVFAS

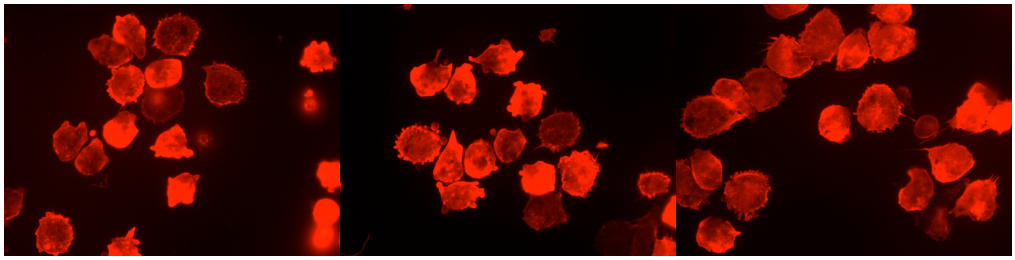

(B) DBP -/- PMN ctx to DBP +/+ CVFAS

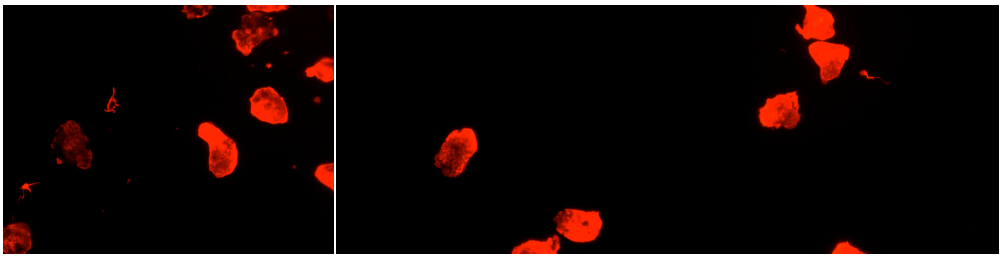

(C) DBP +/+ PMN ctx to DBP -/- CVFAS

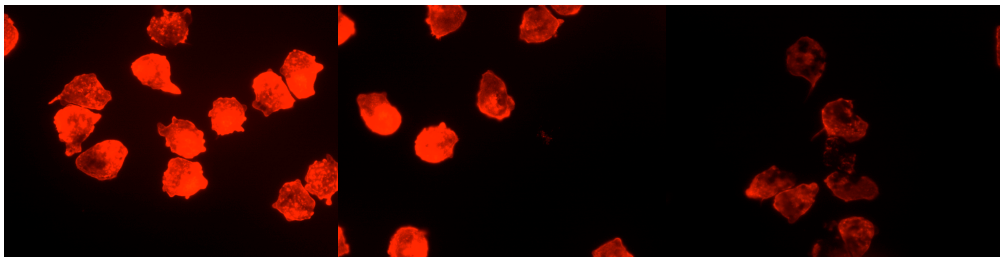

(D) DBP +/+ PMN ctx to DBP +/+ CVFAS

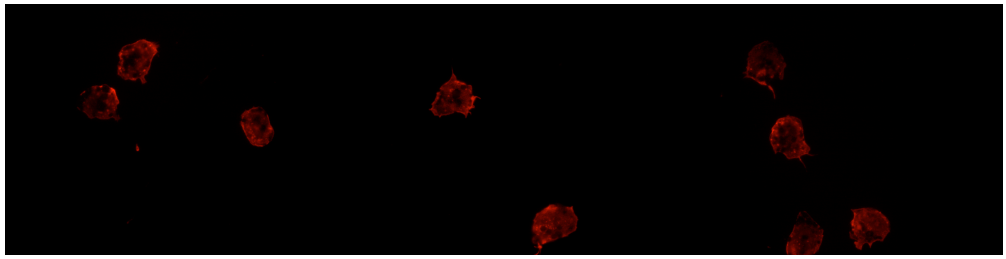

Figure 18 DBP -/- bone marrow neutrophils have a polarization defect during chemotaxis.

Bone marrow neutrophils were purified from one DBP +/+ or DBP -/- mouse and resuspended in HBSS at a concentration of 20 million cells per ml. 0.5 million cells were loaded into a collagen coated coverslip in an under agarose chemotaxis plate, and the cells were allowed to migrate to DBP +/+ or DBP -/- complement activated serum or HBSS (control). After 4.5 hours, the cells were fixed in 2% paraformaldehyde overnight. The agarose was then discarded and the coverslip was stained F-actin with alexa flour 594-conjugated phalloidin (Life Technologies), then mounted on to a microscope slide and analyzed using a Nikon Ti fluorescent microscope at 1000x magnification, shown above. Three representative pictures of DBP -/- bone marrow neutrophils migrating towards DBP -/- (A) or DBP +/+ (B) complement activated sera and of DBP +/+ bone marrow neutrophils migrating towards DBP -/- (C) or DBP +/+ (D) complement activated sera are shown above. This experiment was performed twice using the bone marrow of 2 DBP +/+ mice and once using the bone marrow of 1 DBP -/- mouse.

3.9. DBP -/- bone marrow neutrophils generated a reduced amount of superoxide anions as compared to DBP +/+ bone marrow neutrophils.

Figures 16-18 suggests that DBP -/- bone marrow neutrophils might have an intrinsic defect in chemotaxis. Therefore, other neutrophil functions, such as superoxide anion generation and phagocytosis, were examined to determine whether the intrinsic defect observed in DBP -/- bone marrow neutrophils was specific to chemotaxis. The capacity of bone marrow neutrophils to generate superoxide anions was determined by stimulating DBP +/+ and DBP -/- bone marrow neutrophils with a receptor dependent stimulus, 10% DBP +/+ or DBP -/- complement activated serum, or a receptor independent stimulus, 10 ng/ml of PMA, followed by incubation with Cytochrome c, which becomes reduced upon exposure to superoxide anions. The amount of reduced Cytochrome c was detected using a fluorescent plate reader as described in the materials and methods. Unstimulated cells were used as a control. There was no significant difference in the amount of reduced Cytochrome c between DBP +/+ and DBP -/- bone marrow neutrophils stimulated with DBP +/+ or DBP -/- complement activated sera. However, there was a slight but significant reduction in the amount of reduced Cytochrome c when either neutrophils were stimulated with DBP -/- complement activated serum versus DBP +/+ complement activated serum (figure 19a). This suggests that DBP may play a role in the activation of NADPH oxidase and the generation of superoxide anions in bone marrow neutrophils. To test the full superoxide anion generation capacity of DBP +/+ and DBP -/- bone marrow neutrophils, PMA, a strong receptor independent stimulus, was used. There was a significant reduction in the amount of Cytochrome c reduced by DBP -/- bone marrow neutrophils as compared to DBP +/+ neutrophils stimulated with PMA. This suggests that the capacity to generate superoxide anion is deficient in DBP -/- bone marrow neutrophils.

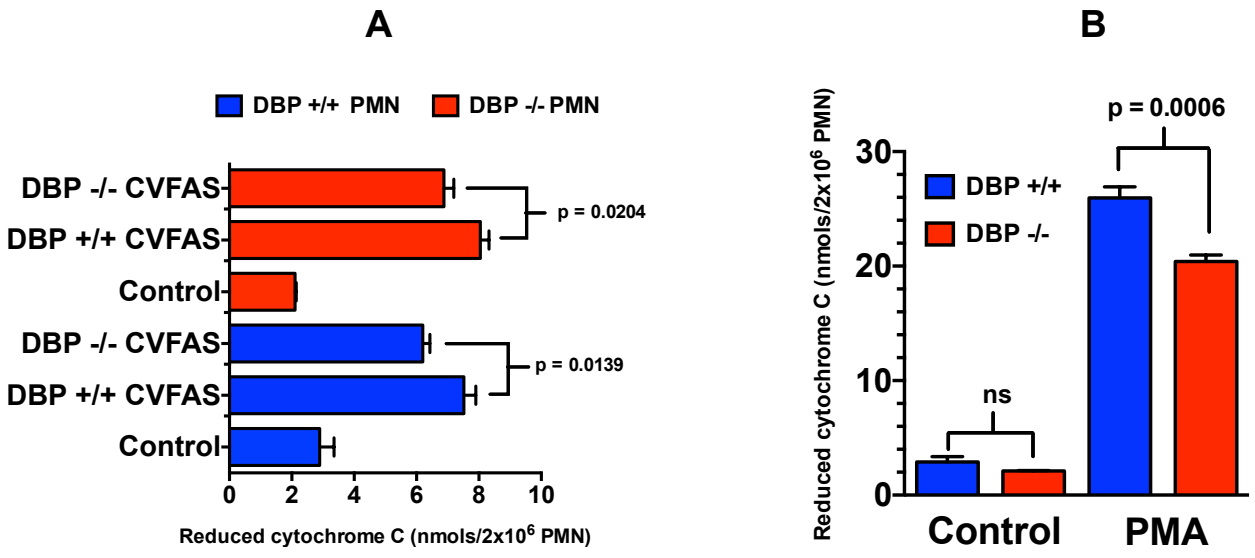

Figure 19 Superoxide anion generation by bone marrow neutrophils.

Bone marrow neutrophils from 3 DBP +/+ and DBP -/- mice were enriched. The cells were then stimulated with 10% DBP +/+ or DBP -/- complement activated serum (A), 10 ng/ml of PMA (B) or HBSS buffer as a control (controls in A and B) in the presence of 120 µM of Cytochrome c for 30 minutes at 37 ºC. The reaction was stopped by placing the cells on ice for 5 minutes and spinning the cells down at 4 ºC. The supernatant was transferred into a 96 well plate and the absorbance was measured at 550 nm using a plate reader (Spectramax M2, Molecular Devices). Nano moles of reduced Cytochrome c were calculated by multiplying the absorbance at 550 nm by 71.4. Panel A and B shows the average of Cytochrome c reduced from 3 DBP +/+ and DBP -/- mice.

3.10. There was no difference in the phagocytic capacity of DBP +/+ and DBP -/- bone marrow neutrophils.

The phagocytic capacity of bone marrow neutrophils was determined next. DBP +/+ and DBP -/- bone marrow neutrophils were incubated with alexa flour 594 conjugated complement opsonized zymosan for 1 hour at 37 ºC. The extracellular bound zymosan was quenched by the addition of trypan blue and the cells were analyzed by flow cytometry. To control for any non-quenched cell surface bound zymosan, cells were mixed with alexa flour 594 conjugated complement opsonized zymosan and incubated on ice for 1 hour. As shown in figure 20, there was more zymosan fluorescence in neutrophils incubated at 37 ºC as compared to neutrophils incubated on ice, indicating that at 37 ºC, cells phagocytosed the opsonized zymosan. However, there was no significant difference in the amount of phagocytosed zymosan by DBP +/+ or DBP -/- bone marrow neutrophils. This suggests that the phagocytic capacity in DBP -/- neutrophils was not affected by the absence of DBP.

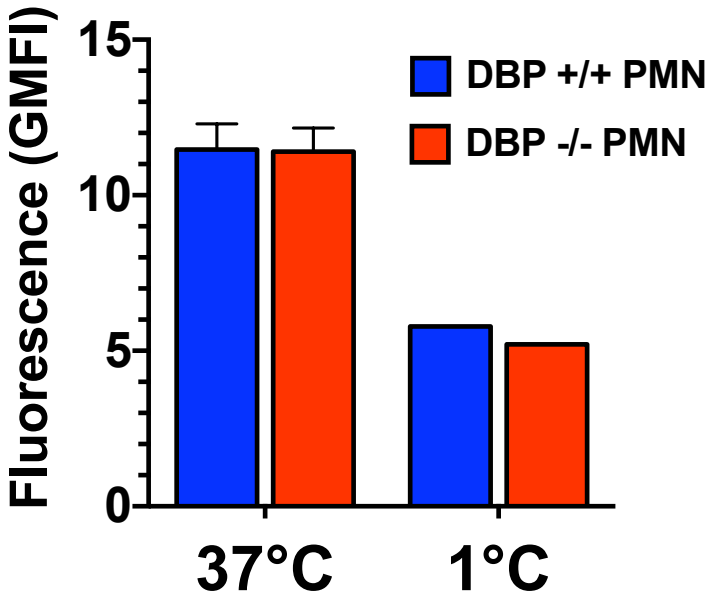

Figure 20 Phagocytosis of opsonized zymosan by bone marrow neutrophils.

Bone marrow neutrophils were isolated from 4 DBP +/+ and DBP -/- mice. The cells were then mixed 1:1 with alexa flour 594 conjugated zymosan, which was complement opsonized in DBP +/+ serum for 30 minutes at 37 ºC. The cells were incubated with the opsonized zymosan for 1 hour at 37 ºC. To control for non-phagocytosed, cell surface bound zymosan, cells were incubated with opsonized zymosan for 1 hour at 1 ºC. Non-phagocytosed zymosan was quenched by adding trypan blue. The cells were washed once with HBSS and then analyzed by flow cytometry. The difference in fluorescence intensity between cells incubated at 1 ºC and at 37 ºC represents fluorescence from phagocytosed zymosan particles. The fluorescence intensity observed at 1 ºC represents fluorescence from cell surface bound zymosan particles. Shown above is the average geometric mean fluorescence intensity from enriched bone marrow neutrophils purified from 4 DBP +/+ and DBP -/- mice.

4. Chapter 2

4.1. DBP may amplify inflammation by inducing the release of S100A8/A9 from neutrophils.

In the first chapter evidence was presented that shows DBP may play a role in neutrophil differentiation, development and chemotaxis. However, a mechanism by which DBP exerts its function on neutrophils is not known. In this chapter, a mechanism will be proposed which will describe how DBP can exert both extrinsic and intrinsic functions on neutrophils.

4.1.a. S100A8 and S100A9 are released by neutrophils in DBP treated conditioned neutrophil supernatants as determined by mass spectrometric analysis.

DBP has been previously shown to bind and subsequently shed from the cell surface of neutrophils; both binding and shedding are required for its chemotactic cofactor function. However, whether this binding and subsequent shedding induces any changes in neutrophil granular exocytosis or secretion of any neutrophil proteins has not been determined. To this end, a proteomic approach was utilized to address this question. Purified human neutrophils were treated with DBP for 30 minutes at 37 °C, centrifuged and the conditioned supernatants were collected. As a control, neutrophils were incubated with the same volume of buffer at 37 °C for 30 minutes and the cell-free supernatant was collected. The conditioned supernatants were separated by SDS-PAGE and visualized by silver staining. Analysis of the silver stained gel revealed 4 protein bands, which were of lower molecular weight than DBP but with a higher intensity in the DBP treated neutrophil supernatant as compared to the control (figure 21). These bands were cut out, trypsin digested and their protein content was identified by mass spectrometric analysis. The mass spectrometric results are shown in table 1. According to table

1, many neutrophil proteins were detected in both the control DBP treated conditioned supernatants, including lactate dehydrogenase which is a marker for cellular death. However, there were only two proteins in this analysis that has been previously shown to play a role in cellular migration, cellular polarization, actin polymerization and superoxide anion generation in neutrophils, S100A8 and S100A9. As shown in figure 21 and table 1, bands 5 (DBP treated conditioned supernatant) and 6 (control conditioned supernatant) contained S100A8 and S100A9 as detected by mass spectrometry. The intensity of band 5 is higher than band 6, suggesting that there is more protein in band 5 as compared to band 6 and that DBP might induce the secretion of these proteins.

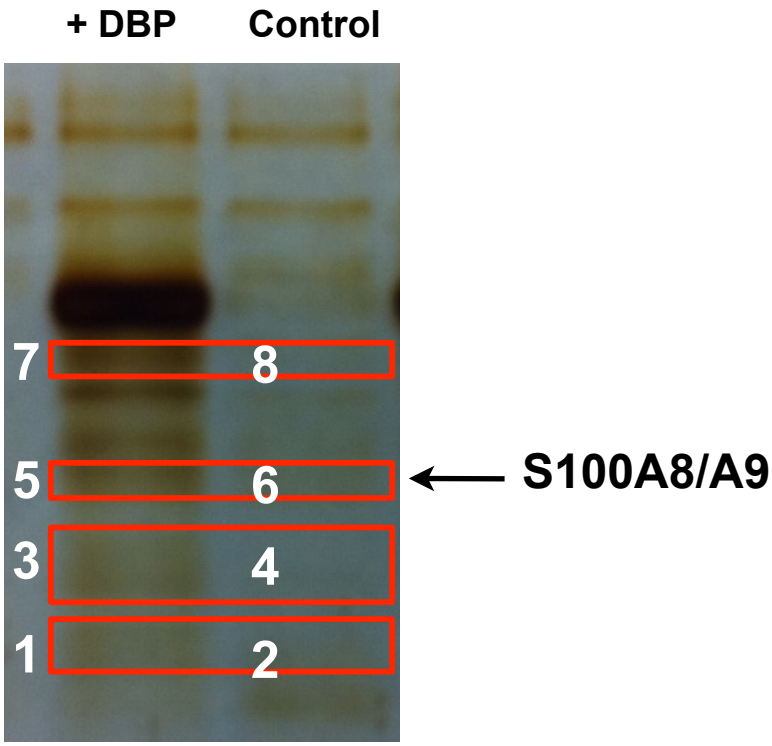

Figure 21 S100A8 and S100A9 are secreted from neutrophils treated with DBP as determined by mass spectrometric analysis of neutrophil conditioned supernatants.

Neutrophils were purified from whole blood and resuspended in HBSS. The cells were treated with 1 μM DBP or PBS as a control for 30 minutes at 37 °C and 5% CO_2. The cells were then spun down at 4 °C and the conditioned supernatants were loaded into an SDS-PAGE gel and subsequently silver stained. Four bands that had a higher intensity in the DBP treated supernatants (left lane) as compared to the control treated supernatants (right lane) were cut out, and their protein contents were identified by mass spectrometry.

Table 1

protein	coverage	Band 1	Band 2	Band 3	Band 4	Band 5	Band 6	Band 7	Band 8
sp|P02774|VTDB_HUMAN Vitamin D-binding protein GC	44.10%	12		26		31		26	
sp|P60709|ACTB_HUMAN Actin, cytoplasmic 1 ACTB	42.70%	8	3	11	13	6	5		
17PM_#3_ALBU_BOVIN	42.80%			51	1				
17PM_#11_CAS1_BOVIN	22.40%			9	3	2	4		
sp|P05109|S10A8_HUMAN Protein S100-A8 S100A8	32.30%					6	6		
sp|P05164|PERM_HUMAN Myeloperoxidase MPO	7.90%					6	6		
sp|P06702|S10A9_HUMAN Protein S100-A9 S100A9	56.10%					5	6		
sp|P12429|ANXA3_HUMAN Annexin A3 ANXA3	24.10%			3	8				
17PM_#11_CAS2_BOVIN	13.10%			5	3				
sp|P02788|TRFL_HUMAN Lactotransferrin LTF	7.20%			2					
sp|P04075|ALDOA_HUMAN Fructose-bisphosphate aldolase A ALDOA	6.30%					4	3		
sp|Q5D862|FILA2_HUMAN Filaggrin-2 FLG2	2.80%				7				
sp|P20930|FILA_HUMAN Filaggrin FLG	1.40%				6				
sp|P02765|FETUA_HUMAN Alpha-2-HS-glycoprotein AHSG	3.50%			4					
sp|P20160|CAP7_HUMAN Azurocidin AZU1	8.00%	2	2						
sp|P30740|ILEU_HUMAN Leukocyte elastase inhibitor SERPINB1	7.90%					1	3		
17PM_#12_CASB_BOVIN	8.50%			3					
sp|P00338|LDHA_HUMAN L-lactate dehydrogenase A chain LDHA	5.70%			1	2				
17PM_#6_TRFE_BOVIN	2.60%			2					
sp|P04083|ANXA1_HUMAN Annexin A1 ANXA1	6.90%			2					

Table 1 Neutrophil proteins identified in DBP treated neutrophil conditioned supernatants by mass spectrometry.

4.1.b. DBP induces the formation of S100A8/A9 heterodimers/heterotetramers in human neutrophils.

S100A8 and S100A9 are abundant cytosolic proteins that are predominantly expressed as a heterodimers, S100A8/A9, in neutrophils. There is some evidence showing that S100A8 and S100A9 can form homodimers, with a significantly reduced half-life as compared to the heterodimers. Upon cytosolic calcium elevation, the two heterodimers bind to each other forming a heterotetramer. To determine the role of DBP in the formation of cytosolic S100A8/A9 heterodimers and/or heterotetramers, purified human neutrophils were treated with DBP for 30 minutes at 37 ºC. The cells were then spun down, fixed, permabilized and stained with a monoclonal antibody, 27E10, which recognizes a neo-epitope found only in the heterodimer and the heterotetramer, but not homodimers or monomers [203]. As shown in figure 22, neutrophil treatment with DBP induced the formation of S100A8/A9 heterodimers and/or heterotetramers, as evident by the doubling in the percentage of cells which were positive for S100A8/A9 (figure 22, compare the right panel to the left panel) and by an average 2 fold increase in the mean fluorescence intensity in the DBP treated samples (data not shown). Non-permabilized neutrophils were negative for S100A8/A9, suggesting that the observed induction of S100A8/A9 heterodimers and/or heterotetramers was intracellular (data not shown). This suggests that DBP might induce the formation of S100A8/A9 heterodimers and/or heterotetramers in human neutrophils.

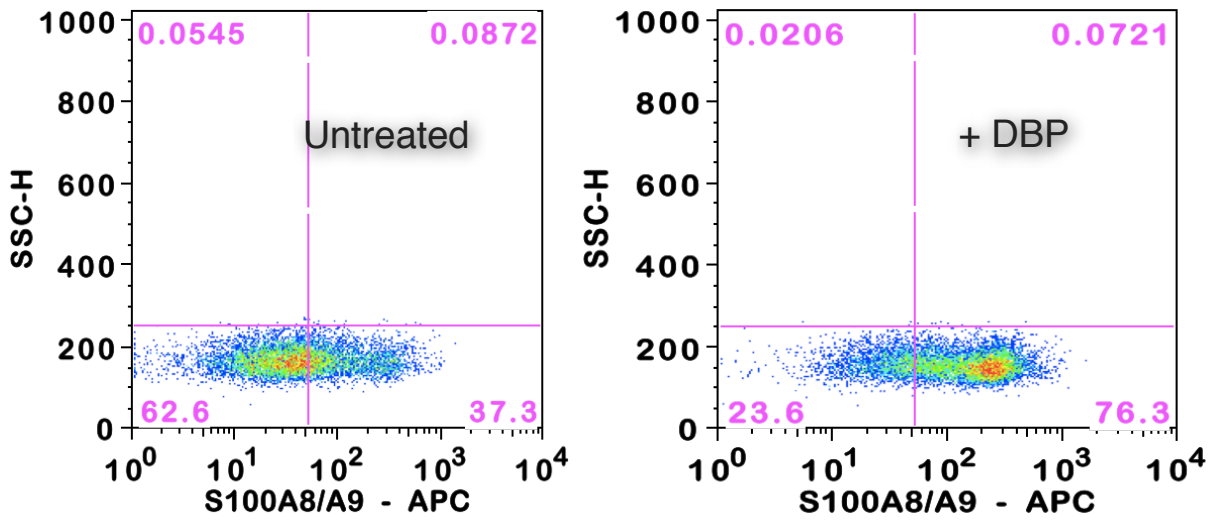

Figure 22 DBP induces the formation of S100A8/A9 heterodimers/heterotetramers in human neutrophils.

Neutrophils were purified from whole blood and resuspended in HBSS. The cells were treated with 1 µM DBP or DPBS as a control (untreated) for 30 minutes at 37 ºC and 5% CO2. The cells were then spun down at 4 ºC, the supernatant was transferred into another microfuge tube and the cells were fixed in 2% paraformaldehyde for 30 minutes at 4 ºC. The cells were permabilized using 1x perm/wash buffer (BD biosciences) and stained with mouse anti human S100A8/A9 monoclonal antibody (27E10, Hycult biotech) followed by APC conjugated goat anti mouse IgG (Biolegend). Flow cytometric data were collected using a BD FACS calibur II and the data were analyzed using FlowJo (tree stars Inc.). Shown above is a representative of the side scatter versus S100A8/A9 staining dot blot of sham treated and DBP treated cells. This experiment was performed 5 times in neutrophils obtained from one donor.

4.1.c. DBP-actin complexes are generated by DBP treated neutrophils and subsequently induce the release of S100A8/A9.

S100A8/A9 is considered to be a DAMP once secreted [207], with many pleotropic functions in neutrophils. DBP induces the formation of S100A8/A9 heterodimer and/or heterotetramer in neutrophils (figure 22), and its secretion (figure 21 and table 1). Previously, it has been shown that the binding of DBP and subsequent shedding is required for its chemotactic cofactor function, a process that is dependent on the degranulation of neutrophils [117,118,208]. We therefore hypothesized that the shedding of DBP is required for its chemotactic cofactor function because DBP might complex with neutrophil protein(s), and this complex is the active chemotactic cofactor. To test this hypothesis, cells were treated with DBP for 30 minutes at 37 ºC. As a control, cells were treated with C5a, a combination of DBP and C5a or PBS as a negative control. After treatment, the cells were spun down and the conditioned supernatants were loaded onto a native gel, subjected to electrophoresis and blotted with anti-DBP. As shown in figure 23, DBP treated neutrophil supernatant, three DBP containing bands were observed. To identify the protein content in these bands, the native gel was re-run and silver stained, these three bands were cut out, trypsinized and subjected to mass spectrometric analysis. Mass spectrometric analysis revealed that, the bottom band contained DBP only; the middle band contained DBP, lactoferrin, NGAL and defensin; and the top band contained DBP, actin and albumin (figure 23).

DBP is a known G-actin binding protein. Previously, it has been shown that cell surface actin is a binding site for DBP in neutrophils and U937 cells; this interaction is needed for its chemotactic cofactor function (figure 28b and McVoy et al, manuscript in preparation). Mass spectrometric analysis shown in figure 23 suggests that, in addition to the binding of DBP to cell surface actin, DBP-actin complexes might be subsequently shed from DBP treated neutrophils.

Since actin is predominantly a cytosolic protein, which is only known to be released from necrotic cells, it was hypothesized that the generated DBP-actin complexes may be the inducers for S100A8/A9 release from neutrophils. Therefore, to determine whether DBP-actin complexes induce the release of S100A8/A9 from neutrophils, DBP-actin complexes were prepared *in vitro* with purified DBP and actin and were subsequently incubated with purified human neutrophils for 30 minutes at 37 ºC. After 30 minutes, neutrophils were spun down, the condition supernatants were loaded into a native gel, subjected to electrophoresis and blotted with anti S100A8/A9 monoclonal antibody (27E10). As shown in figure 24, DBP-actin complexes were potent inducers of the release of S100A8/A9 from neutrophils obtained from 4 different donors. This confirms our hypothesis, and suggests that DBP-actin complexes are generated basally from neutrophils and that these complexes subsequently induce the release of S100A8/A9 from neutrophils.

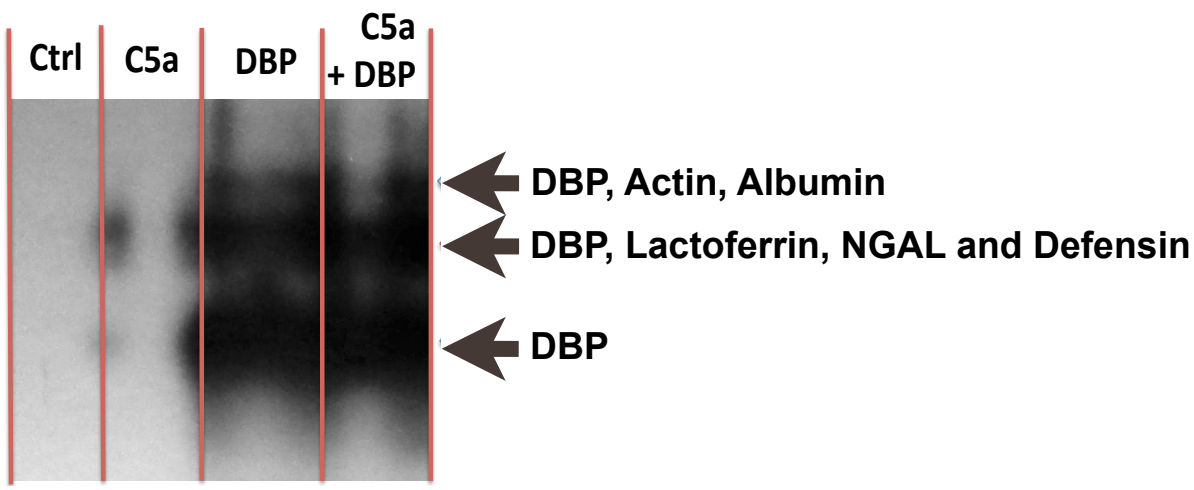

Figure 23 DBP-actin complexes are generated in conditioned supernatants of neutrophils treated with DBP.

Neutrophils were purified from whole blood and resuspended in HBSS. The cells were treated with 1 μM DBP, 400 pM C5a + 1 μM DBP, 400 pM C5a or PBS for 30 minutes at 37 ºC and 5% CO_2. After 30 minutes, the cells were spun down at 4 ºC and the conditioned supernatants were loaded into native gel, transferred to a PVDF membrane and a western blot was performed using chicken anti human DBP antibody (Gallus Immunotech). Three DBP containing bands were detected in the native gel western blot. To determine the identity of the proteins in these bands, the conditioned supernatants were loaded into a native gel, subjected to electrophoresis and silver stained. The bands were cut out and identified by mass spectrometry. The protein content of all the DBP containing bands is shown above.

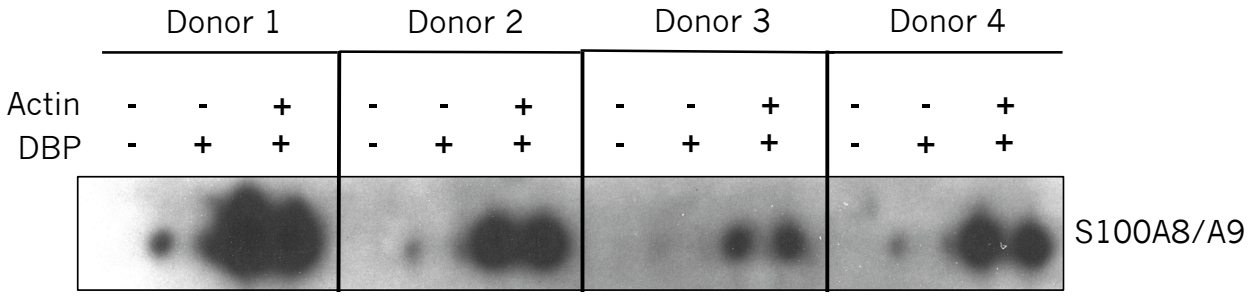

Figure 24 DBP-actin complexes are potent inducers of S100A8/A9 release from human neutrophils.

Neutrophils were purified from whole blood obtained from four donors and resuspended in HBSS. The cells were treated with 1 μM DBP, 1 μM DBP-actin complexes, or DPBS as a control (untreated) for 30 minutes at 37 ºC and 5% CO_2. The cells were then spun down at 4 ºC and the conditioned supernatants were loaded into native gel, transferred to a PVDF membrane and a western blot was performed using a mouse anti human S100A8/A9 monoclonal antibody (27E10, Hycult biotech) shown above.

4.1.d. DBP-actin complex generation and the release of S100A8/A9 by neutrophils are specific for DBP.

The C5a chemotactic cofactor function of DBP has been previously shown to be very specific *in vitro* [92]. To determine whether the generation of extracellular actin and the subsequent release of S100A8/A9 was specific to DBP, neutrophils were incubated for 30 minutes at 37 °C with two plasma proteins which are of a similar size and charge as DBP: histidine rich glycoprotein (HRGP) and α1 acid glycoprotein (α1AGP). In addition, HMGB1 BoxA mutant was used as an irrelevant protein control and DBP-actin complexes as the positive control. The cell free conditioned supernatants were collected, loaded into a native gel, subjected to electrophoresis and blotted with the monoclonal antibody 27B10 to detect S100A8/A9. After detecting S100A8/A9, the membrane was re-blotted with anti-actin to detect the generated DBP-actin complexes from neutrophils. As shown in figure 25, DBP induced the secretion of actin, presumably as DBP-actin complexes, and S100A8/A9 (figure 25, lane 2). DBP-actin complexes induced the secretion of a higher amount of S100A8/A9 as compared to what was observed to be induced by DBP, confirming our previous results (figure 25, lane 3). However, HRGP, α1AGP and HMGB1 boxA mutant did not induce the secretion of actin or S100A8/A9 (figure 25, lanes 4-6 respectively) suggesting that the secretion of actin and S100A8/A9 by neutrophils is specific for DBP.

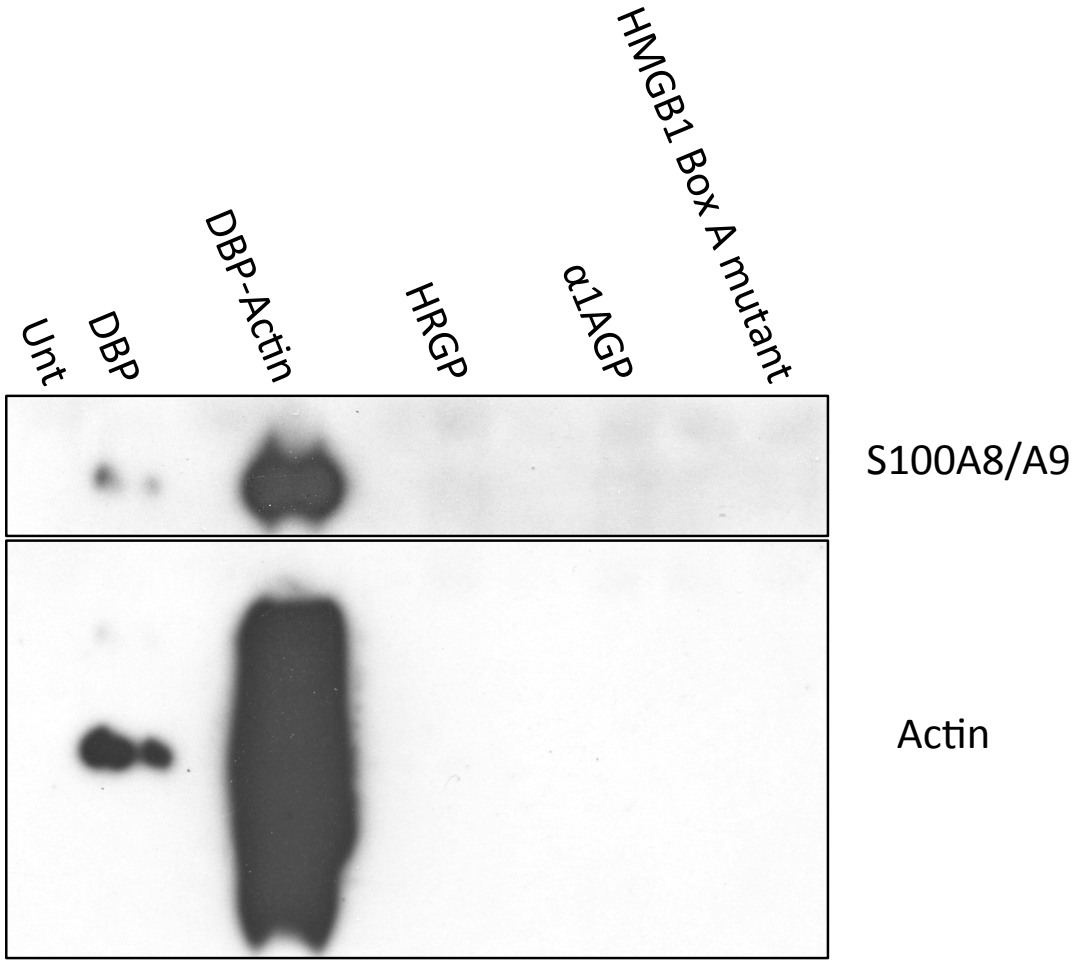

Figure 25 Specificity of actin and S100A8/A9 release from human neutrophils.

Neutrophils were purified from whole blood and resuspended in HBSS. The cells were treated with 1 μM DBP, DBP-actin complexes, HRGP, α1AGP, HMGB1 BoxA mutant or DPBS (Untreated) for 30 minutes at 37 ºC and 5% CO_2. The cells were then spun down at 4 ºC and the conditioned supernatants were loaded into native gel, transferred to a PVDF membrane and a western blot was performed using a mouse anti human S100A8/A9 monoclonal antibody (27E10, Hycult Biotech), shown at the top panel. The blot was then re-blotted with mouse anti actin antibody (Fisher Scientific), shown at the bottom panel.

4.1.e. DBP-actin complexes were detected in vivo in the BALF of DBP +/+ mice after the induction of alveolitis by C5a.

All of the previous experiments were performed *in vitro,* and thus the *in vivo* relevance for the generation of DBP-actin complexes by inflammatory cells is not known. Therefore, to determine whether DBP-actin complexes are generated in an inflammatory setting, BALF was collected from DBP +/+ and DBP -/- mice 4 hours after instillation of purified C5a, spun down and the cell free BALF was loaded into a native gel, subjected to electrophoresis and blotted with a polyclonal anti-DBP antibody. As a control for the migration of uncomplexed DBP, sera from DBP +/+ and DBP -/- mice were loaded and blotted for DBP. As expected, DBP was only detected in the BALF and serum of DBP +/+ mice. Unexpectedly, most of the DBP in the BALF was complexed with another protein, as evident by the upward shift in the DBP band, as compared to the normal mouse serum control (figure 26). This upward shift is very similar to the shift observed when purified DBP-actin complexes, prepared *in vitro,* or DBP +/+ serum spiked with actin are blotted for DBP in a native gel. This suggests that DBP-actin complexes might be formed in large amounts during inflammation *in vivo*, and suggests that these complexes may then subsequently amplify inflammation by inducing the release of S100A8/A9 from neutrophils.

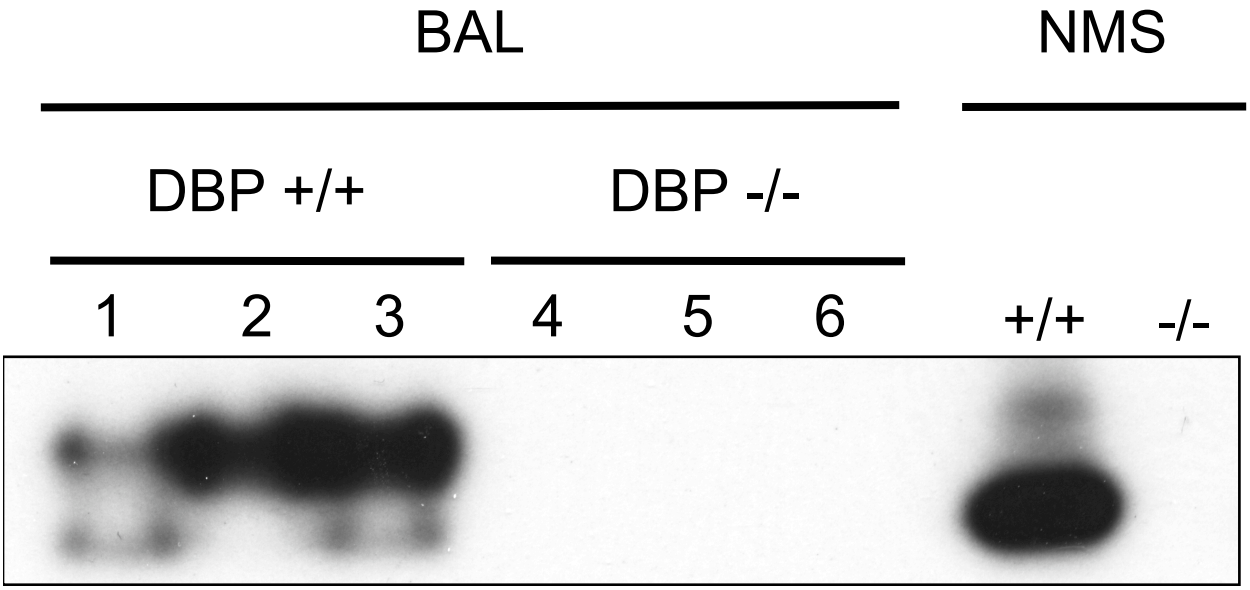

Figure 26 DBP-actin complexes are generated in an inflammatory model of alveolitis in vivo.

Three DBP +/+ (lanes 1-3) and DBP -/- (lanes 4-6) mice were instilled with 1 μg of C5a per 24 gram of mouse. After 4 hours, the mice were sacrificed and their lungs were lavaged with HBSS containing 5 mM EDTA. The BALF was spun down and the cell free supernatants were loaded into a native gel and subjected to electrophoresis. As a control for unbound DBP, normal mouse sera from one DBP +/+ and DBP -/- mouse were also loaded into the native gel. The gel was transferred to a PVDF membrane and blotted with chicken anti human DBP, shown above.

4.1.f. DBP binds to migrating neutrophils, a process which might be partially dependent on the surface expression of actin during migration.

As previously mentioned, DBP is a chemotactic cofactor for the chemotaxis of neutrophils to C5a, a function which requires the cell surface binding and subsequent shedding of DBP by neutrophils. However, all of the previous experiments to analyze binding and shedding of DBP by neutrophils were performed in suspension and not with migrating or adherent cells. The binding and localization of DBP on a polarized migrating neutrophil is not known. Therefore, to answer this question, the under agarose chemotaxis assay was utilized. Purified human neutrophils were loaded on collagen coated coverslips in an under agarose plate and allowed to migrate to C5a or formylated peptides in the presence or absence of DBP for 3.25 hours at 37 ºC. The cells were then fixed, the agarose was discarded and the coverslips were stained with a polyclonal anti DBP antibody followed with alexa flour 488-conjugated secondary antibody. The coverslips were then mounted onto a microscope slide and fluorescent pictures were taken at 200x magnification using a fluorescent microscope. As shown in figure 27a, migrating neutrophils were strongly positively for DBP only when DBP was exogenously added. We also noticed that when DBP-actin complexes were added to migrating neutrophils, the intensity of DBP on migrating neutrophils decreased (figure 27a, compare the fluorescence intensity of DBP on cells migrating with DBP and DBP-actin). The average fluorescence intensity of 250 or more cells indicated that there was an approximate 50% reduction in the average fluorescence intensity of DBP on cells migrating in the presence of DBP-actin complexes as compared to cells migrating in the presence of DBP (figure 27b). This suggests that the actin-binding site on DBP might contribute to the binding of DBP to migrating neutrophils, and that cell surface actin may be the docking site for DBP on migrating neutrophils.

To determine the presence of cell surface actin on migrating neutrophils, neutrophils were allowed to migrate under agarose as previously described, then fixed, stained with anti-actin followed by an alexa flour 488 conjugated secondary antibody and the cover slips were mounted on microscope slides. Fluorescent pictures were then taken at 1000x magnification using a fluorescent microscope. Cells migrating to C5a in the absence of DBP were positive for cell surface actin suggesting that migrating neutrophils do express cell surface actin (figure 28a, top row). However, when cells were migrating in the presence of DBP, there was a substantial decrease in the cell surface actin staining on migrating neutrophils (figure 28a, middle row). This suggests that the binding of DBP to migrating neutrophils may have either masked the actin epitope from detection by the anti actin antibody or that DBP might have induced the shedding of cell surface actin from migrating neutrophils.

DBP has been previously shown to bind to the human lymphoma cell line U937 cells transfected with the C5aR (CD88) [122,127,128]. DBP also has been shown to augment the chemotaxis to C5a in these cells . Therefore, to study the requirement of cell surface binding of DBP to leukocytes, surface plasmon resonance (SPR) chips were coated with DBP, and the binding of U937 cells was measured by Biacore SPR in the presence or absence of blocking antibodies. Untreated cells bound to the immobilized DBP as previously described (figure 28b, red line). However, when cells were treated with an anti-actin antibody, there was a large reduction in the binding of U937 cells to immobilized DBP (figure 28b, black line). This reduction was specific to the anti-actin antibody as the binding of non-immune IgG treated U937 cells to DBP was similar to untreated cells (figure 28b, compare red line to the blue line). This indicates that cell surface actin mediates the binding of DBP to U937 cells, and cell surface actin may contribute to DBP binding on migrating neutrophils.

(A) DBP binds to migrating neutrophils

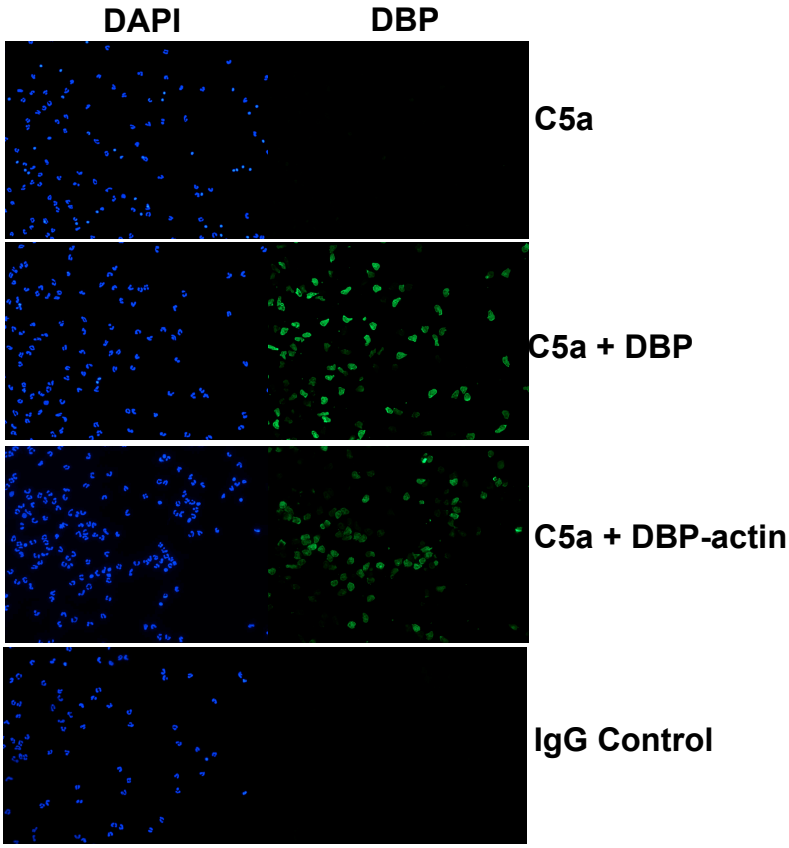

(B) DBP fluoresence intensity

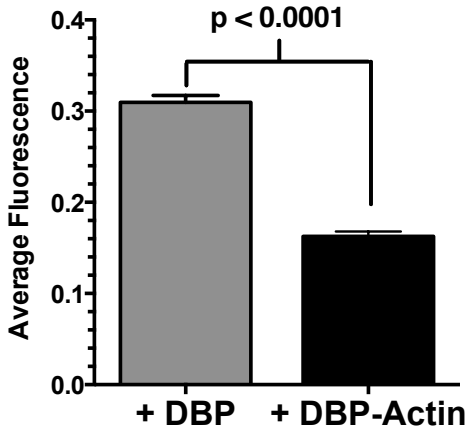

Figure 27 DBP binds to migrating human neutrophils.

Neutrophils were purified from whole blood and resuspended in HBSS at a concentration of 20 million cells per ml. 0.5 million cells were loaded into a collagen coated coverslip in an under agarose chemotaxis plate, and the cells were allowed to migrate to 1 nM C5a, 1 nM C5a + 1 μM DBP or 1 nM C5a + 1 μM DBP-actin for 3.25 hours at 37 ºC. As a control, the cells were allowed to migrate to HBSS, 1 μM DBP or 1 μM DBP-actin. After 3.25 hours, the cells were fixed in 2% paraformaldehyde overnight. The agarose was then discarded and the coverslips were stained with chicken anti human DBP (Gallus Immunotech) followed by alexa flour 488-conjugated goat anti chicken antibody (Life Technologies). As a control, the cells were stained with non-immune chicken IgG followed by alexa flour 488-conjugated goat anti chicken antibody. The coverslips were then mounted and analyzed using a Nikon Ti fluorescent microscope at 200x magnification, shown above. To quantify the average fluorescence of DBP staining, 250 or more cells were individually highlighted and the average fluorescence was determined using Macnification (Interface Design Software). Part A was repeated twice and the quantitation shown in part B was done by calculating the average DBP fluorescence on 252 migrating cells or more from one of the two experiments.

A

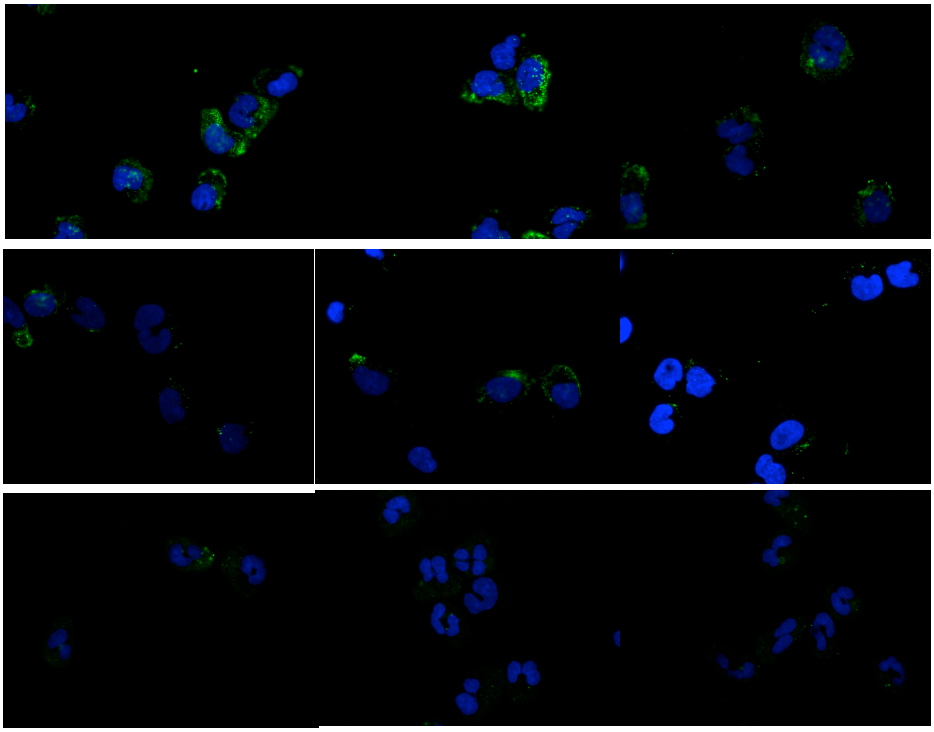
C5a
C5a + DBP
IgG Control

B

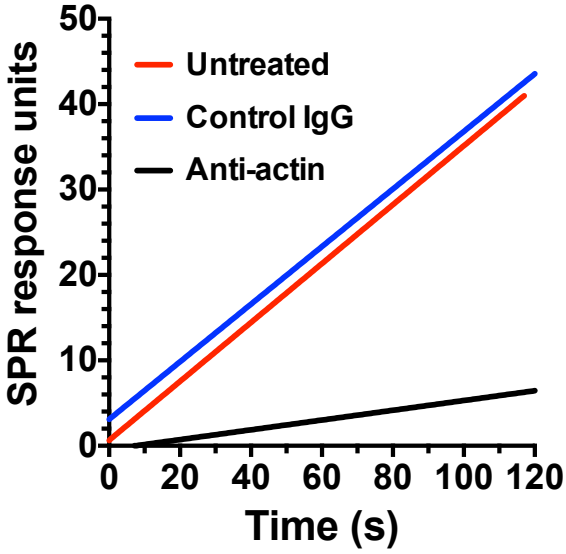
SPR response units
50
40
30
20
10
0
Untreated
Control IgG
Anti-actin
0
20
40
60
80
100
120
Time (s)

Figure 28 Migrating neutrophils express cell surface actin. DBP binds to cell surface actin on U937 cells.

A) Actin is expressed on the cell surface of migrating neutrophils. Neutrophils were purified from whole blood and resuspended in HBSS at a concentration of 20 million cells per ml. 0.5 million cells were loaded into a collagen coated coverslip in an under agarose chemotaxis plate, and the cells were allowed to migrate to 1 nM C5a or 1 nM C5a + 1 μM DBP for 3.25 hours at 37 ºC. As a control, the cells were allowed to migrate to HBSS, or 1 μM DBP. After 3.25 hours, the cells were fixed in 2% paraformaldehyde overnight. The agarose was then discarded and the coverslips were stained with mouse anti actin monoclonal antibody (Fisher Scientific) followed by alexa flour 488-conjugated donkey anti mouse antibody (Life Technologies). As a control, the cells were stained with non-immune mouse IgG followed by alexa flour 488-conjugated donkey anti mouse antibody. The coverslips were then mounted on a microscope slide and analyzed using a Nikon Ti fluorescent microscope at 1000x magnification, shown above. **B)** DBP binds to cell surface actin on U937 cells as assessed by Biacore surface plasmon resonance. DBP was coupled to a biacore CM5 sensor ship using N-ethyl-N-(dimethylaminopropyl) carbodiimide/N-hydroxysuccinimide (EDC/NHS). As a control, a flow cell was activated in the absence of any protein and subsequently deactivated. Undifferentiated U937 cells were pretreated with rabbit anti-actin polyclonal antibody (Sigma), rabbit IgG or buffer (untreated) for 30 minutes at 37 ºC. The cells were then spun down and re-suspended in HBSS prior to injection into the DBP coated and the control biacore cells at a flow rate of 5 μl/minute. The binding curve was generated using BiaEvaluation software (GE Healthcare) and graphed using Prism (GraphPad Software). Shown above is a representative of two experiments.

4.1.g. S100A8/A9 binds to migrating neutrophils and colocalizes with DBP on protrusions extending out of migrating neutrophils.

The previous results have showed that DBP binds to the surface of migrating neutrophils, and that DBP-actin complexes are shed from neutrophils. After shedding of the DBP-actin complexes, these complexes can then induce the secretion of S100A8/A9 from neutrophils as shown in figures 24 & 25. However, the binding of the secreted S100A8/A9 on migrating neutrophils and its localization is not known. Therefore, the under agarose chemotaxis assay was utilized to determine the capacity of migrating neutrophils to bind to S100A8/A9, and the location of the bound S100A8/A9 on polarized neutrophils relative to DBP. Neutrophils were allowed to migrate under agarose as previously described, fixed and stained with anti DBP and anti S100A8/A9 (27E10) antibodies followed by an alexa flour 488 conjugated (DBP) and alexa flour 594 conjugated (S100A8/A9) secondary antibodies. The cover slips were then mounted on microscope slides and fluorescent pictures were acquired at 200x magnification using a fluorescent microscope. All migrating neutrophils stained positively for S100A8/A9 (figure 29, red color in the first three panels from the top). When DBP was exogenously added, DBP and S100A8/A9 colocalized on 50-70% of the migrating neutrophils (figure 29, two middle panels).

To identify the regions on migrating neutrophils where DBP and S100A8/A9 localize, neutrophils were allowed to migrate to formylated peptides, fixed and stained anti DBP and anti S100A8/A9 (27E10). As previously shown, DBP induces the formation of S100A8/A9 in neutrophils (figure 22). Therefore, to determine the location of intracellular S100A8/A9 relative to the cell surface bound DBP; some samples were permabilized prior to staining with anti DBP and anti S100A8/A9 antibodies. After staining, the cells where mounted on to a microscope slide and analyzed using a fluorescent microscope at 1000x magnification. As shown in figure

30a, in both permabilized and non-permabilized, there was strong colocalization between DBP and S100A8/A9 on protrusions extending out of migrating neutrophils. Interestingly, all the cells stained with S100A8/A9, but there was a subset of cells that stained negatively for DBP. Protrusions extending out neutrophils were observed to be F-actin rich (figure 30b, arrows), and thus this suggests that DBP and/or S100A8/A9 might be capable of inducing the polymerization of actin and thus may affect neutrophil polarization or migration. Additionally, not all migrating neutrophils stained positively for DBP, suggesting that DBP might only affect a subset of migrating neutrophils.

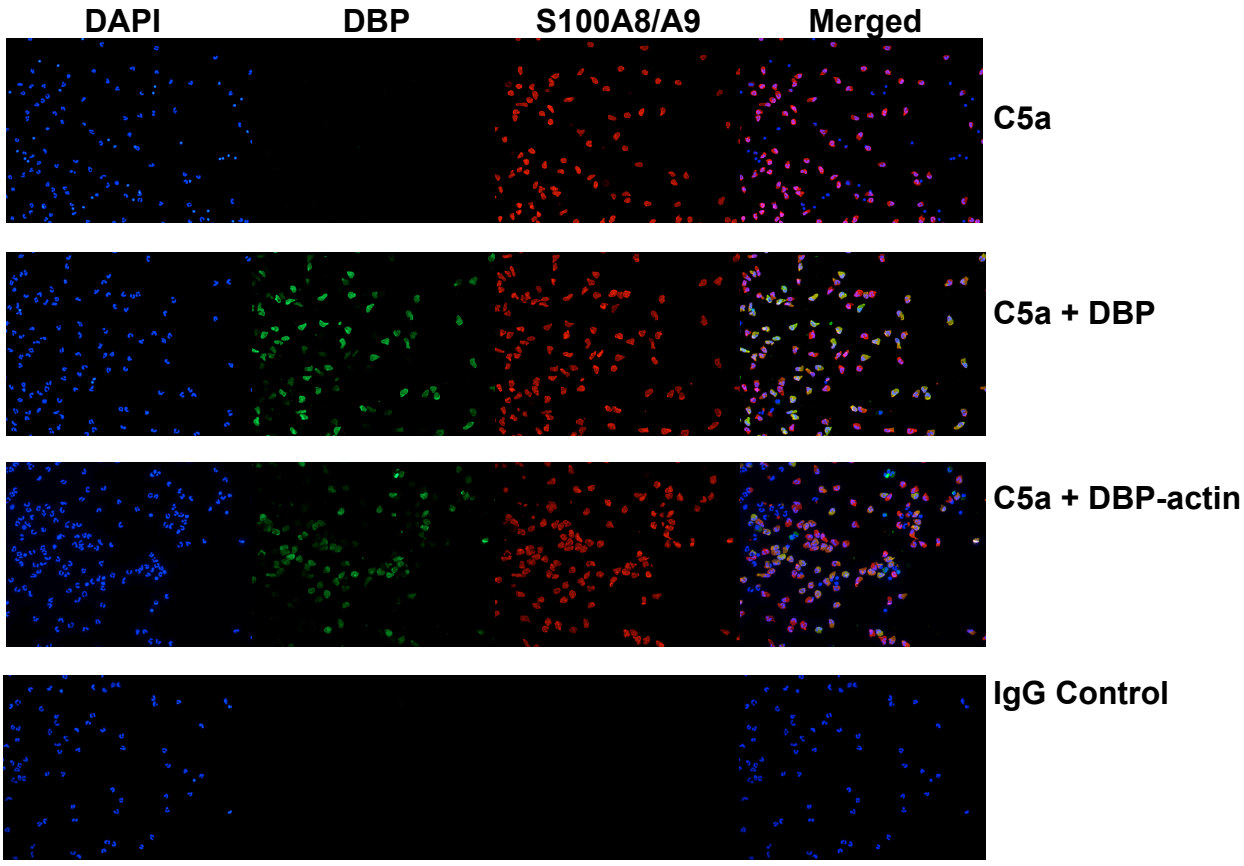
DAPI
DBP
S100A8/A9
Merged
C5a
C5a + DBP
C5a + DBP-actin
IgG Control

Figure 29 S100A8/A9 binds to and colocalizes with DBP on a subset of migrating neutrophils.

Neutrophils were purified from whole blood and resuspended in HBSS at a concentration of 20 million cells per ml. 0.5 million cells were loaded on a collagen coated coverslip in an under agarose chemotaxis plate, and the cells were allowed to migrate to 1 nM C5a, 1 nM C5a + 1 μM DBP or 1 nM C5a + 1 μM DBP-actin for 3.25 hours at 37 ºC. As a control, the cells were allowed to migrate to HBSS, 1 μM DBP or 1 μM DBP-actin. After 3.25 hours, the cells were fixed in 2% paraformaldehyde overnight. Then, the agarose was discarded and the coverslips were stained with chicken anti human DBP (Gallus Immunotech) and mouse anti human S100A8/A9 (27E10, Hycult Biotech) antibodies followed by alexa flour 488 conjugated goat anti chicken and alexa flour 594 conjugated donkey anti mouse antibodies (Life Technologies). As a control, the cells were stained with non-immune chicken and mouse IgG followed by alexa flour 488-conjugated goat anti chicken and alexa flour 594-conjugated donkey anti mouse antibodies. The coverslips were then mounted on a microscope slide and analyzed using a Nikon Ti fluorescent microscope at 200x magnification, shown above. The pictures taken above are representative from 3 separate experiments performed using neutrophils from 1 donor.

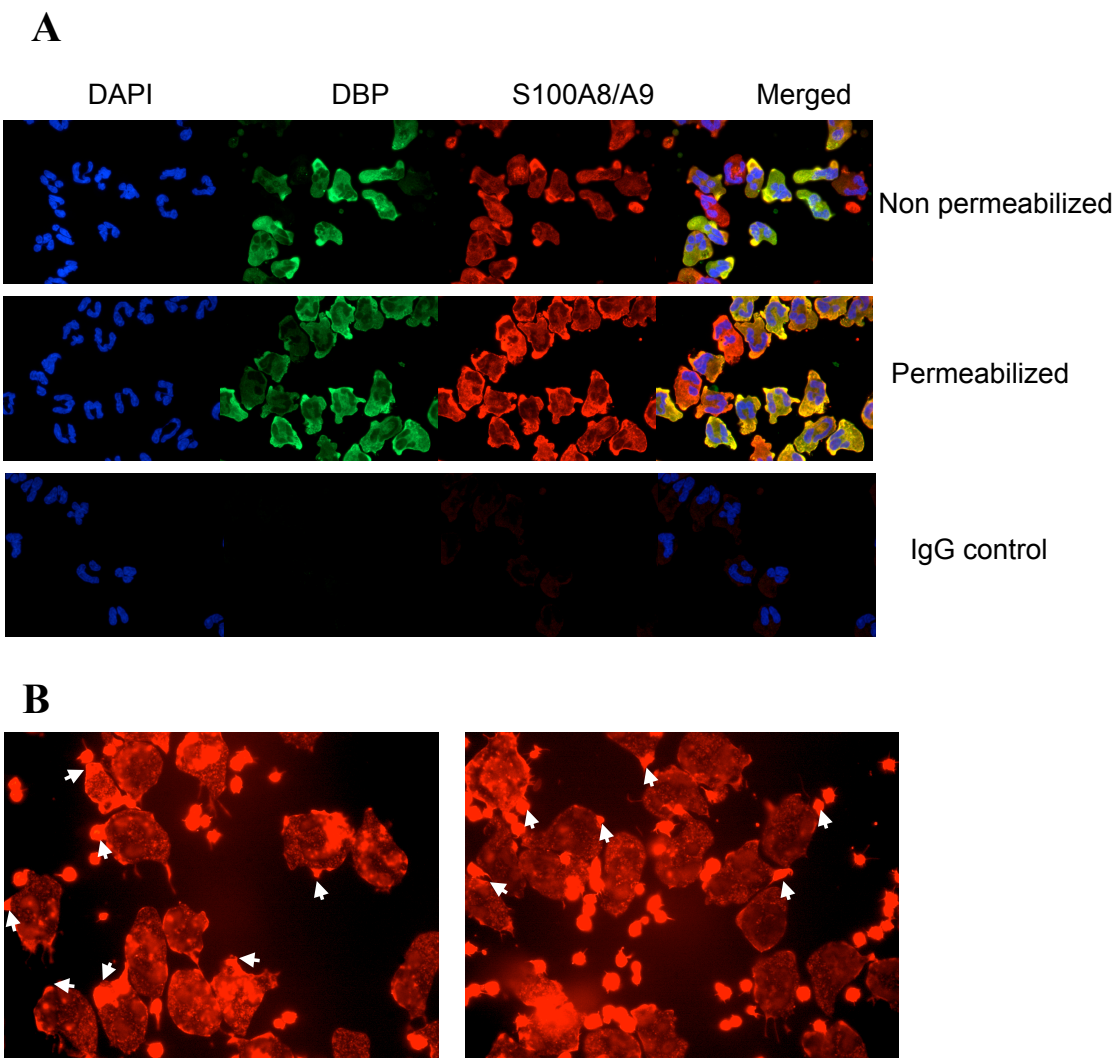

Figure 30 DBP and S100A8/A9 colocalize on protrusions extending out of migrating neutrophils.

Neutrophils were purified from whole blood and resuspended in HBSS at a concentration of 20 million cells per ml. 0.5 million cells were loaded on a collagen coated coverslip in an under agarose chemotaxis plate, and the cells were allowed to migrate to 10 nM fNLP + 1 µM DBP for 3.25 hours at 37 ºC. As a control, the cells were allowed to migrate to 1 µM DBP. After 3.25 hours, the cells were fixed in 2% paraformaldehyde overnight. Then, the agarose was discarded and the coverslips were stained with chicken anti human DBP (Gallus Immunotech) and mouse anti human S100A8/A9 (27E10, Hycult Biotech) antibodies followed by alexa flour 488

conjugated goat anti chicken and alexa flour 594 conjugated donkey anti mouse antibodies (Life Technologies) (A). As a control, the cells were stained with non-immune chicken and mouse IgG followed by alexa flour 488-conjugated goat anti chicken and alexa flour 594-conjugated donkey anti mouse antibodies. In panel B, the cells were permabilized and stained with alexa flour 594-conjugated Phalloidin. The coverslips were then mounted on a microscope slide and analyzed using a Nikon Ti fluorescent microscope at 1000x magnification, shown above.

4.2. DBP may be required for optimal neutrophil differentiation in the bone marrow.

The alveolitis results presented in chapter 1 indicate that DBP is required for the optimal recruitment of neutrophils into an inflammatory site *in vivo*. *Ex vivo* analysis of DBP -/- bone marrow neutrophils revealed reduced chemotaxis, superoxide anion generation and a decrease in the side scatter and the surface expression of CD88, CD44 and CD11b as compared to DBP +/+ bone marrow neutrophils. These results suggest that there might be an intrinsic defect in the bone marrow neutrophil pool of DBP -/- mice.

4.2.a. Culturing HL-60 cells with DMSO for 4-5 days induces the differentiation and surface expression of CD88.

To study neutrophil differentiation in the presence or absence of DBP, a promyelocytic cell line, HL-60 cells, was utilized. HL-60 cells have previously been reported to differentiate into myelocytes, metamyelocytes and banded neutrophils in response to DMSO treatment for 3 to 5 days. To confirm HL-60 differentiation into neutrophil like cells, HL-60 cells were treated with 1.3% (w/v) DMSO, and starting from day 0 (D0, the day of the treatment), cells were removed from the culture dish and stained with PE conjugated anti CD88 (C5aR), a differentiation marker which was previously shown to be expressed only by differentiated HL-60 cells [209], and analyzed by flow cytometry. As a control for background staining, cells were stained with a PE conjugated isotype control antibody. As shown in figure 31a, starting from day 2 after the addition of DMSO, there were two major populations of HL-60 cells, a large population with low side scatter, and a small population with high side scatter. The small population increased progressively until day 4, were it was the major population. Cellular survival analysis by

annexin V and PI staining indicated that the small population was composed of dead cells (both apoptotic and necrotic) and the large population to be composed of live cells (data not shown). Therefore, for all subsequent experiments, the live population was gated and analyzed for the surface expression of several markers such as CD88 and CD44. Undifferentiated HL-60 cells (day 0) were negative for cell surface CD88 and remained negative after the addition of DMSO until day 3 (figure 31c). Peak cell surface expression of CD88 was observed at days 4 and 5 after the addition of DMSO (figure 31c). The isotype control antibody stained cells were negative for PE fluorescence (figure 31b) suggesting that the CD88 staining observed on differentiated HL-60 cells was specific. Due to the strong induction of CD88 expression on the surface of differentiated HL-60 cells at day 5, these cells were used for all subsequent experiments.

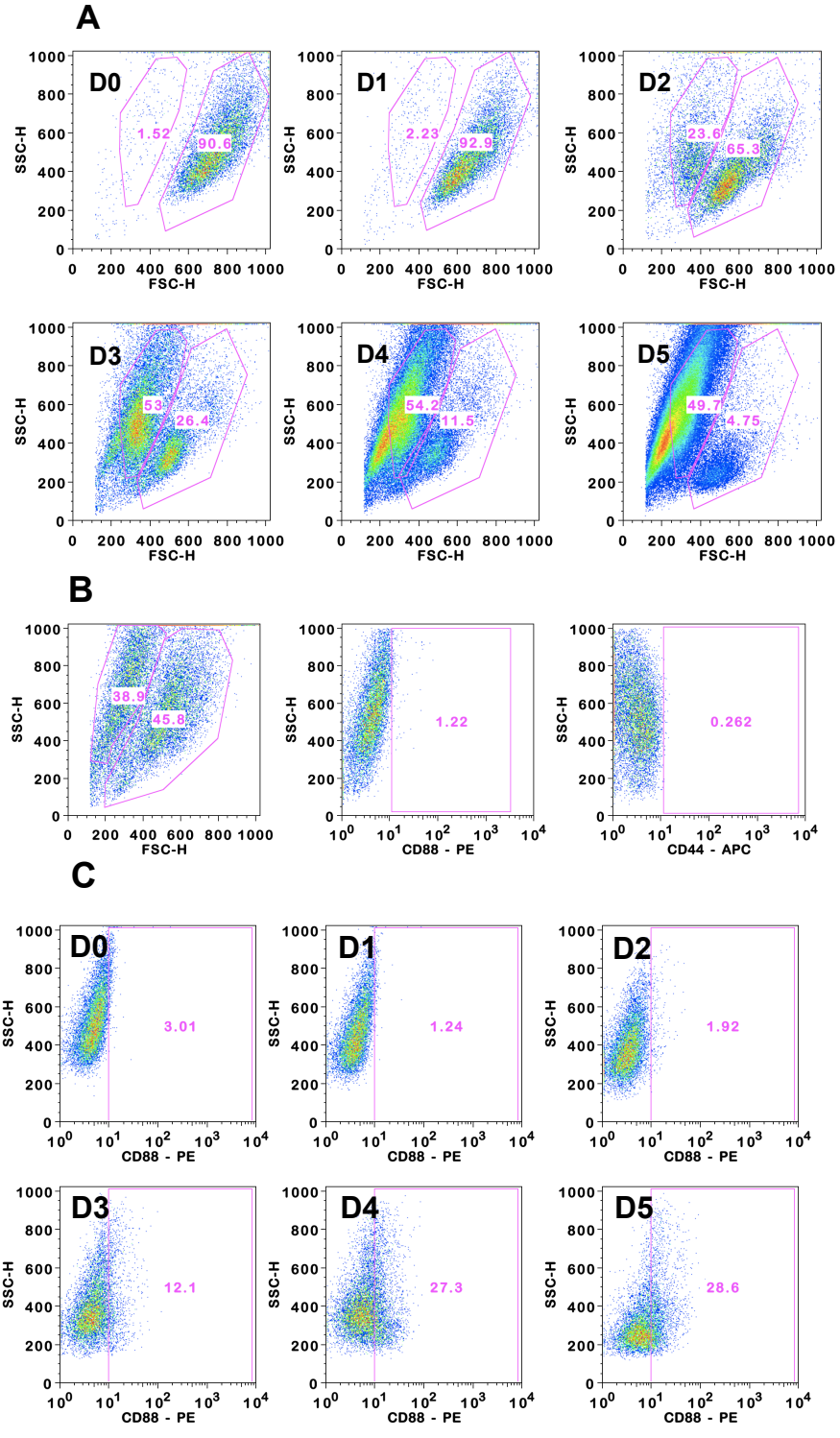
A
D0
1.52
90.6
D1
2.23
92.9
D2
23.6
65.3
D3
53
26.4
D4
54.2
11.5
D5
49.7
4.75
SSC-H
FSC-H
B
38.9
45.8
1.22
0.262
CD88 - PE
CD44 - APC
C
3.01
1.24
1.92
12.1
27.3
28.6

Figure 31 DMSO differentiation of HL-60 cells.

Two million HL-60 cells were differentiated with 1.3% DMSO in RPMI 1640 + 5% FBS for 5 days at 37 ºC and 5% CO_2. Every day, starting from the day DMSO was added to the cells (Day 0) and ending on the fifth day, cells were removed from the culture dish and stained with alexa flour 594-conjugated mouse anti human CD88 (Biolegend) or alexa flour 594-conjugated non-immune mouse IgG. Flow cytometric data were acquired using a BD FACS Calibur II flow cytometer. The data was then analyzed using FlowJo. Panel A shows a dot plot of the forward and side scatter of HL-60 cells undergoing differentiation from day 0 to day 5. Panel B shows a dot plot of the side scatter and the CD88 fluorescence staining of the isotype control stained cells. Panel C shows a dot plot of the side scatter and the percentage of cells that stained positive for CD88 from day 0 to day 5.

4.2.b. Bovine DBP in FBS is not functional.

To study the role of DBP in the differentiation of HL-60 cells, cells must be grown and differentiated in medium containing no or non-functional DBP. DBP binds to 25 OH D_3 (5×10^{-8} M) with a higher affinity than to 1, 25 $(OH)_2$ D_3 (4×10^{-7} M). Therefore, the binding of DBP to 25 OH D_3 was utilized to determine the functionality of bovine DBP in FBS. HL-60 cells have been previously shown to differentiate upon exposure to as little as 5 nM of 1, 25 $(OH)_2$ D_3 . However, their response to 25 OH D_3, the more stable vitamin D metabolite, is not known. Preliminary experiments using 1 μM 25 OH D_3 indicated that this vitamin D metabolite can also induce the surface expression of CD88 on HL-60 cells (data not shown). Therefore, to determine the functionality of bovine DBP in FBS, HL-60 cells were differentiated with 1 μM 25 OH D_3, in the presence or absence of exogenously added DBP for 5 days at 37 ºC. After 5 days, the cells were stained with PE conjugated anti CD88 and APC conjugated anti CD44 antibodies and analyzed by flow cytometry. As a control, untreated cells incubated for 5 days at 37 ºC, were stained and analyzed by flow cytometry as previously described. As shown in figure 32, only a few untreated HL-60 cells expressed cell surface CD88. 25 OH D_3 induced the expression cell surface CD88 on HL-60 cells (figure 32, top row, middle dot plot). 25 OH D_3 treated HL-60 cells also acquired the ability to migrate to purified C5a on collagen coated coverslips in an under agarose chemotaxis assay (data not shown). However, when HL-60 cells were incubated with DBP and 25 OH D_3, the percentage of cells which stained positively for CD88 was similar to the percentage observed in untreated cells (figure 32, compare the right panel to the left panel). The isotype control antibody stained cells were negative for PE and APC fluorescence (figure 31b) suggesting that the CD88 and CD44 staining observed on HL-60 cells was specific.

This suggests that by binding and sequestering 25 OH D_3, exogenously added DBP was capable of blocking its differentiation inducing function. This also suggests that bovine DBP in FBS used in the culture medium was not functional because it failed to bind to, sequester and block the induction of HL-60 cellular differentiation by 25 OH D_3. Therefore, one can utilize DMSO differentiation of HL-60 cells in the presence or absence of exogenously added DBP as a model for studying the role of DBP in neutrophil differentiation in the bone marrow.

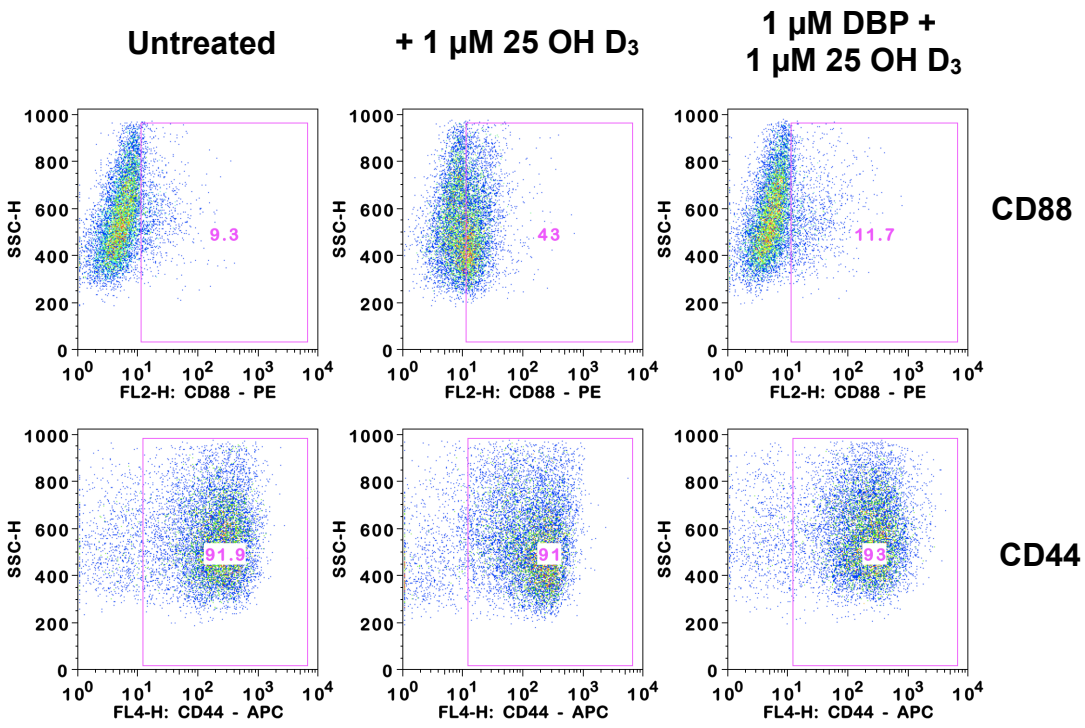

Figure 32 Bovine DBP is not functional.

Shown above is the percentage of cells that stained positively for CD88 and CD44 after 5 days of culture with DBP or 25 OH D_3 (Vitamin D). Two million HL-60 cells were plated in RPMI 1640 + 5% FBS in the presence of 1 µM DBP, 25-OH D_3 or DBP + 25 OH D_3 for 5 days at 37 ºC and 5% CO_2. After 5 days the cells were stained with alexa flour 594-conjugated mouse anti human CD88 and alexa flour 647-conjugated mouse anti human CD44 (Biolegend). As a control, cells were stained with alexa flour 594 and 647-conjugated mouse IgG. Flow cytometric data were acquired using a BD FACS calibur II flow cytometer and the data were analyzed using FlowJo (Tree Stars Inc.). The CD88 and CD44 positive gates were determined using the isotype control samples, which were negative for both fluorescent signals (figure 31b).

4.2.c. Differentiated HL-60 cells in the presence of DBP, DBP-actin complexes and LPS had higher surface expression of CD88 and CD44 as compared to untreated differentiated cells.

As previously shown, bone marrow neutrophils from DBP -/- mice might have an intrinsic migratory defect. In addition, human neutrophils treated with DBP for 30 minutes generated DBP-actin complexes, which then subsequently induced the release of S100A8/A9. This suggests that DBP-actin complexes might be basally generated from neutrophils and that these complexes can induce the basal release of S100A8/A9. Therefore, in addition to the lack of DBP in the DBP -/- mouse, one would hypothesize that there will be no basally generated DBP-actin complexes and a reduced basal level of S100A8/A9. Thus, the intrinsic defect observed in the bone marrow neutrophils of DBP -/- mice might be due to the lack of DBP-actin complexes and reduced levels of exogenous S100A8/A9. To determine the role of DBP and DBP-actin in neutrophil differentiation, HL-60 cells were differentiated for 5 days at 37 ºC with DBP, DBP-actin complexes or 100 ng/ml LPS, a positive control and the prototypic TLR4 agonist. As a negative control, undifferentiated and untreated DMSO differentiated HL-60 cells were incubated at 37 ºC for 5 days. The cells were then stained with PE conjugated anti CD88 and APC conjugated anti CD44 antibodies and analyzed by flow cytometry. Differentiating HL-60 cells with DMSO for 5 days induced a significant increase in the percentage of cells expressing cell surface CD88 and in the mean fluorescence intensity of CD88 staining (figure 33a and 33b). The percentage of CD88 positive cells and the mean fluorescence intensity of CD88 staining increased gradually with the differentiation of HL-60 cells in the presence of DBP and DBP-actin complexes as compared untreated differentiated HL-60 cells (figure 33a and 33b). The percentage of CD88 positive cells was also increased when HL-60 cells were differentiated in the

presence of LPS (figure 33a) but the mean fluorescence intensity was similar to the mean fluorescence intensity observed in untreated differentiated HL-60 cells.

Differentiation of HL-60 cells with DMSO induced a slight decrease of CD44 expression in a sub population of cells (figure 33a and 33c). However, when HL-60 cells were differentiated in the presence of DBP, DBP-actin or LPS, there was a significant increase in the mean fluorescence intensity staining for CD44 as compared to undifferentiated and untreated differentiated HL-60 cells (figure 33c). Furthermore, DBP, DBP-actin complexes and LPS treatment induced an increase in the side scatter of the differentiated cells as compared to the side scatter of untreated differentiated HL-60 cells (figure 33a and 33d). A similar differentiation phenotype was also observed when HL-60 cells were differentiated in the presence of 10 ng/ml LPS (data not shown). These data suggests that exogenous DBP and DBP-actin complexes can alter the differentiation of HL-60 cells by inducing higher cell surface CD88 and CD44 expression and by increasing cellular granularity (as evident by the increase in side scatter). However, the same phenotype was also observed when cells were differentiated in the presence of LPS, suggesting that the phenotype observed in the presence of DBP and DBP-actin complexes might be due to endotoxin contamination in our DBP stock.

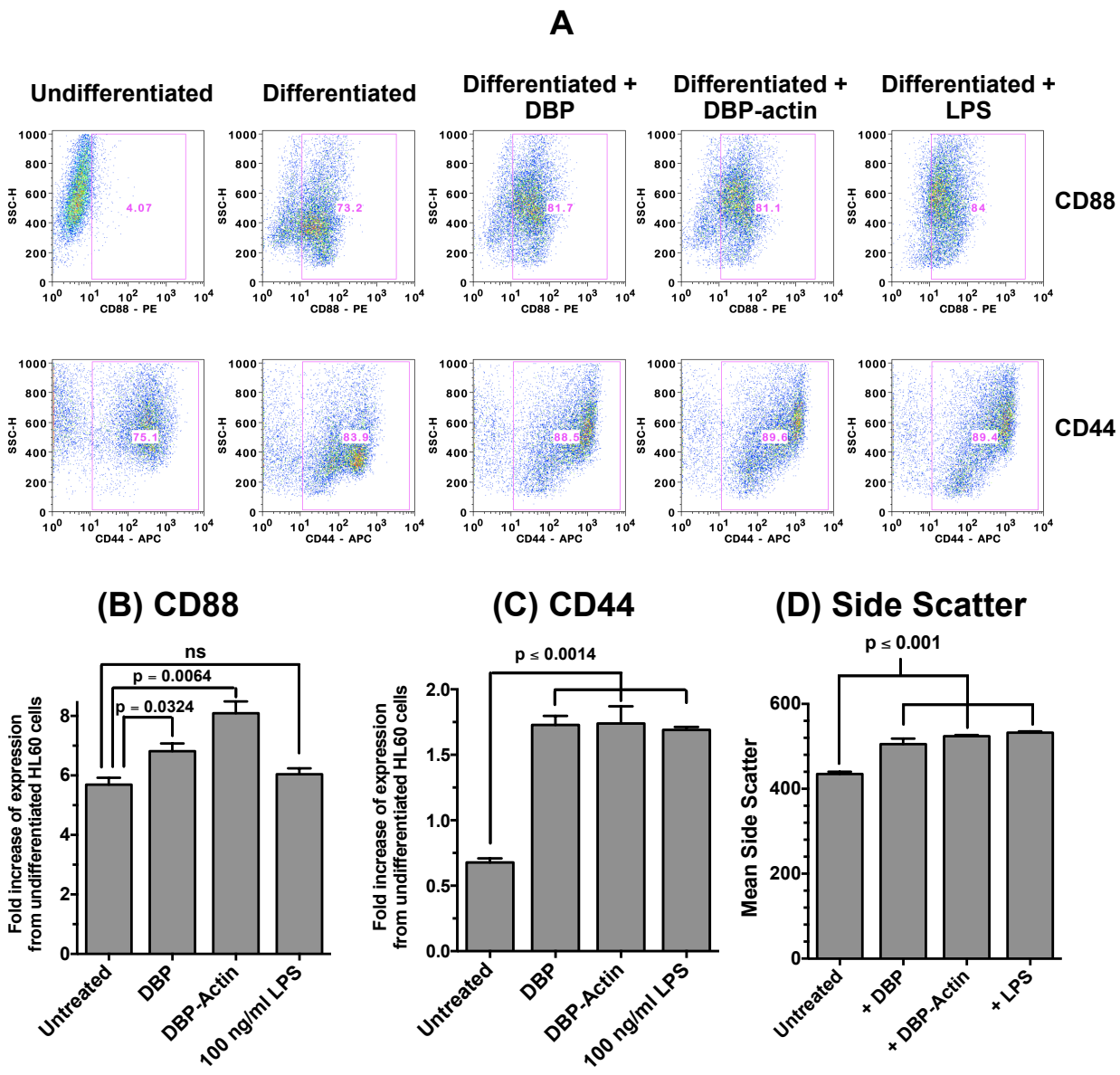
A
Undifferentiated
Differentiated
Differentiated + DBP
Differentiated + DBP-actin
Differentiated + LPS
CD88
CD44
SSC-H
CD88 - PE
CD44 - APC
4.07
73.2
81.7
81.1
84
75.1
83.9
88.5
89.6
89.4
(B) CD88
(C) CD44
(D) Side Scatter
ns
p = 0.0064
p = 0.0324
p ≤ 0.0014
p ≤ 0.001
Fold increase of expression from undifferentiated HL60 cells
Mean Side Scatter
Untreated
DBP
DBP-Actin
100 ng/ml LPS
+ DBP
+ DBP-Actin
+ LPS

Figure 33 The surface expression of CD88 and CD44 on HL-60 cells differentiated in the presence of DBP, DBP-actin or LPS.

Shown above is the percentage of HL-60 cells that stained positively for CD88, and CD44 after 5 days of DMSO induced differentiation in the presence of DBP, DBP-actin or LPS. Two million HL-60 cells were plated in RPMI 1640 + 5% FBS and differentiated with 1.3% (w/v) DMSO in the presence of 1 μM DBP, DBP-actin or 100 ng/ml LPS for 5 days at 37 ºC and 5% CO_2. As a control, undifferentiated HL-60 cells were incubated at 37 ºC and 5% CO_2 for 5 days. After 5 days, the cells were stained with alexa flour 594-conjugated mouse anti human CD88 and alexa flour 647-conjugated mouse anti human CD44 (Biolegend) antibodies. To control for non-specific staining, cells were stained for alexa flour 594 and 647-conjugated mouse IgG. Flow cytometric data were acquired using a BD FACS calibur II flow cytometer and the data was analyzed using FlowJo (Tree Stars Inc.). The CD88 and CD44 positive gates were determined using the isotype control samples, which were negative for both fluorescent signals (figure 31b). The experiment was repeated three times. Shown above is a representative scatter plot from one of the three replicates. The fold change in mean fluorescence intensity for CD88 (B) and CD44 (C) in differentiated cells relative to undifferentiated cells was determined using FlowJo. The mean side scatter was also determined using FlowJo (D).

4.2.d. Polymyxin B does not block the HL-60 differentiation phenotype induced by DBP.

To determine whether the differentiation phenotype observed when HL-60 cells were differentiated in the presence of DBP was due to endotoxin contamination, Polymyxin B, an antibiotic that binds to and sequesters LPS, was utilized. HL-60 cells were differentiated in the presence of Polymyxin B alone or Polymyxin B with DBP or LPS. The cells were then stained with PE conjugated anti CD88 antibody and analyzed by flow cytometry. There was no significant difference in the percentage of cells which were CD88 positive or in the side scatter of the differentiated HL-60 cells when the cells were differentiated in the presence of Polymyxin B and LPS suggesting that the Polymyxin B sequestered and inhibited LPS and confirming the specificity of the phenotype observed when cells were differentiated in the presence of LPS. However, when cells were differentiated in the presence of DBP, there was an increase in the percent of CD88 positive cells and in the side scatter of the differentiated cells suggesting that the phenotype observed in figure 33 was not due to endotoxin contamination in the DBP stock solution (figure 34 middle panel).

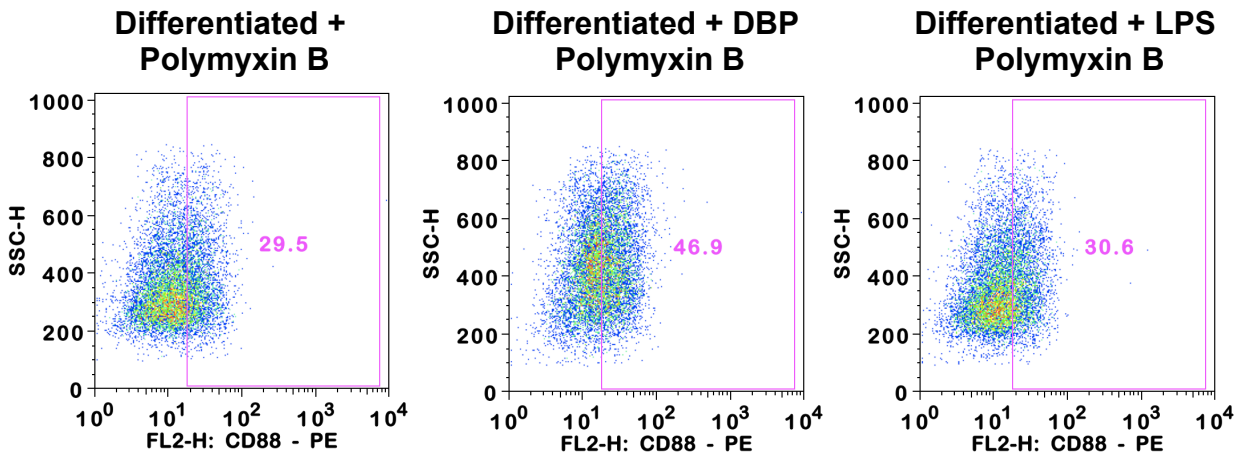

Figure 34 Polymyxin B does not inhibit the increased surface CD88 expression induced by DBP in differentiating HL-60 cells.

Shown above is the percentage of cells which stained positively for CD88 after 5 days of culture with Polymyxin B, Polymyxin B + DBP, and Polymyxin B + LPS. Two million HL-60 cells were plated in RPMI 1640 + 5% FBS and differentiated with 1.3% DMSO in the presence of 50 ng/ml Polymyxin B, 50 ng/ml Polymyxin B + 1 μM DBP or 50 ng/ml Polymyxin B + 100 ng/ml LPS for 5 days at 37 ºC and 5% CO_2. After 5 days, the cells were stained with alexa flour 594-conjugated mouse anti human CD88 antibody (Biolegend). As a control, cells were stained for alexa flour 594-conjugated mouse IgG. Flow cytometric data were acquired using a BD FACS Calibur II flow cytometer and the data were analyzed using FlowJo (Tree Stars Inc.). The CD88 positive gate was determined using the isotype control sample, which was negative for PE fluorescence (figure 31b). The experiment was repeated twice, shown above is a representative of one of the two experiments.

4.2.e. HL-60 differentiation in the presence of DBP leads to a higher basal activity in the NF-κB and the MAPK pathways.

When HL-60 cells are differentiated in the presence of DBP and LPS, there was an increase in the percentage of cells, which were CD88 positive, in the surface expression of CD44 and CD88 and the side scatter of the differentiated cells. This suggests that DBP and LPS might induce the observed differentiation phenotype using a similar mechanism. LPS is known to bind to and signal through TLR4-MD2 complex, which in turn activates the NF-κB and the MAPK pathways. Therefore, we hypothesized that DBP might induce higher basal activity of the NF-κB and the MAPK pathways in differentiating HL-60 cells as compared to untreated differentiated cells. To test this hypothesis, HL-60 cells were differentiated in the presence or absence of DBP in triplicates for 5 days at 37 ºC. After 5 days, cells were pelleted, and lysed. The protein was quantified in the cellular lysates, and equal amount of protein was loaded into an SDS-PAGE gel and subjected to electrophoresis. As a control, undifferentiated HL-60 cells were grown for 5 days at 37 ºC and then processed as previously described. The SDS-PAGE gel was transferred into a PVDF membrane and blotted with anti phospho-IKK α/ß followed by anti phospho-p38 MAPK followed by anti GAPDH antibodies. Undifferentiated HL-60 cells had low levels of phospho-IKK α/ß and phospho-p38 MAPK (figure 35, first 3 lanes). When the cells were induced to differentiate by DMSO for 5 days, the level of phospho-IKK α/ß and p38 MAPK detected was increased relative to what was observed in undifferentiated cells, suggesting higher basal activity of the NF-κB and the MAPK pathways during differentiation (figure 35, middle 3 lanes). However, when HL-60 cells were differentiated in the presence of DBP, there was a substantial increase in the level of phospho IKK α/ß and p38 MAPK detected as compared to untreated differentiated HL-60 cells (figure 35, compare the middle 3 lanes to the last 3 lanes).

This observed increase was not due to a difference in the amount of protein loaded as evident by the equal amount of GAPDH observed on the same gel (figure 35, bottom). This suggests that DBP might induce the differentiation phenotype observed in figure 33 by inducing higher basal activity of the NF-κB and the MAPK pathways during differentiation.

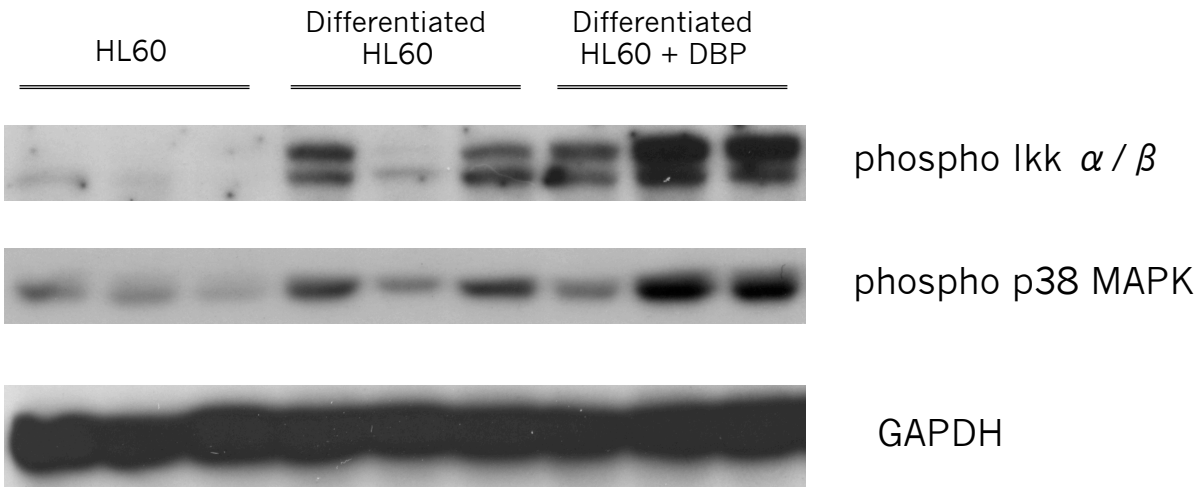

Figure 35 Cells differentiated in the presence of DBP have higher basal level NF-κB and MAPK activity.

Shown above is western blot analysis for phospho IKK α/ß, phospho p38 MAPK and GAPDH of undifferentiated HL-60 cells and differentiated HL-60 cells in the presence or absence of DBP in triplicates. Two million HL-60 cells were plated in RPMI 1640 + 5% FBS, and then differentiated with 1.3% DMSO in the presence or absence of 1 μM DBP for 5 days at 37 ºC and 5% CO_2. As a control, undifferentiated HL-60 cells were incubated at 37 ºC and 5% CO_2 for 5 days. After 5 days, the cells were pelleted and lysed in the presence of protease/phosphatase inhibitors (Cell Signaling). The protein in the lysates was quantified and equal amount of protein was loaded into an SDS-PAGE gel, subjected to electrophoresis, transferred on to a PVDF membrane and blotted for phospho IKK α/ß, then for phospho p38 MAPK and then for GAPDH.

4.2.f. Differentiated HL-60 cells release S100A8/A9 in response to DBP-actin complexes.

As previously shown, human neutrophils treated with DBP for 30 minutes generated DBP-actin complexes, which then subsequently induced the release of S100A8/A9. S100A8/A9 has been previously shown to bind to and signal through TLR4-MD2 complex in bone marrow cells, monocytes and T-cells [22,23,168]. Therefore, we hypothesized that the increase in basal activation of the NF-κB and the MAPK pathways observed in figure 35 might be due to the basal secretion of S100A8/A9 when HL-60 cells are differentiated in the presence of DBP. To test this hypothesis, the capacity of HL-60 cells to respond to DBP-actin complexes by secreting S100A8/A9 was first determined. Intracellular staining for S100A8/A9 using a monoclonal anti S100A8/A9 antibody (27B10) indicated that undifferentiated HL-60 cells did not express S100A8/A9, but upon DMSO differentiation, 50-60% of the cells were positive for S100A8/A9 (data not shown). To determine whether HL-60 cells responded to DBP and DBP-actin complexes by secreting S100A8/A9, HL-60 cells were treated with 25 OH D_3, DBP or DBP + 25 OH D_3 in the presence or absence of DMSO for 5 days at 37 ºC. As a control, untreated undifferentiated and DMSO differentiated cells were incubated for 5 days at 37 ºC. The cells were then spun down, washed once with DPBS and resuspended in HBSS at a concentration of 5 million cells per ml. The cells were then treated with DBP, actin or DBP-actin complexes for 30 minutes at 37 ºC. As a control, untreated cells were also incubated for 30 minutes at 37 ºC. The cells where then spun down, the conditioned supernatants were collected, loaded into a native gel, subjected to electrophoresis and blotted with a monoclonal anti-S100A8/A9 antibody (27B10). As shown in figure 36a, undifferentiated HL-60 cells, in the presence or absence of DBP or DBP + 25 OH D_3 did not secrete S100A8/A9 in response to DBP or DBP-actin complexes. This was expected due to the lack of S100A8/A9 expression by undifferentiated HL-

60 cells. When HL-60 cells were differentiated by the addition of 1 μM 25 OH D_3, or DMSO in the presence or absence of 25 OH D_3, DBP or DBP + 25 OH D_3, DBP-actin complexes induced the release of S100A8/A9 (figure 36a and 36b). Actin treatment of differentiated HL-60 cells was also observed to induced the release of S100A8/A9 from HL-60 cells, however, the intensity of the detected S100A8/A9 in response to actin was lower in most samples than the intensity observed in response to DBP-actin complexes. Additionally, the secreted S100A8/A9 in response to actin was observed at several molecular weights, which might be due to the binding of S100A8/A9 to different length F-actin polymers [210]. Only the HL-60 cells that were differentiated in the presence of DBP responded to DBP by releasing S100A8/A9 (figure 36b). All DBP treated HL-60 cells generated DBP-actin complexes (data not shown). This data suggests that differentiated HL-60 cells can both generate DBP-actin complexes and respond to DBP-actin complexes by releasing S100A8/A9.

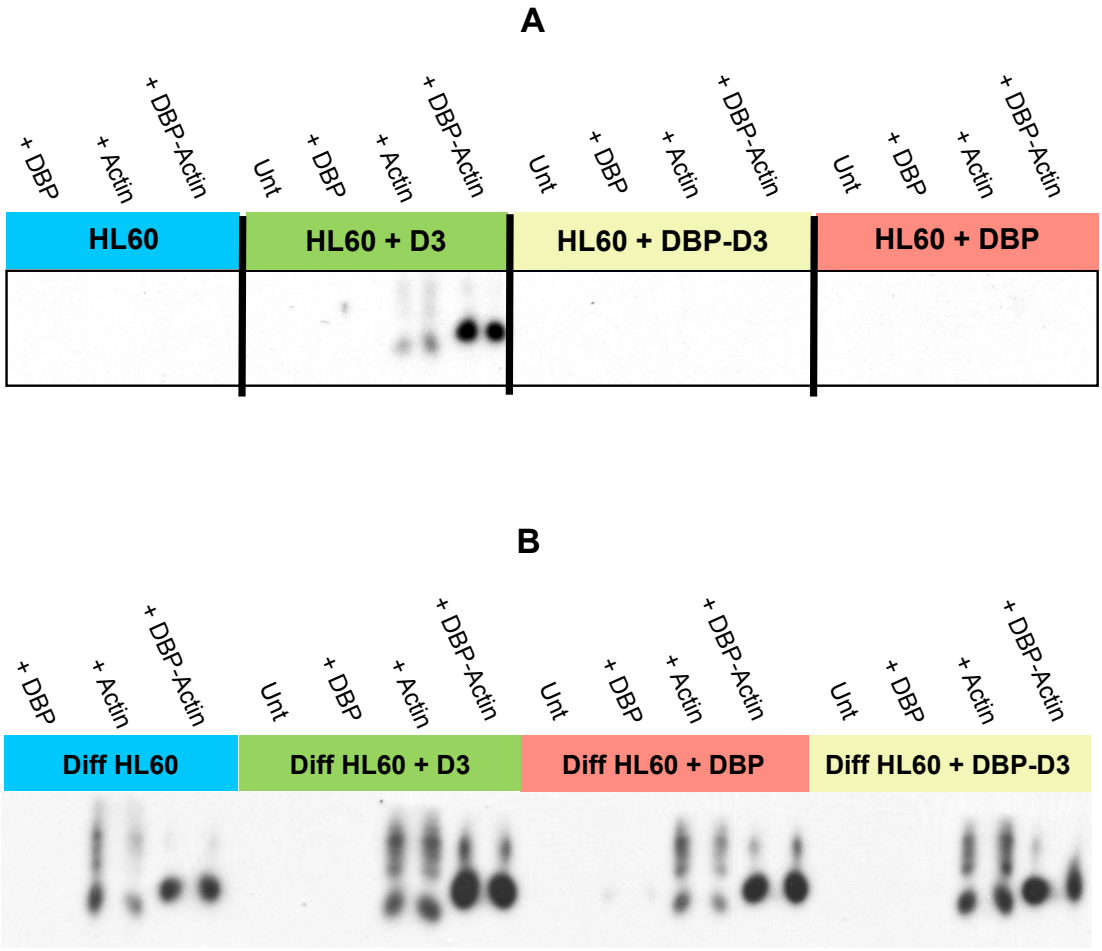

Figure 36 Differentiated HL-60 cells secrete S100A8/A9 when treated with DBP-actin complexes.

HL-60 cells were grown in complete medium (RPMI 1640 + 5% FBS) treated with or without 1 µM 25-OH D3, DBP or DBP-25-OH D3 in the absence (A) or presence 1.3% (w/v) DMSO (B) for 5 days at 37 ºC and 5% CO_2. After 5 days, the cells were spun down, resuspended in HBSS and treated with 1 µM DBP, actin or DBP-actin complexes for 30 minutes at 37 ºC and 5% CO_2. After 30 minutes, the cells were spun down and the conditioned supernatants were loaded into a native gel and a western blot was performed using mouse anti human S100A8/A9 monoclonal antibody (27E10, Hycult Biotech). This experiment was performed three times. Shown above is a representative blot from one of the experiments.

4.2.g. TLR4 signaling is required for the survival of HL-60 cells during differentiation.

The results presented in figure 36 suggest that HL-60 cells can both generate DBP-actin complexes and respond to these complexes by releasing S100A8/A9. Since S100A8/A9 is a known TLR4-MD2 ligand, it was hypothesized that the observed phenotype when HL-60 cells are differentiated in the presence of DBP was due to secretion of S100A8/A9 and a basal stimulation of TLR4. This was supported by the observed increase in the basal activity of the NF-κB and the MAPK pathways (figure 35). To further test this hypothesis, TLR4 was specifically inhibited using a peptide derived from a vaccinia virus protein (A46), VIPER . HL-60 cells were differentiated in the presence or absence of DBP and LPS for 5 days at 37 ºC. To inhibit TLR4 signaling during differentiation, the cells were differentiated in the presence of 20 μM of VIPER. To control for any non-specific effects of the peptide treatment, cells were differentiated in the presence of another peptide, CP7, derived from the same vaccinia virus protein, which has been previously shown to not interfere with TLR signaling [211]. Undifferentiated HL-60 cells were used as a baseline control. Inhibiting TLR4 activity during differentiation led to the death of all HL-60 cells, independent of DBP and LPS treatment (figure 37a, middle row, gated population represents the live cell population). However, the CP7 control peptide did not affect cellular differentiation, the phenotype observed in the presence of DBP and LPS or cellular viability (figure 37a and 37b). This suggests that TLR4 activity is required for HL-60 cell survival during differentiation. An alternative approach must be taken to determine whether the phenotype observed when cells are differentiated in the presence of DBP is due to an increase in the basal activity of TLR4.

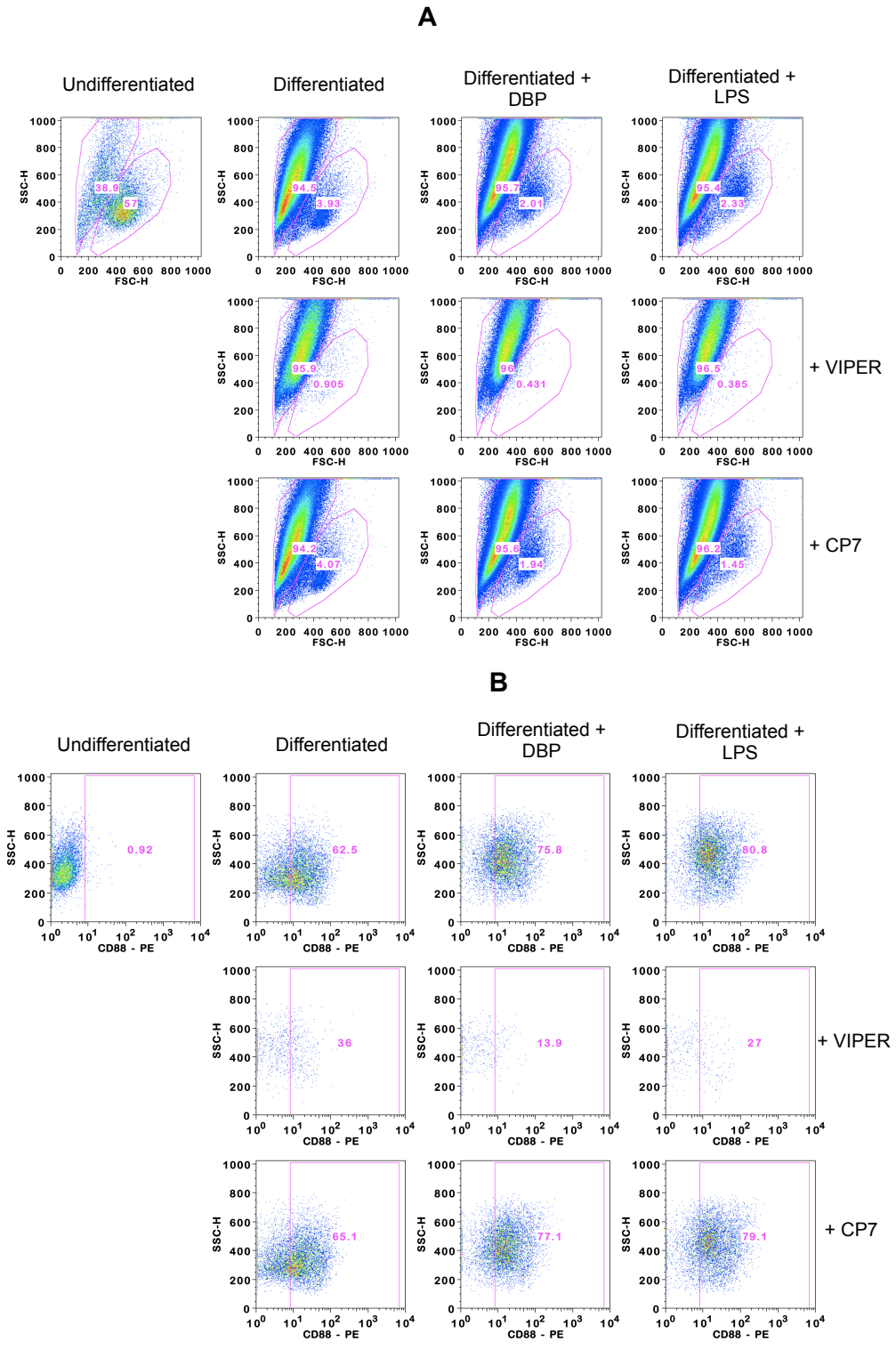
A
Undifferentiated
Differentiated
Differentiated + DBP
Differentiated + LPS
+ VIPER
+ CP7
SSC-H
FSC-H
38.9
57
94.5
3.93
95.7
2.01
95.4
2.33
95.9
0.905
96
0.431
96.5
0.385
94.2
4.07
95.6
1.94
96.2
1.45
B
Undifferentiated
Differentiated
Differentiated + DBP
Differentiated + LPS
+ VIPER
+ CP7
SSC-H
CD88 - PE
0.92
62.5
75.8
80.8
36
13.9
27
65.1
77.1
79.1

Figure 37 Inhibiting TLR4 activity leads to HL-60 cell death during differentiation.

Two million HL-60 cells were plated in RPMI 1640 + 5% FBS for 5 days or differentiated with 1.3% DMSO with our without 1 μM DBP or 100 ng/ml LPS for 5 days at 37 ºC and 5% CO_2. To inhibit TLR4 activity, all samples were treated with 20 μM of the peptide VIPER (Imgenex, San Diego, CA). As a control, cells were treated with 20 μM of the peptide CP7 (Imgenex). After 5 days, the cells were stained with alexa flour 594-conjugated mouse anti human CD88 (Biolegend) or mouse IgG isotype control (Biolegend). Flow cytometric data were acquired using a BD FACS Calibur II flow cytometer and analyzed using FlowJo (Tree Stars Inc.). The CD88 positive gate was determined using the isotype control sample, which was negative for PE fluorescence (figure 31b). The experiment was repeated twice, shown above is a representative of one of the two experiments. Panel A shows the forward versus side scatter of the HL-60 cells and panel B shows CD88 fluorescence staining versus side scatter on a dot plot and the percentage of cells which were positive for CD88.

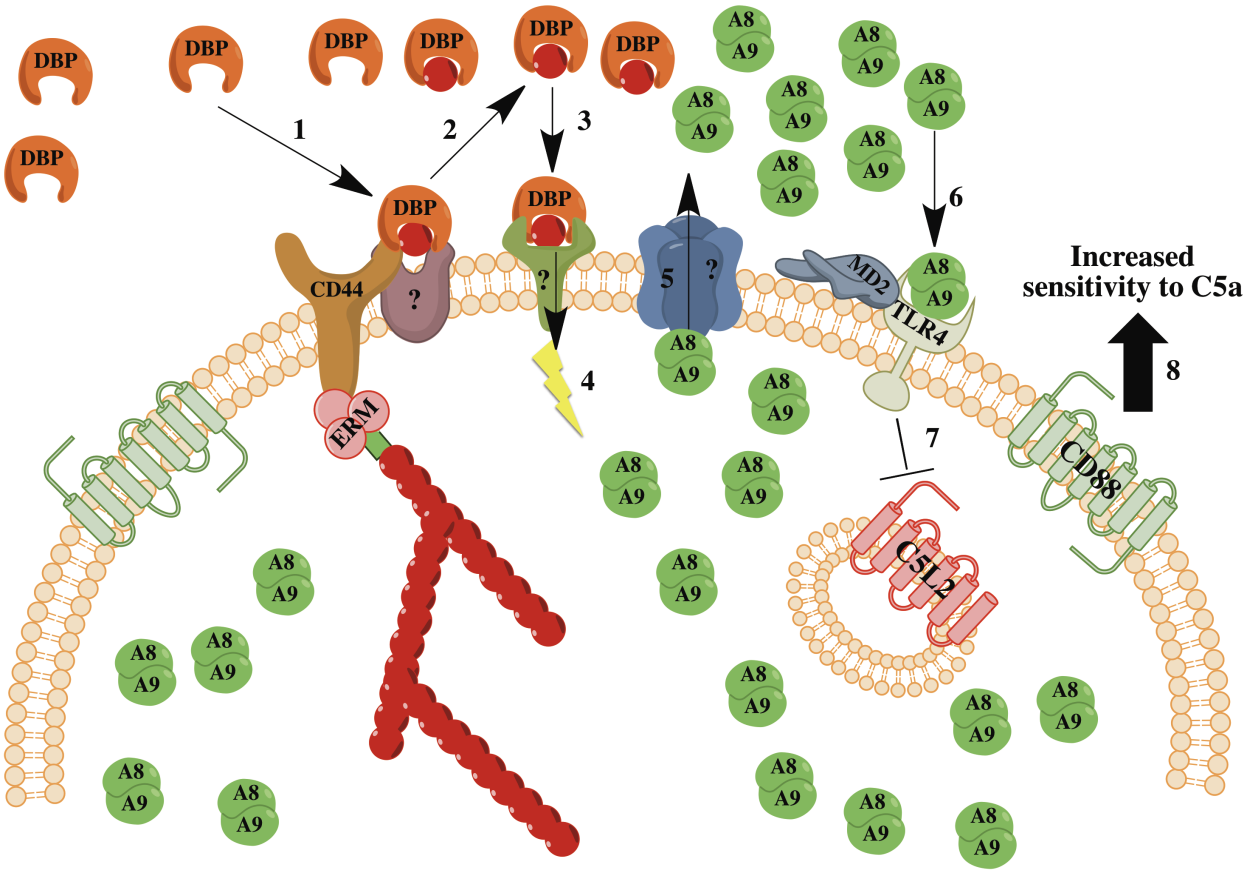

Figure 38 Proposed model.

Shown above is a proposed model for DBP's chemotactic cofactor function. Activated neutrophils express cell surface actin, which, in conjunction with CD44, induces the binding of DBP to the cell surface (1). Surface bound DBP and actin are then shed as DBP-actin complexes (2). DBP-actin complexes then induce the secretion of cytosolic S100A8/A9 from neutrophils (3-5), which bind to and activate TLR4 in an autocrine/paracrine fashion (6). TLR4 activation down regulates C5L2, a C5a decoy receptor and a down regulator for C5aR (7). Finally, the down regulation of C5L2 by TLR4 increases the sensitivity of C5aR for C5a, which increases the chemotaxis of neutrophils to suboptimal concentrations of C5a (8).

5. Discussion

5.1. A potential mechanism behind DBP's chemotactic cofactor function.

5.1.a. DBP might exert its chemotactic cofactor function through the generation of DBP-actin complexes and subsequent secretion of S100A8/A9.

DBP has been shown to be a chemotactic cofactor for neutrophils in vitro by several groups [92,93,115-119,126]. To exert its chemotactic cofactor function, DBP binds to the surface of neutrophils [118,124-128,208] and subsequently is shed in a process that is dependent on neutrophil elastase [118,126]. However, the reason why DBP needs to both bind and shed from the cell surface to induce the chemotactic cofactor function is not known. The model proposed is that DBP by itself is not the active chemotactic cofactor but an essential upstream molecule needed to generate this activity (figure 38). The model is supported by current and previous published data: 1) step one is that DBP binds to actin on the surface of activated and/or migrating neutrophils (figures 27, 28 and McVoy et al, manuscript in preparation). 2) Step two is that the DBP-actin complex is shed into the extracellular environment. 3) Step three is that the DBP-actin complexes re-bind to a yet to be identified neutrophil receptor. 4) Step four is that DBP-actin binding induces a calcium flux that induces formation and release of the calcium dependent cytosolic complex S100A8/A9. 5) Step five is that S100A8/A9 interacts with its receptor TLR4 to generate a chemotactic cofactor signal. Thus, in this model, S100A8/A9 is the actual chemotactic cofactor and there is abundant evidence to support this premise since it has been shown that this complex functions to facilitate cell migration [155,158,163,165,212-215].

The following is a summary of the experimental evidence that gave rise to this model. First, DBP binding partners were investigated by incubating neutrophil with purified DBP for 30

minutes at 37 °C to generate conditioned supernatants. These conditioned supernatants were then subjected to native gel (non-denaturing) electrophoresis and blotted for DBP. Two potential DBP-neutrophil protein complexes were observed and identified by mass spectrometry (figure 23). One of the proteins was actin, a known DBP binding protein [105,106,109,110]. Since the binding of DBP to the surface of leukocytes has been shown to be partially dependent on cell surface actin (figures 27, 28 and McVoy et al, manuscript in preparation), and actin is an intracellular protein that is generally released during necrotic cell death, it was speculated that DBP-actin might be the active chemotactic cofactor that is generated by neutrophils during inflammation. This model also states that DBP produces its effect on neutrophils indirectly, by inducing the release of another pro-inflammatory chemotactic cofactor protein from neutrophils. A mass spectrometric approach was taken to identify this protein in conditioned supernatants from DBP treated neutrophils. As shown in figure 21 and table 1, only one secreted neutrophil protein identified in the conditioned supernatant has been previously implicated in neutrophil chemotaxis, superoxide anion generation, and polarization, a complex of S100A8 and S100A9.

S100A8/A9 is a heterodimer that makes up approximately 40% of all cytosolic proteins in neutrophils [147,148]. Upon the elevation of cytosolic calcium, S100A8/A9 has been shown to form calcium bound heterotetramers [151,152]. As previously mentioned, in addition to DBP-actin complexes, S100A8 and S100A9 also were detected in mass spectrometric analysis in DBP treated neutrophil conditioned supernatants, so the role of DBP and DBP-actin complexes in S100A8/A9 formation and secretion was determined. DBP induced an approximate 2 fold increase in the amount of S100A8/A9 heterodimer/heterotetramer detected in neutrophils (figure 22) and induced the secretion of the complex into the conditioned supernatant (figure 24). However, DBP-actin complexes were much more potent in inducing the secretion of S100A8/A9

from neutrophils than DBP (figure 24) suggesting that the observed S100A8/A9 released by DBP treated neutrophils was in response to the generated DBP-actin complexes. Neutrophils treated with actin were also induced to secrete S100A8/A9, but to a lesser extent in most donors (data not shown), suggesting that actin portion of the DBP-actin complex may be the main inducer of S100A8/A9 release from neutrophils. However, under physiological conditions extracellular actin is bound to DBP and so all of the experiments presented were performed with the physiologically relevant DBP-actin complexes. Moreover, DBP-actin complexes were observed in BALF of DBP +/+ mice after the induction of inflammation supporting the hypothesis that DBP-actin complexes are generated during inflammation (figure 26). It is important to point out that in this analysis, the antibody detects both the heterodimeric and heterotetrameric forms of S100A8/A9, so it is not known whether DBP induces the formation of the heterodimeric or heterotetrameric form. However, since all of the assays were performed in HBSS containing both calcium and magnesium, one would hypothesize that the detected S100A8/A9 in the conditioned supernatants is in a heterotetrameric form.

The C5a chemotactic cofactor function of DBP was previously shown to be very specific for DBP [92]. Therefore, the specificity of secretion of extracellular actin and S100A8/A9 to DBP was determined. As shown in figure 25, the generation of DBP-actin complexes and the release of S100A8/A9 were specific to DBP because other proteins with a similar molecular weight and charge as DBP, such as HRGP and α1AGP, did not induce the secretion of actin or S100A8/A9 from neutrophils (figure 25). This also suggests that the actin secreted from DBP treated neutrophils is most likely specific to DBP and is not due to cell death, since there was no actin detected in HRGP and α1AGP treated neutrophils (figure 25, bottom panel). By performing annexin V and PI staining of untreated and DBP treated neutrophils, there was no significant

difference in the percentage of annexin V or PI positive neutrophils between the two groups (data not shown) also suggesting that the observed generation of DBP-actin complexes was not due to the liberation of actin from necrotic cells.

5.1.b. DBP binds to migrating neutrophils in a process that is partially dependent on cell surface actin.

For DBP to exert its chemotactic cofactor function it first must bind to neutrophils. However, all previous experiments performed to study the binding of DBP to neutrophils utilized non-activated cells in suspension or neutrophil membrane fractions [118,124-128,208]. Therefore, to study the binding of DBP on migrating cells under agarose, migrated neutrophils were fixed, stained with anti-DBP and the surface bound DBP was visualized using fluorescence microscopy. As shown in figure 27a, exogenously added DBP bound to migrating neutrophils. However, to our surprise, approximately 65% of migrating neutrophils were positive for DBP staining (data not shown) suggesting that there may be a subset of neutrophils possessing a putative DBP receptor or binding site. DBP has been shown to bind to a CSPG on the surface of neutrophils [125], which was later identified to be CD44 [122,127]. In addition to CD44, there is evidence that cell surface actin is required for the tight binding of DBP to neutrophils and U937 cells (McVoy et al, manuscript in preparation). To determine whether cell surface actin contributes to the binding of DBP to migrating neutrophils, cells were allowed to migrate in the presence of DBP-actin complexes. As shown in figure 27a and 27b, the intensity of DBP staining on migrating neutrophils was lower when neutrophils were allowed to migrate in the presence of DBP-actin complexes instead of DBP alone. This suggests that the actin-binding site on DBP is required for the optimal binding of DBP to migrating neutrophils. It should be noted that when DBP is mixed with actin to make DBP-actin complexes, only 60-80% of the DBP becomes

complexed with actin (data not shown). This suggests that uncomplexed DBP is present when neutrophils migrate in the presence of DBP-actin complexes. Therefore, some of the observed DBP staining in the DBP-actin complex treated migrating neutrophils might be due to the presence of free DBP and thus these data might under estimate the importance of DBP's actin binding site and cell surface actin in the binding of DBP to migrating neutrophils. Cell surface actin expression on migrating neutrophils was confirmed (figure 28) by immuno-fluorescent staining of non-permabilized migrated neutrophils for actin. The observed cell surface actin was substantially decreased when cells were migrating in the presence of DBP presumably due to the masking of actin or the shedding of actin by DBP (figure 28a, compare the middle and the top panels). The requirement for cell surface actin in the binding of DBP to leukocytes was further confirmed by utilizing SPR showing that anti-actin pre-treated U937 cells had a substantial reduction in binding to immobilized DBP (figure 28b). These results are in agreement with the results of Zhang et al, which showed that the actin binding site in DBP is required for optimal binding of DBP to U937 cells [128] and suggests that DBP binds to the cell surface of migrating neutrophils and that this binding is partially dependent on the actin binding site on DBP and the surface expression of actin by migrating neutrophils.

5.1.c. Purified DBP-actin or DBP-actin treated neutrophil conditioned supernatants are not chemotactic to neutrophils.

As previously mentioned, neutrophils treated with DBP were observed to generate DBP-actin complexes and subsequently release S100A8/A9. Murine S100A8 and S100A8/A9 have been previously shown to be chemotactic to mouse neutrophils and monocytes in vitro and in vivo [212-215]. However, the role of S100A8/A9 in human neutrophil chemotaxis has been controversial. Newton et al observed no significant chemotaxis of human neutrophils to purified

S100A8 and S100A9 [165]. However, Ryckman et al showed that S100A8, S100A9 and S100A8/A9 were potent chemoattractants for human neutrophils [163]. This discrepancy between the two studies was thought to be due to the oxidative inactivation of S100A8 by hypochlorite [216]. Since DBP-actin complexes were observed to induce the release of S100A8/A9 from neutrophils, chemotaxis assays were performed to determine whether the DBP-actin treated neutrophil conditioned supernatants were chemotactic or whether DBP-actin treatment of neutrophils enhanced neutrophil chemotaxis to C5a. We did not detect any significant chemotaxis to DBP-actin treated neutrophil conditioned supernatants using the modified Boyden chamber and under agarose chemotaxis assays (data not shown). We also did not observe any difference in the chemotaxis of neutrophils to 1 nM C5a in the presence or absence of DBP-actin complexes (data not shown). S100A8/A9 has been shown to be a potent chemoattractant for human neutrophils only at the narrow concentration range of 10^{-12} to 10^{-10} M [163,214]. Therefore, the lack of chemotactic activity in the conditioned supernatants might be due to a concentration of S100A8/A9 in these supernatants that was outside the reported chemotactic range. Alternatively, S100A8 in the conditioned supernatant might be inactive due to oxidative modification and thus no chemotaxis was observed to the conditioned supernatants. In addition to inducing neutrophil chemotaxis, S100A8/A9 has been shown to play a major role in neutrophil trans endothelial migration [155,158], through its induction of neutrophil degranulation [164], surface expression and activation of CD11b [165], and microtubule polymerization [155]. Therefore, by inducing the release of S100A8/A9, DBP-actin complexes may play a role in the trans endothelial migration of neutrophils in inflammation.

5.1.d. S100A8/A9 binds to migrating neutrophils and colocalizes with DBP on F-actin rich protrusions extending out of the migrating cells.

S100A8/A9 has been shown to bind to CSPGs, carboxylated glycans, RAGE, CD36 and TLR4 on endothelial cells, bone marrow cells, and several cancer cell lines [22,159-161,166]. However, the binding of S100A8/A9 to migrating neutrophils has never been investigated or visualized. Like S100A8/A9, DBP has also been observed to bind to the CSPG on neutrophils [125,127]. As shown in figure 29, the majority of migrating neutrophils (~80%) stained strongly for S100A8/A9 suggesting that the heterodimer/heterotetramer binds to migrating cells. There was a subset of migrating neutrophils where DBP and S100A8/A9 staining colocalized and at high magnification (1000x), DBP and S100A8/A9 were observed to colocalize on F-actin rich protrusions extending out of the migrating neutrophils (figure 30a) suggesting that DBP and/or S100A8/A9 might induce F-actin polymerization, thus potentially play a role in neutrophil chemotaxis.

McVoy et al has previously shown that DBP binds to a CSPG on neutrophils, CD44 [127], which was later confirmed by Trujillo et al[122]. Since S100A8/A9 has also been previously shown to bind to a CSPG [160], and S100A8/A9 colocalizes with DBP on migrating neutrophils, it is possible that S100A8/A9 might bind to CD44. The activation of CD44 is known to induce the recruitment and phosphorylation of the actin binding proteins, ezrin/radixin/moesin (ERM), to its intracellular domain that subsequently leads to actin polymerization at pseudopods [217,218]. Therefore, by binding to CD44, DBP and/or S100A8/A9 might induce actin polymerization and subsequently play a role in cellular polarization and/or chemotaxis.

5.1.e. The chemotactic cofactor function of DBP is specific to C5a: A potential role of S100A8/A9 and TLR4.

Collectively, the data presented indicate that DBP-actin complexes are generated from DBP treated neutrophils, and that these complexes subsequently induce the release of S100A8/A9. In vitro, the chemotactic cofactor function of DBP has been shown to be specific to C5a [92]. Additionally, this chemotactic cofactor function of DBP was only observed at suboptimal concentrations of C5a and C5a des arg (10-100 pM and 100-1000 pM respectively), suggesting that DBP increases the sensitivity of C5aR to C5a and C5a des arg [92,93,115,117,118,126]. S100A8/A9 has been previously shown to directly bind to and activate TLR4 [22,23,168]. TLR4 activation in peripheral blood mononuclear cells has been recently shown to increase the sensitivity of C5aR to low concentrations of C5a by down regulating the activity of C5L2, a negative regulator of C5aR [219]. Therefore, by inducing the secretion of S100A8/A9 from migrating neutrophils and thus activating TLR4, DBP might increase the sensitivity of C5aR to C5a and C5a des arg and thus augment chemotaxis of neutrophils to suboptimal concentrations of these chemoattractants. Therefore, the specificity of DBP's chemotactic cofactor function to C5a and C5a des arg might be due to the specific down regulation of C5L2 by the secreted S100A8/A9 through TLR4 in migrating neutrophils.

5.2. DBP's chemotactic cofactor function is observed in vivo.

5.2.a. DBP is required for the optimal recruitment of neutrophils into the alveolar spaces in a C5a induced alveolitis model of acute inflammation.

To study the role of DBP in the chemotaxis of neutrophils in vivo, an alveolitis model was developed. The complement activation peptide, C5a, has been previously shown to induce

alveolitis in rats [220-222]. C5a is known to be a very potent cellular activator, capable of activating several cell types including endothelial cells, macrophages, neutrophils, dendritic and mast cells (for reviews, see [223,224]). The presence of C5a in the lungs has been shown to induce the secretion of CXC and CC chemokines, cytokines and the induction of expression of adhesion molecules, cytokines and chemotactic factors by endothelial cells [220-222,225,226]. Activated endothelial cells then apically present chemotactic factors, such as KC in mouse and IL-8 in human, [71-73], which induces secretory vesicle and secondary granule exocytosis in rolling neutrophils and the up regulation of CD11b/CD18 [75,76]. The binding of neutrophils to endothelial cells may also lead to the secretion of S100A8/A9 [157], which also acts on rolling neutrophils by inducing the exocytosis of CD11b/CD18 containing secretory vesicles, and secondary granules [164]. The up-regulation and activation of surface CD11b/CD18 on neutrophils will then lead to the tight adhesion of rolling neutrophils on endothelial cells and trans endothelial migration [155,158].

To induce alveolitis, purified mouse C5a was instilled directly into the lungs of DBP +/+ and DBP -/- mice by oropharyngeal aspiration. In vitro, the chemotactic cofactor function of DBP was observed only at suboptimal concentrations of C5a; therefore to determine the role of DBP in neutrophil chemotaxis to C5a in vivo, two doses of C5a were used, a "high" dose 1 μg per 24 grams of mouse and a "low" dose 0.25 μg per 24 grams of mouse. Results shown in figures 3 and 4 suggest that DBP is required for the optimal recruitment of neutrophils into the alveolar spaces 4, 6, and 24 hours after the instillation of 1 μg of C5a and 4 hours after the instillation of 0.25 μg of C5a. To rule out the possibility that the reduced numbers in the DBP-/- mice were due to cells trapped in the lung interstitium, lavaged and non lavaged lungs were homogenized 4 hours after the instillation of 1 μg of C5a to obtain a single cell suspension and

the number of neutrophils in the whole lung of DBP +/+ and DBP -/- mice was determined (figure 6). There was a significant reduction in the total number of neutrophils in the homogenized lungs of DBP -/- mice as compared to the lungs of DBP +/+ mice pre and post lavage indicating a migration defect into the lung.

Histological analysis of the lungs was performed 4 hours after the instillation of C5a to confirm our previous results and to determine the extent of inflammation in the lungs. Results, shown in figure 5, show that C5a treated lungs from DBP +/+ mice contained more leukocytes, hemorrhage and interstitial edema as compared to C5a treated lungs from DBP -/- mice. This suggests that there was less inflammation in the lungs of DBP -/- mice as compared to the lungs of DBP +/+ mice. To confirm this observation, we examined the vascular leakage by measuring the protein concentration in the BALF from C5a treated DBP +/+ and DBP -/- mice. There was a significant reduction in the protein concentration in the BALF from DBP -/- mice as compared to the BALF from DBP +/+ mice (data not shown), suggesting that there was less vascular leakage in DBP -/- mice as compared to DBP +/+ mice in response to the instillation of C5a into the lungs. These data suggest that in addition to its role in neutrophil chemotaxis, DBP might play a role in the amplification of inflammation in vivo.

DBP-actin complexes are generated from human neutrophils in vitro (figure 23 and 25) and during inflammation in our alveolitis model in vivo (figure 26). DBP-actin complexes were shown to induce the release of S100A8/A9 from neutrophils (figures 24 and 25). S100A8/A9 is known to be an inflammatory amplifier (for a review see [207]) due to its capacity to amplify the production of pro-inflammatory cytokines from macrophages [182], attract neutrophils [163,212,214], activate endothelial cells [162] and induce trans endothelial migration of neutrophils and monocytes [155,158]. The lack of DBP-actin generation and subsequent S100A8/A9 release from neutrophils in

DBP -/- mice might explain the observed decreased inflammation in the histological analysis of the inflamed lungs of DBP -/- mice.

5.2.b. DBP reconstitution in the alveolar spaces during inflammation partially rescues the inflammatory phenotype in DBP -/- mice by increasing the number of migrated neutrophils into the alveolar spaces.

The DBP-actin-S100A8/A9 model described above suggests an extrinsic role for DBP in vivo. Therefore, it was hypothesized that the reconstitution of DBP at the inflammatory site in DBP -/- mice would induce greater neutrophil recruitment and inflammation. To test this hypothesis, DBP +/+ or DBP -/- complement activated sera were instilled into the lungs of DBP +/+ or DBP -/- mice. Results from this experiment showed that reconstituting DBP increased the number of neutrophils recruited into the lungs of DBP -/- mice 4 hours after instillation, however this increase did not reach statistical significance (figure 7a) suggesting only a partial rescue. This observed increase in the number of neutrophils recruited in response to DBP +/+ complement activated serum was not due to a difference in the level of C5a/C5a des arg between the two sera as determined by ELISA (figure 7b). In our experimental model, alveolitis was induced for 4 hours, which may not be long enough to reverse a potential intrinsic defect in DBP -/- mice. Therefore, the partial rescue observed in figure 7a suggests that DBP exerts an extrinsic function during acute inflammation, but the lack of a full rescue also indicates that there might be an intrinsic defect in one or more inflammatory cell(s) in the DBP -/- mouse. This observed extrinsic function may be due to its capacity to induce the generation of DBP-actin complexes and subsequent S100A8/A9 release which is a known neutrophil chemoattractant and an inducer of trans endothelial migration [155,163,165,212-214].

5.3. Bone marrow neutrophils from DBP -/- mice exhibit intrinsic defects.

5.3.a. Reductions in the numbers of bone marrow neutrophils and their surface expression of CD88, CD44 and CD11b in DBP -/- vs. DBP +/+ mice.

The generation of DBP-actin and subsequent formation and secretion of S100A8/A9 complexes from neutrophils provides a potential mechanism where DBP can influence development and differentiation of neutrophils in the DBP -/- mouse. There is approximately twice the amount of S100A8/A9 detected in human neutrophils treated with DBP as compared to untreated neutrophils (figure 22), suggesting that there might be a reduced amount of S100A8/A9 in bone marrow neutrophils of DBP -/- mice as compared to DBP +/+ mice. This decrease in S100A8/A9 might be responsible for the development of a potential intrinsic defect. Unfortunately, this cannot be tested easily due to the lack of a mouse S100A8/A9 specific antibody or a commercially available mouse S100A8/A9 ELISA. However, this hypothesis is supported by results published by Mantiz et al where they show that in the S100A9 knockout mouse, there was a reduction in the number of Gr-1 positive neutrophils in the bone marrow, suggesting a role of S100A8/A9 in neutrophil differentiation and maturation [158]. A reduction in the blood or bone marrow neutrophil count in the DBP -/- mice as compared to DBP +/+ mice might lead to the observed reduction in neutrophil recruitment to the lungs of DBP -/- mice in the alveolitis model. Therefore, the total number of white blood cells, blood neutrophils, bone marrow cells and bone marrow neutrophils was determined from five different DBP +/+ and DBP -/- mice. There was no significant difference in the total white blood cell, blood neutrophil (figure 9) or whole bone marrow cell count (figure 10a) but there was a significant reduction in the number of bone marrow neutrophils in DBP -/- as compared to DBP +/+ mice (figure 10b). Furthermore, analysis of bone marrow neutrophils revealed that DBP -/- bone marrow

neutrophils had lower side scatter, expressed less Gr-1, CD88 and CD44 as compared to DBP +/+ bone marrow neutrophils (figures 11-14). There were no observed differences in the expression of any of these proteins on blood neutrophils. This further supports our previous observations indicating that there might be an intrinsic defect in DBP -/- bone marrow neutrophils.

5.3.b. Evidence of an intrinsic defect in integrin exocytosis and/or recycling and chemoattractant receptor recycling in DBP -/- bone marrow derived BAL neutrophils 4 hours after the initiation of inflammation.

In mice, lymphocytes make up approximately 88%, monocytes make up 1-4% and neutrophils make up 8-10% of white blood cells in circulation [227]. In contrast, in human, lymphocytes make up 20-40%, monocytes make up 2-8% and neutrophils make up 50-65% of all WBC in circulation. Mice compensate for the small number of neutrophils in their blood by utilizing bone marrow neutrophils during inflammation, a process that has been shown to peak at 3-4 hours after the initiation of inflammation and to be dependent on the secretion of S100A8/A9 into the circulation [215]. Therefore, a functional defect in the bone marrow neutrophil pool can lead to reduced neutrophil recruitment to an inflammatory site in mice. To examine the possibility of an intrinsic defect, BAL neutrophils were first characterized by quantifying the surface expression of the adhesion molecules CD11b, CD11c and CD44. As shown in figure 8, there was a significant increase in the surface expression of CD11b and CD11c on the BALF neutrophils from DBP -/- mice as compared to DBP +/+ mice 4 hours after the instillation of C5a into the lung. However, there was no observed difference in the surface expression of these integrins at the any other time point examined (2.5, 6, and 24 hours). Surface expression of

CD44 on neutrophils was not altered after the instillation of C5a. In addition, preliminary data shows that there was a substantial reduction in the surface expression of CD88 on the surface of DBP -/- BAL neutrophils as compared to DBP +/+ BAL neutrophils 4 hours after the instillation of C5a (data not shown). A similar trend was observed with CXCR2 when KC was instilled into the lungs of DBP +/+ and DBP -/- mice (data not shown). Since the peak recruitment of bone marrow neutrophils to the site of inflammation occurs at 4 hours after the initiation of inflammation, these results suggest that there might be a defect in granular exocytosis, receptor internalization and/or recycling in the bone marrow neutrophil pool of DBP -/- mice.

To maintain polarized chemotaxis, neutrophils must recycle their adhesion molecules and chemoattractant receptors so that there are free receptors and integrins available to sense and respond to the chemoattractant gradient. In neutrophils, approximately 95% of CD11b/CD18 integrins are localized in secretory vesicles and secondary granules [75]. Additionally, it has been previously shown in several cell types that integrins are internalized upon binding to their ligands and trafficked into sorting endosomes where they are subsequently trafficked into lysosomes for degradation or into recycling endosomes for recycling on the plasma membrane [228-231]. Directional exocytosis of integrin containing granules and polarized recycling of integrins towards the leading edge of migrating neutrophils has been previously shown [84,229,231] and are thought to play a role in the polarized chemotaxis of neutrophils. Similar to integrins, chemoattractant receptors such as CD88 and CXCR2 have been previously shown to be internalized upon ligand binding and subsequently degraded or recycled back to the plasma membrane [232-235]. The recycling of chemoattractant receptors is thought to be important for persistent directional migration.

Manitz et al have reported a defect in CD11b exocytosis and/or recycling in the S100A9 -/- mouse, as evident by the reduced amount of cell surface CD11b after the stimulation of bone marrow neutrophils with IL-8 [158]. The reduced CD11b surface expression observed in S100A9 -/- bone marrow neutrophils may also be due reduced microtubules polymerization, as reported by [155], since microtubules are known to be major regulators for endosomal and granular trafficking [236-239]. As previously discussed, DBP was observed to induce a 2-fold increase in the amount of intracellular S100A8/A9 in human neutrophils, and similar to the S100A9 -/- mouse, there was a reduction in the number of bone marrow neutrophils in DBP -/- mice as compared to DBP +/+ mice. In the alveolitis model of inflammation at the 4-hour time point, DBP -/- BALF neutrophils expressed higher levels of the integrins CD11b/CD18 and CD11c/CD18 suggesting that, similar to what was observed in the S100A9 -/- mouse, DBP -/- bone marrow neutrophils might have increased granular exocytosis or a defect in integrin internalization and recycling. Additionally, DBP -/- BAL neutrophils also had a substantial reduction in the surface expression of the chemoattractant receptors used for migration suggesting that these neutrophils might have an intrinsic defect in receptor recycling. These data suggest that DBP -/- bone marrow neutrophils might not be capable of persistent migration towards a chemoattractant due to the loss of the surface expression of chemoattractant receptors and the non-polarized integrin exocytosis and recycling during chemotaxis.

5.3.c. Evidence of an intrinsic defect in the migration of DBP -/- bone marrow neutrophils.

To further confirm the presence of an intrinsic defect in DBP -/- bone marrow neutrophils, bone marrow neutrophils were functionally characterized utilizing two chemotaxis assays, one adhesion dependent and the other independent. A modified Boyden chamber

chemotaxis assay was is largely adhesion independent, cells migrate in three dimensions through a cellulose nitrate filter, which separates the neutrophils from the chemoattractant in the bottom chamber. The distance migrated into the 120 μm thick filter is measured using a microscope at 400x. This assay does not measure the number of cells which specifically respond to the chemoattractant, it only measures the distance migrated by the cells in a relatively short time (30 minutes). However, this assay is very sensitive in measuring cell movement towards a weak or small gradient of a chemoattractant. In contrast, in an under agarose chemotaxis assay, cells migrate in two dimensions over type 1 collagen coated coverslips. The assay was designed such that the cells can freely migrate to either buffer or chemoattractant containing wells. This assay analyzes both the net distance and number of migrating cells. Migration in this assay is highly dependent on adhesion to the substratum and polarization towards a chemoattractant is readily observed. In addition, this assay can be used to study polarization by staining the migrated cells with phalloidin to visualize F-actin, making this assay a powerful tool to study neutrophil polarization and chemotaxis.

Results using the Boyden chamber chemotaxis assay showed that there was no difference in the distance migrated between DBP +/+ and DBP -/- bone marrow neutrophils to purified C5a (figure 15) or to DBP +/+ or DBP -/- complement activated sera (data not shown). However, in the under agarose chemotaxis assay, there was a significant decrease in the net distance migrated by DBP -/- bone marrow neutrophils to DBP -/- complement activated serum and in the net number of migrated cells to both complement activated sera (figure 16). The reduction in the distance migrated was partially reversed when the cells were allowed to migrate to DBP +/+ complement activated serum (figure 16c). This data suggests that there is an intrinsic migratory defect in DBP -/- bone marrow neutrophils, which can be partially reversed by extrinsic DBP.

As previously mentioned, preliminary analysis of the chemoattractant receptors on DBP -/- and DBP +/+ BAL neutrophils revealed that there might be a chemoattractant receptor-recycling defect in DBP -/- BAL neutrophils. Ex vivo analysis of bone marrow neutrophil migration was performed using two different chemotaxis assays, the modified Boyden chamber assay, where neutrophils are allowed to migrate for 30 minutes, and the under agarose chemotaxis assay, where neutrophils are allowed to migrate for 4.5 hours. Due to the difference in the duration of migration in both assays, optimal receptor recycling will be more important for sustained neutrophil chemotaxis in the under agarose chemotaxis assay as compared to the shorter modified Boyden chamber chemotaxis assay. Therefore, the lack of a migratory phenotype in the modified Boyden chamber chemotaxis assay might be due to the short duration of the assay. In addition, the observed reduction in the net number of migrating neutrophils in the under agarose chemotaxis assay might be due to a defect in chemoattractant receptor recycling, specifically CD88, in DBP -/- bone marrow neutrophils which would prevent sustained chemotaxis to C5a due to the depletion of CD88 from the cell surface.

5.3.d. DBP -/- bone marrow neutrophils present an intrinsic defect in their polarization during chemotaxis.

CD11b and CD11c are integrins required for neutrophil tight adhesion to endothelial cells and subsequent trans endothelial migration. They are normally expressed as heterodimers with the common $ß_2$ integrin, CD18. Approximately 95% of neutrophil CD11b is expressed in secretory vesicles and secondary granules [75], which is exocytosed during inflammation in response to neutrophil activation by chemoattractants. As previously mentioned, it is thought that the exocytosis and the endosomal recycling of these integrins occurs in a polarized fashion [84,229], and thus a defect in exocytosis or recycling can lead to unpolarized CD11b or CD11c

surface expression on neutrophils. The cross linking of CD11b/CD18 by antibodies has been previously shown to induce actin polymerization, suggesting that actin polymerization occurs at the site of adhesion of CD11b/CD18 to endothelial cells or to matrix proteins [85,86]. This suggests that polarized granular exocytosis and integrin recycling may play a role in cellular polarization during chemotaxis, where actin is induced to polymerize at the leading edge of migrating cells. As shown in figure 8, there was an increase in the surface expression of CD11b and CD11c on DBP -/- BAL neutrophils 4 hours after the instillation of C5a into the lung that may be due to a defect in the exocytosis of granular CD11b and CD11c or in the recycling of these integrins. In the under agarose chemotaxis assay, cells were allowed to migrate on type 1 collagen, a process which has been previously shown to be dependent on the surface expression of CD11b/CD18 [240]. Therefore, a defect in the polarized exocytosis and/or recycling of CD11b/CD18 might lead to unregulated, unpolarized actin polymerization and ultimately a defect in cellular migration in the under agarose assay. As shown in figure 17, higher non-polarized actin polymerization was observed when DBP +/+ bone marrow neutrophils were allowed to migrate to DBP -/- complement activated serum as compared to cells migrating to DBP +/+ complement activated serum on type 1 collagen coated cover slips. Morphological analysis indicated that cells migrating in the absence of DBP were not as well polarized as cells migrating in the presence of DBP (figure 17a). When DBP -/- bone marrow neutrophils were allowed to migrate to DBP -/- complement activated serum, there was a striking difference in the morphology of the migrating neutrophils under these conditions as compared to the morphology of DBP +/+ bone marrow neutrophils. Most of the observed DBP -/- bone marrow neutrophils were round, with F-actin present at all poles and with no clear polarized morphology (figure 18a). This is in contrast to DBP +/+ bone marrow neutrophils migrating in the absence of DBP where only a few cells

showed a round morphology but most cells had increase non-polarized actin polymerization (figure 18c). When DBP -/- bone marrow neutrophils were allowed to migrate to DBP +/+ complement activated serum, there was a partial restoration of polarization in most of the migrating neutrophils. This phenotype was similar to the phenotype observed when DBP +/+ bone marrow neutrophils were allowed to migrate to DBP -/- complement activated serum (compare figures 18b and 18c) suggesting only a partial reversal of the polarization defect by exogenous DBP. When DBP +/+ bone marrow neutrophils were allowed to migrate to DBP +/+ complement activated serum, all of the cells showed a polarized morphology with polarized actin polymerization. However, only a small subset of DBP -/- bone marrow neutrophils migrating to DBP +/+ complement activated serum had a similar polarized phenotype. This suggests that the polarization defect in some DBP -/- bone marrow neutrophils is partially reversed by adding extrinsic DBP (compare figures 18b, right panel, and 18d).

The lack of polarized actin polymerization in DBP -/- and DBP +/+ bone marrow neutrophils migrating in the absence of DBP may be due to non-polarized granular exocytosis and/or integrin recycling. As shown in figure 18, it is clear that addition of exogenous DBP can partially restore polarization in DBP -/- neutrophils, confirming the previous results observed in the alveolitis model of inflammation and the under agarose chemotaxis assay. Partial restoration of polarization by DBP might be due to generation of DBP-actin complexes by migrating neutrophils and the induction of S100A8/A9 formation and secretion. Intracellular S100A8/A9 can then increase microtubule polymerization and thus enhance endosomal trafficking, which enhances integrin recycling. As previously mentioned, mouse S100A8/A9 has been previously shown to be chemotactic to mouse neutrophils *in vitro* and *in vivo* [212-215]. Therefore, DBP-actin induced secreted S100A8/A9 can bind to migrating neutrophils and induce chemotaxis.

5.3.e. Superoxide anion generation by DBP -/- bone marrow neutrophils is defective.

In addition to neutrophil migration, S100A8/A9 has been shown to play an important role in the optimal generation of superoxide anions by NADPH oxidase [170-175]. Since DBP was observed to induce the formation of S100A8/A9 in human neutrophils one would hypothesize that if the same is true in bone marrow neutrophils, DBP might influence the superoxide anion generation capacity in DBP +/+ and DBP -/- bone marrow neutrophils. To induce superoxide anion generation in bone marrow neutrophils the receptor dependent stimulus complement activated serum (C5a) was utilized. There was no difference in the generation of superoxide anions between DBP +/+ or DBP -/- bone marrow neutrophils. However, there was a slight increase in the amount of superoxide anions generated when DBP +/+ or DBP -/- bone marrow neutrophils were treated with DBP +/+ complement activated serum as compared to DBP -/- complement activated serum, suggesting that DBP can extrinsically influence the generation of superoxide anions (figure 19a).

The activation of NADPH oxidase is known to be dependent on the translocation of several of its components from neutrophil granules to the plasma membrane (reviewed in [241]). This process is dependent proper granular trafficking and exocytosis. As previously discussed, DBP -/- bone marrow neutrophils might have a defect in granular and endosomal trafficking. Therefore, one would hypothesize that if DBP -/- bone marrow neutrophils were stimulated to produce superoxide anion with a strong receptor independent stimulus, one would observe reduced levels in these neutrophils as compared to DBP +/+ cells. When DBP +/+ and DBP -/- bone marrow neutrophils were treated with 10 ng/ml PMA, there was a significant reduction in the amount of superoxide anions generated in DBP -/- compared to DBP +/+ cells, supporting this hypothesis and suggesting that there might a defect in granular and endosomal trafficking in

DBP -/- bone marrow neutrophils. Alternatively, a decrease in intracellular S100A8/A9 formation in DBP-/- bone marrow neutrophils may lead to reduced NADPH oxidase activity and subsequently to the reduction in superoxide anion generation in these cells.

5.3.f. DBP +/+ and DBP -/- bone marrow neutrophils have a similar phagocytic capacity for complement-opsonized zymosan.

Phagocytes, including neutrophils, monocytes, macrophages and dendritic cells, make up a class of immune cells that are known for their high capacity to phagocytose antigens (pathogens). Phagocytosis is greatly enhanced by the opsonization of pathogens by either antibodies or complement proteins. To study phagocytosis, complement opsonized zymosan or IgG coated beads are used. In macrophages, microtubules are required for the phagocytosis of complement opsonized zymosan and sheep erythrocytes coated with iC3b, but not IgG coated sheep erythrocytes or beads [242,243]. As previously discussed, it is hypothesized that DBP -/- bone marrow neutrophils may have reduced intracellular S100A8/A9 and thus reduced microtubules polymerization. Therefore, opsonized zymosan was utilized to compare the phagocytic capacity of DBP +/+ and DBP -/- bone marrow neutrophils and to determine whether DBP -/- bone marrow neutrophils had any defect in microtubule dependent phagocytosis. As shown in figure 20, there was no observed difference in the phagocytosis of opsonized zymosan particles between DBP +/+ and DBP -/- bone marrow neutrophils suggesting that the intrinsic defect observed in DBP -/- bone marrow neutrophils does not affect their capacity to phagocytose complement opsonized zymosan.

5.4. HL-60 cells as an *in vitro* model for bone marrow neutrophil differentiation to dissect DBP's mechanism of action.

5.4.a. DMSO induces the differentiation of HL-60 cells after 5 days.

To further study the role of DBP in neutrophil differentiation and development, the promyelocytic cell line HL-60 cell was utilized to study differentiation in the presence or absence of DBP. HL-60 cells can be induced to differentiate into myelocytes, metamyelocytes and banded neutrophils by treating them with 1.3% DMSO for 3-6 days [55,56,58]. The differentiation of HL-60 cells was confirmed by assessing the surface expression of the C5a receptor, CD88. As shown in figure 31c, optimal differentiation of HL-60 cells was observed after 4-5 days of incubation with 1.3% DMSO. However, at days 4 and 5, only 5-10% of the differentiated HL-60 cells were viable as assessed by annexin V and PI analysis (figure 31a and data not shown). HL-60 cell death after differentiation has been previously observed [244], and is thought to be due to the down regulation of the anti apoptotic protein bcl-2 during differentiation [245,246]. Therefore for all of the subsequent experiments were performed by differentiating cells for 5 days with DMSO followed by flow cytometric analysis where the live cellular population was gated and analyzed.

5.4.b. Bovine DBP in FBS was inactivated by the incubation of FBS at 4 ºC for 2-3 weeks.

Due to the long duration of time required for the differentiation of HL-60 cells into neutrophil like cells (5 days), the cells must be differentiated in 5% FBS to ensure survival. However, FBS contains a large amount of bovine DBP. Therefore, to study HL-60 cellular differentiation in the presence or absence of DBP, bovine DBP had to be removed or inactivated.

The latter was achieved by incubating FBS at 4 ºC for 2-3 weeks prior to its use for HL-60 differentiation as evident by the inability of bovine DBP to bind to, sequester and block the induction of differentiation of HL-60 cells by 25 OH D_3. Therefore, exogenously added DBP during the differentiation of HL-60 cells to neutrophil-like cells can be used as a model to study the differentiation of bone marrow neutrophils in the DBP -/- mouse.

5.4.c. DBP, DBP-actin complexes and LPS increase the surface expression of CD88 and CD44 and side scatter of differentiating HL-60 cells.

As previously shown and discussed, DBP-actin complexes are generated basally by human neutrophils, which then induce the release of S100A8/A9. Therefore, DBP may affect neutrophil differentiation indirectly by inducing S100A8/A9 heterodimer/heterotetramer formation and release from differentiating or blood neutrophils. S100A8/A9 is known to bind to and signal through TLR4 [22], which has been shown to be expressed on hematopoetic stem cells and granulocyte/macrophage progenitors (GMPs) [247] and HL-60 cells [248]. In addition, S100A8/A9 has been shown to bind to and signal through the ubiquitously expressed RAGE [166]. A role of S100A8/A9 in neutrophil differentiation is supported by the observation that there was a decrease in the number of neutrophils in the bone marrow of S100A9 knockout mice [158]. Therefore, to study the role of DBP, DBP-actin and TLR4 in HL-60 cellular differentiation, HL-60 cells were differentiated in the presence or absence of DBP, DBP-actin or 100 ng/ml of LPS. As shown in figure 33, DBP, DBP-actin complexes and LPS increased the percentage of cells which stained positively for cell surface CD88, increased the surface expression of the adhesion molecule CD44 and increased the side scatter of differentiated HL-60 cells relative to untreated differentiated cells (figure 33a and 33d). This observed difference in differentiation phenotype is

very similar to that observed in the bone marrow of DBP +/+ and DBP -/- mice (figures 11-13). Therefore, this suggests that DBP might play a role in the differentiation of HL-60 and bone marrow cells into neutrophils.

Treatment of HL-60 with LPS, DBP and DBP-actin during differentiation induced a similar differentiation phenotype suggesting that the phenotype observed with the addition of DBP and DBP-actin during differentiation might be due to endotoxin contamination in the purified DBP stock. As shown in figure 34, this possibility was excluded because Polymyxin B only inhibited the action of LPS but not DBP on differentiating HL-60 cells suggesting that that the DBP and DBP-actin induced differentiation phenotype was not due to endotoxin contamination in the purified DBP stock.

5.4.d. DBP enhances the activation of NF-κB IKK signalsome and p38 kinases in differentiating HL60 cells.

Treatment of HL-60 with 100 ng/ml or 10 ng/ml (data not shown) of LPS induced a similar differentiation phenotype as when cells were differentiated in the presence of DBP or DBP-actin complexes, suggesting that the LPS signaling receptor TLR4 might play a role in the induction of this phenotype. DBP-actin complexes induce the secretion of S100A8/A9, a TLR4 agonist [22,23,168]. Therefore, to determine the potential activation of TLR4 by DBP during differentiation of HL-60 cells, the activation (phosphorylation) of NF-κB and MAPK pathways, two pathways which are known to be activated by TLR4 (for a review see [3]), was determined by western blot analysis of cell lysates from HL-60 cells. As shown in figure 35, there was a substantial increase in the amount of phospho IKK α/ß and phospho p38 MAPK detected in DBP treated differentiated HL-60 cells as compared to untreated differentiated HL-60 cells suggesting

that DBP may induce or maintain the differentiation phenotype in part by sustaining the activities of NF-κB and MAPK activating kinases. There are many known activators of the NF-κB and MAPK pathways so it is not known if TLR4 activation triggered these pathways. However, since a similar differentiation phenotype was observed when HL-60 cells were exposed to DBP or LPS, a known TLR4 activator, it was speculated that the activation of the NF-κB and MAPK pathways observed in Figure 35 was due to the indirect activation of TLR4 by DBP through S100A8/A9.

5.4.e. DBP treated differentiating HL-60 cells generate DBP-actin complexes, express S100A8/A9 and are induced to release the S100A8/A9 heterodimer/heterotetramer in response to DBP-actin complexes.

To further test the proposed TLR4 activation by DBP during differentiation, the expression of S100A8/A9, the capacity of HL-60 cells to generate DBP-actin complexes and the capacity of DBP-actin to induce the secretion of S100A8/A9 from differentiated HL-60 cells was determined. Undifferentiated and differentiated HL-60 cells were treated with DBP for 30 minutes at 37°C and the conditioned supernatants were analyzed by native gel electrophoresis for the presence of DBP-actin complexes and S100A8/A9. S100A8/A9 was not detected in undifferentiated HL-60 cells, but after 5 days of DMSO differentiation, HL-60 cells expressed intracellular S100A8/A9 (data not shown). Surprisingly, both undifferentiated and differentiated HL-60 cells generated DBP-actin complexes when treated with DBP (data not shown). This suggests that DBP-actin complexes are generated by HL-60 cells before the induction of S100A8/A9 expression. Finally, the response of undifferentiated and differentiated HL-60 cells to DBP-actin complexes was then determined. As expected, when cells were differentiated with

vitamin D, DMSO, or DMSO + vitamin D, DBP or DBP + vitamin D, DBP-actin induced the release of S100A8/A9 from these cells (figure 36a and 36b) indicating that differentiated HL-60 cells are capable of responding to DBP-actin complexes by releasing S100A8/A9. As previously observed with primary human neutrophils, actin treated differentiated HL-60 cells also released S100A8/A9 suggesting that actin may be the main stimulus for the induction of S100A8/A9 release from both neutrophils and HL-60 cells, independent of DBP. However, as previously discussed, the generation of DBP-actin complexes from neutrophils was dependent on the exogenous presence of DBP (figure 23 and 25). Actin released from necrotic cells is quickly depolymerized by the extracellular actin scavenger system and bound to DBP in circulation [105,106,109,110]. Therefore, in a physiological setting extracellular actin is bound to DBP so the results observed in response to DBP-actin complexes are thought to be physiologically relevant.

5.4.f. TLR4 activity is required for the survival of differentiating HL-60 cells.

TLR4 signals through MyD88 dependent and independent signaling pathways. To the best of my knowledge, TLR4 knockout bone marrow neutrophils were never characterized, and thus role of TLR4 in the maturation and differentiation of bone marrow neutrophils remains unknown. However, an intrinsic migratory defect was observed in bone marrow neutrophils from MyD88 knockout mice due to decreased surface expression of chemoattractant receptors after peritoneal migration of these cells, suggesting a receptor recycling defect similar to what was observed in the DBP -/- mouse [249]. This suggests that TLRs might be required for optimal differentiation of bone marrow neutrophils in mice. Therefore, to examine the requirement of TLR4 in the differentiation of HL-60 cells in the presence of DBP and LPS; TLR4 was specifically inhibited using a specific TLR4 inhibitory peptide, VIPER, which was derived from

the vaccinia virus protein, A46. VIPER has been shown to specifically inhibit both MyD88 dependent and independent signaling pathways of TLR4 by directly binding to the TLR4 adaptors Mal and TRAM [211]. This observed inhibition of TLR4 was specific to VIPER because there was no observed inhibition of TLR4 (or any other TLRs) using a different peptide, CP7, from the A46 protein of a similar length as VIPER. Therefore, to examine the requirement of TLR4 for the DBP and LPS induced differentiation phenotype, HL-60 cells were treated with 20 μM of VIPER, to inhibit TLR4, or CP7, to control for any non-specific effects due to the peptide treatment, during differentiation in the presence or absence of DBP and LPS. To my surprise, there was no cellular survival after 5 days of differentiation of HL-60 cells in the presence of the VIPER peptide (figure 37a). However, differentiated HL-60 cells treated with the control peptide, CP7, were similar to untreated differentiated HL-60 cells suggesting that the cellular death observed in the VIPER treated cells was not due to non-specific toxicity of the peptide treatment (figure 37a, compare the top row to the bottom row). CP7 did not inhibit the differentiation phenotype exerted by DBP or LPS in HL-60 cells (figure 37b). These data suggest that TLR4 activity is required for the survival of HL-60 cells during differentiation. However, the role of TLR4 in the induced differentiation phenotype observed when HL-60 cells are differentiated in the presence of DBP or LPS is not known.

Collectively, these results suggest that when HL-60 cells are differentiated in the presence of DBP, DBP-actin complexes are generated. When differentiating HL-60 begin expressing S100A8/A9, the DBP-actin complexes will then induce the release of S100A8/A9, which subsequently acts in an autocrine/paracrine fashion by binding to and stimulating TLR4. TLR4 stimulation might enhance cellular survival, induce the production of secondary granules

(as evident from the increase in the side scatter) during differentiation and induce higher surface expression of receptors required for optimal neutrophil function.

6. Summary and Conclusion

To summarize, using an alveolitis model of inflammation in DBP +/+ and DBP -/- mice, DBP was required for the optimal recruitment of neutrophils to the site of inflammation. The exogenous addition of DBP in the lungs of DBP -/- mice, or in ex vivo chemotaxis assays partially reversed the phenotype observed in the DBP -/- mice, suggesting that in addition to an extrinsic role of DBP on neutrophils, there was an intrinsic defect in DBP -/- neutrophils. A potential defect in surface expression CD11b, CD44 and CD88 was identified in the bone marrow neutrophil pool of DBP -/- mice. Functionally, DBP -/- bone marrow neutrophils had a polarization and a migratory defect. The defect in the surface expression of CD44 and CD88 reproduced in HL-60 cells differentiated in the absence of DBP, suggesting a role for DBP in neutrophil differentiation. A potential mechanism was then determined by showing that DBP treatment of human neutrophils induced the generation of DBP-actin complexes, which in turn induced the secretion of a pro-inflammatory protein, S100A8/A9. DBP-actin complexes were generated in the BALF of DBP +/+ mice after the induction of alveolitis. In addition, DBP bound to the cell surface of migrating neutrophils, a process that was partially dependent on cell surface actin on the migrating cells. Finally, S100A8/A9 was observed to bind to the surface of migrating neutrophils. Both DBP and S100A8/A9 colocalized at F-actin rich protrusions extending out of the migrating neutrophils suggesting a potential role of these two proteins in neutrophil polarization and migration.

In conclusion, DBP is required for the optimal differentiation of neutrophils in the bone marrow and the optimal migration of neutrophils to the site of inflammation in vivo. DBP might exert its function during inflammation by inducing the generation of DBP-actin complexes at inflammatory sites, which in turn leads to the release of the inflammatory amplifier, S100A8/A9 from migrating neutrophils. This would in turn lead to the amplification of inflammation by activating endothelial cells and macrophages and by recruiting more neutrophils to the site of inflammation.

References

1. Kumagai, Y. & Akira, S. Identification and functions of pattern-recognition receptors. *J. Allergy Clin. Immunol.* **125**, 985–992 (2010).

2. Takeuchi, O. & Akira, S. Pattern recognition receptors and inflammation. *Cell* **140**, 805–820 (2010).

3. Takeda, K. & Akira, S. TLR signaling pathways. *Semin Immunol* **16**, 3–9 (2004).

4. Kawai, T. & Akira, S. TLR signaling. *Cell Death Differ* **13**, 816–825 (2006).

5. Yu, M. *et al.* HMGB1 signals through toll-like receptor (TLR) 4 and TLR2. *Shock* **26**, 174–179 (2006).

6. Okamura, Y. *et al.* The extra domain A of fibronectin activates Toll-like receptor 4. *J Biol Chem* **276**, 10229–10233 (2001).

7. Smiley, S. T., King, J. A. & Hancock, W. W. Fibrinogen stimulates macrophage chemokine secretion through toll-like receptor 4. *J Immunol* **167**, 2887–2894 (2001).

8. Midwood, K. *et al.* Tenascin-C is an endogenous activator of Toll-like receptor 4 that is essential for maintaining inflammation in arthritic joint disease. *Nature medicine* **15**, 774–780 (2009).

9. Guillot, L. *et al.* Cutting edge: the immunostimulatory activity of the lung surfactant protein-A involves Toll-like receptor 4. *J Immunol* **168**, 5989–5992 (2002).

10. Ohya, M. *et al.* Human Pulmonary Surfactant Protein D Binds the Extracellular Domains of Toll-like Receptors 2 and 4 through the Carbohydrate Recognition Domain by a Mechanism Different from Its Binding to Phosphatidylinositol and Lipopolysaccharide †. *Biochemistry* **45**, 8657–8664 (2006).

11. Biragyn, A. *et al.* Toll-like receptor 4-dependent activation of dendritic cells by beta-defensin 2. *Science* **298**, 1025–1029 (2002).

12. Ohashi, K., Burkart, V., Flohé, S. & Kolb, H. Cutting edge: heat shock protein 60 is a putative endogenous ligand of the toll-like receptor-4 complex. *J Immunol* **164**, 558–561 (2000).

13. Asea, A. *et al.* Novel signal transduction pathway utilized by extracellular HSP70: role of toll-like receptor (TLR) 2 and TLR4. *J Biol Chem* **277**, 15028–15034 (2002).

14. Wheeler, D. S. *et al.* Extracellular Hsp72, an endogenous DAMP, is released by virally infected airway epithelial cells and activates neutrophils via Toll-like receptor (TLR)-4.

Respir Res **10**, 31 (2009).

15. Roelofs, M. F. *et al.* Identification of small heat shock protein B8 (HSP22) as a novel TLR4 ligand and potential involvement in the pathogenesis of rheumatoid arthritis. *J Immunol* **176**, 7021–7027 (2006).

16. Warger, T. *et al.* Interaction of TLR2 and TLR4 ligands with the N-terminal domain of Gp96 amplifies innate and adaptive immune responses. *J Biol Chem* **281**, 22545–22553 (2006).

17. Vabulas, R. M. *et al.* The endoplasmic reticulum-resident heat shock protein Gp96 activates dendritic cells via the Toll-like receptor 2/4 pathway. *J Biol Chem* **277**, 20847–20853 (2002).

18. Termeer, C. *et al.* Oligosaccharides of Hyaluronan activate dendritic cells via toll-like receptor 4. *J Exp Med* **195**, 99–111 (2002).

19. Devaney, J. M. *et al.* Neutrophil elastase up-regulates interleukin-8 via toll-like receptor 4. *FEBS Lett* **544**, 129–132 (2003).

20. Curran, C. S., Demick, K. P. & Mansfield, J. M. Lactoferrin activates macrophages via TLR4-dependent and -independent signaling pathways. *Cell. Immunol.* **242**, 23–30 (2006).

21. Johnson, G. B., Brunn, G. J., Kodaira, Y. & Platt, J. L. Receptor-mediated monitoring of tissue well-being via detection of soluble heparan sulfate by Toll-like receptor 4. *J Immunol* **168**, 5233–5239 (2002).

22. Vogl, T. *et al.* Mrp8 and Mrp14 are endogenous activators of Toll-like receptor 4, promoting lethal, endotoxin-induced shock. *Nature medicine* **13**, 1042–1049 (2007).

23. Loser, K. *et al.* The Toll-like receptor 4 ligands Mrp8 and Mrp14 are crucial in the development of autoreactive CD8+ T cells. *Nature medicine* **16**, 713–717 (2010).

24. Feghali, C. A. & Wright, T. M. Cytokines in acute and chronic inflammation. *Front Biosci* **2**, d12–26 (1997).

25. Opal, S. M. & Depalo, V. A. Anti-Inflammatory Cytokines*. *Chest* **117**, 1162–1172 (2000).

26. Serhan, C., Yacoubian, S. & Yang, R. Anti-inflammatory and proresolving lipid mediators. *Annual Review of Pathology: Mechanisms of Diseases* **3,** 279-312 (2008).

27. Epstein, F. H. & Luster, A. D. Chemokines—chemotactic cytokines that mediate inflammation. *The New England journal of medicine* **338**, 436–445 (1998).

28. Baggiolini, M., Walz, A. & Kunkel, S. L. Neutrophil-activating peptide-1/interleukin 8, a novel cytokine that activates neutrophils. *J Clin Invest* **84**, 1045–1049 (1989).

29. Palmblad, J. *et al.* Leukotriene B4 is a potent and stereospecific stimulator of neutrophil chemotaxis and adherence. *Blood* **58**, 658–661 (1981).

30. Carolan, E. J. & Casale, T. B. Degree of platelet activating factor-induced neutrophil migration is dependent upon the molecular species. *J Immunol* **145**, 2561–2565 (1990).

31. Shaw, J., Pinckard, R., Ferrigni, K., McManus, L. & Hanahan, D. Activation of human neutrophils with 1-O-hexadecyl/octadecyl-2-acetyl-sn-glycerol-3-phosphorylcholine (platelet activating factor). *J Immunol* **127**, 1250 (1981).

32. Balamayooran, G., Batra, S., Balamayooran, T., Cai, S. & Jeyaseelan, S. Monocyte chemoattractant protein 1 regulates pulmonary host defense via neutrophil recruitment during Escherichia coli infection. *Infection and Immunity* **79**, 2567–2577 (2011).

33. Wolpe, S. D. *et al.* Identification and characterization of macrophage inflammatory protein 2. *Proc Natl Acad Sci USA* **86**, 612–616 (1989).

34. Okinaga, S. *et al.* C5L2, a Nonsignaling C5A Binding Protein †. *Biochemistry* **42**, 9406–9415 (2003).

35. Yancey, K. B. Biological properties of human C5a: selected in vitro and in vivo studies. *Clin Exp Immunol* **71**, 207–210 (1988).

36. Riedemann, N. C. *et al.* Regulation by C5a of neutrophil activation during sepsis. *Immunity* **19**, 193–202 (2003).

37. Huber-Lang, M. S. *et al.* Complement-induced impairment of innate immunity during sepsis. *J Immunol* **169**, 3223–3231 (2002).

38. Seely, A. J. E. *et al.* Alteration of chemoattractant receptor expression regulates human neutrophil chemotaxis in vivo. *Ann. Surg.* **235**, 550–559 (2002).

39. Solomkin, J. S., Jenkins, M. K., Nelson, R. D., Chenoweth, D. & Simmons, R. L. Neutrophil dysfunction in sepsis. II. Evidence for the role of complement activation products in cellular deactivation. *Surgery* **90**, 319–327 (1981).

40. Gomez-Cambronero, J., Di Fulvio, M. & Knapek, K. Understanding phospholipase D (PLD) using leukocytes: PLD involvement in cell adhesion and chemotaxis. *J Leukoc Biol* **82**, 272–281 (2007).

41. Perianayagam, M. C., Balakrishnan, V. S., King, A. J., Pereira, B. J. G. & Jaber, B. L. C5a delays apoptosis of human neutrophils by a phosphatidylinositol 3-kinase-signaling pathway. *Kidney Int* **61**, 456–463 (2002).

42. Lee, H., Whitfeld, P. L. & Mackay, C. R. Receptors for complement C5a. The importance of C5aR and the enigmatic role of C5L2. *Immunol Cell Biol* **86**, 153–160 (2008).

43. Guo, R.-F., Riedemann, N. C. & Ward, P. A. Role of C5a-C5aR Interaction in Sepsis. *Shock* **21**, 1 (2004).

44. Bamberg, C. E. *et al.* The C5a receptor (C5aR) C5L2 is a modulator of C5aR-mediated signal transduction. *J Biol Chem* **285**, 7633–7644 (2010).

45. Pillay, J. *et al.* In vivo labeling with 2H2O reveals a human neutrophil lifespan of 5.4 days. *Blood* **116**, 625–627 (2010).

46. Borregaard, N. & Cowland, J. B. Granules of the human neutrophilic polymorphonuclear leukocyte. *Blood* **89**, 3503–3521 (1997).

47. Faurschou, M. & Borregaard, N. Neutrophil granules and secretory vesicles in inflammation. *Microbes Infect.* **5**, 1317–1327 (2003).

48. Le Cabec, V., Cowland, J. B., Calafat, J. & Borregaard, N. Targeting of proteins to granule subsets is determined by timing and not by sorting: the specific granule protein NGAL is localized to azurophil granules when expressed in HL-60 cells. *Proc Natl Acad Sci USA* **93**, 6454 (1996).

49. Bainton, D. F. & Farquhar, M. G. Origin of granules in polymorphonuclear leukocytes. Two types derived from opposite faces of the Golgi complex in developing granulocytes. *J Cell Biol* **28**, 277–301 (1966).

50. Bainton, D. F., Ullyot, J. L. & Farquhar, M. G. The development of neutrophilic polymorphonuclear leukocytes in human bone marrow. *J Exp Med* **134**, 907–934 (1971).

51. Brederoo, P., van der Meulen, J. & Mommaas-Kienhuis, A. M. Development of the granule population in neutrophil granulocytes from human bone marrow. *Cell Tissue Res.* **234**, 469–496 (1983).

52. Joiner, K. A., Ganz, T., Albert, J. & Rotrosen, D. The opsonizing ligand on Salmonella typhimurium influences incorporation of specific, but not azurophil, granule constituents into neutrophil phagosomes. *J Cell Biol* **109**, 2771–2782 (1989).

53. Gallagher, R. *et al.* Characterization of the continuous, differentiating myeloid cell line (HL-60) from a patient with acute promyelocytic leukemia. *Blood* **54**, 713–733 (1979).

54. Breitman, T. R., Collins, S. J. & Keene, B. R. Replacement of serum by insulin and transferrin supports growth and differentiation of the human promyelocytic cell line, HL-60. *Exp Cell Res* **126**, 494–498 (1980).

55. Collins, S. J., Ruscetti, F. W., Gallagher, R. E. & Gallo, R. C. Terminal differentiation of human promyelocytic leukemia cells induced by dimethyl sulfoxide and other polar compounds. *Proc Natl Acad Sci USA* **75**, 2458–2462 (1978).

56. Collins, S. J., Ruscetti, F. W., Gallagher, R. E. & Gallo, R. C. Normal functional characteristics of cultured human promyelocytic leukemia cells (HL-60) after induction of differentiation by dimethylsulfoxide. *J Exp Med* **149**, 969–974 (1979).

57. Breitman, T. R., Selonick, S. E. & Collins, S. J. Induction of differentiation of the human promyelocytic leukemia cell line (HL-60) by retinoic acid. *Proc Natl Acad Sci USA* **77**, 2936–2940 (1980).

58. Brackman, D., Lund-Johansen, F. & Aarskog, D. Expression of cell surface antigens during the differentiation of HL-60 cells induced by 1,25-dihydroxyvitamin D3, retinoic acid and DMSO. *Leukemia Research* **19**, 57–64 (1995).

59. Miyaura, C. *et al.* 1α,25-Dihydroxyvitamin D3 induces differentiation of human myeloid leukemia cells. *Biochem Biophys Res Commun* **102**, 937–943 (1981).

60. Mangelsdorf, D. J., Koeffler, H. P., Donaldson, C. A., Pike, J. W. & Haussler, M. R. 1,25-Dihydroxyvitamin D3-induced differentiation in a human promyelocytic leukemia cell line (HL-60): receptor-mediated maturation to macrophage-like cells. *J Cell Biol* **98**, 391–398 (1984).

61. Mccarthy, D. M. *et al.* 1,25-dihydroxyvitamin D3 inhibits proliferation of human promyelocytic leukaemia (HL60) cells and induces monocyte-macrophage differentiation in HL60 and normal human bone marrow cells. *Leukemia Research* **7**, 51–55 (1983).

62. Rovera, G., Santoli, D. & Damsky, C. Human promyelocytic leukemia cells in culture differentiate into macrophage-like cells when treated with a phorbol diester. *Proc Natl Acad Sci USA* **76**, 2779–2783 (1979).

63. Rovera, G., O'Brien, T. & Diamond, L. Induction of differentiation in human promyelocytic leukemia cells by tumor promoters. *Science* **204**, 868–870 (1979).

64. Olsson, I. & Olofsson, T. Induction of differentiation in a human promyelocytic leukemic cell line (HL-60). Production of granule proteins. *Exp Cell Res* **131**, 225–230 (1981).

65. Johnston, J. J. *et al.* Lactoferrin gene promoter: structural integrity and nonexpression in HL60 cells. *Blood* **79**, 2998–3006 (1992).

66. Le Cabec, V. & Calafat, J. Sorting of the Specific Granule Protein, NGAL, During Granulocytic Maturation of HL-60 Cells. *Blood* (1997).

67. Hauert, A. B., Martinelli, S., Marone, C. & Niggli, V. Differentiated HL-60 cells are a valid model system for the analysis of human neutrophil migration and chemotaxis. *Int J Biochem Cell Biol* **34**, 838–854 (2002).

68. Birnie, G. D. The HL60 cell line: a model system for studying human myeloid cell differentiation. *The British Journal of Cancer. Supplement* **9**, 41 (1988).

69. Carlos, T. M. & Harlan, J. M. Leukocyte-endothelial adhesion molecules. *Blood* **84**, 2068–2101 (1994).

70. Norman, K., Moore, K., McEver, R. & Ley, K. Leukocyte rolling in vivo is mediated by P-selectin glycoprotein ligand-1. *Blood* **96**, 3585-3591 (1995).

71. Middleton, J. *et al.* Transcytosis and surface presentation of IL-8 by venular endothelial cells. *Cell* **91**, 385–395 (1997).

72. Zimmerman, G. A., McIntyre, T. M., Mehra, M. & Prescott, S. M. Endothelial cell-associated platelet-activating factor: a novel mechanism for signaling intercellular adhesion. *J Cell Biol* **110**, 529–540 (1990).

73. Huber, A. R., Kunkel, S. L., Todd, R. F. & Weiss, S. J. Regulation of transendothelial neutrophil migration by endogenous interleukin-8. *Science* **254**, 99–102 (1991).

74. Singer, I. I., Scott, S., Kawka, D. W. & Kazazis, D. M. Adhesomes: specific granules containing receptors for laminin, C3bi/fibrinogen, fibronectin, and vitronectin in human polymorphonuclear leukocytes and monocytes. *J Cell Biol* **109**, 3169–3182 (1989).

75. Sengeløv, H., Kjeldsen, L., Diamond, M. S., Springer, T. A. & Borregaard, N. Subcellular localization and dynamics of Mac-1 (alpha m beta 2) in human neutrophils. *J Clin Invest* **92**, 1467–1476 (1993).

76. Borregaard, N. *et al.* Changes in subcellular localization and surface expression of L-selectin, alkaline phosphatase, and Mac-1 in human neutrophils during stimulation with inflammatory mediators. *J Leukoc Biol* **56**, 80–87 (1994).

77. Delclaux, C. *et al.* Role of gelatinase B and elastase in human polymorphonuclear neutrophil migration across basement membrane. *American journal of respiratory cell and molecular biology* **14**, 288–295 (1996).

78. Phillipson, M. & Kubes, P. The neutrophil in vascular inflammation. *Nature medicine* **17**, 1381–1390 (2011).

79. Prince, L. R., Whyte, M. K., Sabroe, I. & Parker, L. C. The role of TLRs in neutrophil activation. *Curr Opin Pharmacol* **11**, 397–403 (2011).

80. Funamoto, S., Meili, R., Lee, S., Parry, L. & Firtel, R. A. Spatial and temporal regulation of 3-phosphoinositides by PI 3-kinase and PTEN mediates chemotaxis. *Cell* **109**, 611–623 (2002).

81. Nishio, M. *et al.* Control of cell polarity and motility by the PtdIns(3,4,5)P3 phosphatase SHIP1. *Nat. Cell Biol.* **9**, 36–44 (2007).

82. Robert H Insall, O. D. W. PIP3, PIP2, and Cell Movement—Similar Messages, Different Meanings? *Developmental cell* **1**, 743 (2001).

83. Eddy, R. J., Pierini, L. M. & Maxfield, F. R. Microtubule asymmetry during neutrophil polarization and migration. *Mol Biol Cell* **13**, 4470–4483 (2002).

84. Jog, N. R. *et al.* The actin cytoskeleton regulates exocytosis of all neutrophil granule subsets. *AJP - Cell Physiology* **292**, C1690–C1700 (2007).

85. Yan, S. R. & Berton, G. Antibody-induced engagement of beta2 integrins in human neutrophils causes a rapid redistribution of cytoskeletal proteins, Src-family tyrosine kinases, and p72syk that precedes de novo actin polymerization. *J Leukoc Biol* **64**, 401–408 (1998).

86. Walzog, B., Seifert, R., Zakrzewicz, A., Gaehtgens, P. & Ley, K. Cross-linking of CD18 in human neutrophils induces an increase of intracellular free Ca2+, exocytosis of azurophilic granules, quantitative up-regulation of CD18, shedding of L-selectin, and actin polymerization. *J Leukoc Biol* **56**, 625–635 (1994).

87. Anderson, D. C. & Springer, T. A. Leukocyte Adhesion Deficiency: An Inherited Defect in the Mac-1, LFA-1, and p150,95 Glycoproteins. *Annu. Rev. Med.* **38**, 175–194 (1987).

88. Bergin, D. A. *et al.* α-1 Antitrypsin regulates human neutrophil chemotaxis induced by soluble immune complexes and IL-8. *J Clin Invest* **120**, 4236–4250 (2010).

89. Webb, L. M., Ehrengruber, M. U., Clark-Lewis, I., Baggiolini, M. & Rot, A. Binding to heparan sulfate or heparin enhances neutrophil responses to interleukin 8. *Proc Natl Acad Sci USA* **90**, 7158 (1993).

90. Simpkins, C. O., Dickey, C. A. & Fink, M. P. Human neutrophil migration is enhanced by beta-endorphin. *Life Sci* **34**, 2251–2255 (1984).

91. Van Epps, D. E., Wiik, A., Garcia, M. L. & Williams, R. C. Enhancement of human neutrophil migration by prostaglandin E2. *Cell. Immunol.* **37**, 142–150 (1978).

92. Kew, R. & Webster, R. Gc-globulin (vitamin D-binding protein) enhances the neutrophil chemotactic activity of C5a and C5a des Arg. *Journal of Clinical Investigation* **82**, 364-369 (1988).

93. Perez, H. D., Kelly, E., Chenoweth, D. & Elfman, F. Identification of the C5a des Arg cochemotaxin. Homology with vitamin D-binding protein (group-specific component globulin). *J Clin Invest* **82**, 360–363 (1988).

94. Kawakami, M., Blum, C. B., Ramakrishnan, R., Dell, R. B. & Goodman, D. S. Turnover of the Plasma Binding Protein for Vitamin D and Its Metabolites in Normal Human Subjects. *The Journal of clinical endocrinology and metabolism* **53**, 1110–1116 (1981).

95. Ray, K., Wang, X., Zhao, M. & Cooke, N. The rat vitamin D binding protein (Gc-globulin) gene. Structural analysis, functional and evolutionary correlations. *Journal of Biological Chemistry* **266**, 6221-6229 (1991).

96. Ena, J., Esteban, C., Perez, M., Uriel, J. & Calvo, M. Fatty acids bound to vitamin D-binding protein (DBP) from human and bovine sera. *Biochem Int* **19**, 1–7 (1989).

97. Rehder, D. S., Nelson, R. W. & Borges, C. R. Glycosylation status of vitamin D binding protein in cancer patients. *Protein Science* **18**, 2036–2042 (2009).

98. Daiger, S. P., Schanfield, M. S. & Cavalli-Sforza, L. L. Group-specific component (Gc) proteins bind vitamin D and 25-hydroxyvitamin D. *Proc Natl Acad Sci USA* **72**, 2076–2080 (1975).

99. Cooke, N. & Haddad, J. Vitamin D binding protein (Gc-globulin). *Endocrine reviews* **10**, 294-307 (1989).

100. Zella, L. A., Shevde, N. K., Hollis, B. W., Cooke, N. E. & Pike, J. W. Vitamin D-Binding Protein Influences Total Circulating Levels of 1,25-Dihydroxyvitamin D3 but Does Not Directly Modulate the Bioactive Levels of the Hormone in Vivo. *Endocrinology* **149**, 3656–3667 (2008).

101. Nykjaer, A. *et al.* Cubilin dysfunction causes abnormal metabolism of the steroid hormone 25 (OH) vitamin D3. *Proc Natl Acad Sci USA* **98**, 13895-13900 (2001).

102. Nykjaer, A. *et al.* An Endocytic Pathway Essential for Renal Uptake and Activation of the Steroid 25-(OH) Vitamin D3. *Cell* **96**, 507–515 (1999).

103. Safadi, F. F. *et al.* Osteopathy and resistance to vitamin D toxicity in mice null for vitamin D binding protein. *J Clin Invest* **103**, 239–251 (1999).

104. Lee, W. M. & Galbraith, R. M. The extracellular actin-scavenger system and actin toxicity. *The New England journal of medicine* **326**, 1335–1341 (1992).

105. Harper, K. D., McLeod, J. F., Kowalski, M. A. & Haddad, J. G. Vitamin D binding protein sequesters monomeric actin in the circulation of the rat. *J Clin Invest* **79**, 1365–1370 (1987).

106. Lind, S. E., Smith, D. B., Janmey, P. A. & Stossel, T. P. Role of plasma gelsolin and the vitamin D-binding protein in clearing actin from the circulation. *J Clin Invest* **78**, 736–742 (1986).

107. Kwiatkowski, D. J., Mehl, R., Izumo, S., Nadal-Ginard, B. & Yin, H. L. Muscle is the major source of plasma gelsolin. *J Biol Chem* **263**, 8239–8243 (1988).

108. Harris, H. & Weeds, A. Plasma gelsolin caps and severs actin filaments. *FEBS Lett* **177**, 184–188 (1984).

109. Janmey, P. A., Stossel, T. P. & Lind, S. E. Sequential binding of actin monomers to plasma gelsolin and its inhibition by vitamin D-binding protein. *Biochem Biophys Res Commun* **136**, 72–79 (1986).

110. van Baelen, H., Bouillon, R. & De Moor, P. Vitamin D-binding protein (Gc-globulin) binds actin. *J Biol Chem* **255**, 2270–2272 (1980).

111. Yamamoto, N. & Kumashiro, R. Conversion of vitamin D3 binding protein (group-specific component) to a macrophage activating factor by the stepwise action of beta-galactosidase of B cells and sialidase of T cells. *J Immunol* **151**, 2794–2802 (1993).

112. Kanda, S., Mochizuki, Y., Miyata, Y., Kanetake, H. & Yamamoto, N. Effects of Vitamin D3-Binding Protein-Derived Macrophage Activating Factor (GcMAF) on Angiogenesis. *JNCI Journal of the National Cancer Institute* **94**, 1311 (2002).

113. Kalkunte, S., Brard, L., Granai, C. O. & Swamy, N. Inhibition of angiogenesis by vitamin D-binding protein: characterization of anti-endothelial activity of DBP-maf. *Angiogenesis* **8**, 349–360 (2005).

114. Kisker, O. *et al.* Vitamin D binding protein-macrophage activating factor (DBP-maf) inhibits angiogenesis and tumor growth in mice. *Neoplasia* **5**, 32–40 (2003).

115. Metcalf, J. P. *et al.* GcGlobulin Functions as a Cochemotaxin in the Lower Respiratory Tract: A Potential Mechanism for Lung Neutrophil Recruitment in Cigarette Smokers. *American Journal of Respiratory and Critical Care Medicine* **143**, 844-849 (1991).

116. Robbins, R. A. & Hamel, F. G. Chemotactic factor inactivator interaction with Gc-globulin (vitamin D-binding protein). A mechanism of modulating the chemotactic activity of C5a. *J Immunol* **144**, 2371–2376 (1990).

117. Kew, R., Mollison, K. & Webster, R. Binding of Gc globulin (vitamin D binding protein) to C5a or C5a des Arg is not necessary for co-chemotactic activity. *J Leukoc Biol* **58**, 55–58 (1995).

118. Kew, R. R., Fisher, J. A. & Webster, R. O. Co-chemotactic effect of Gc-globulin (vitamin D binding protein) for C5a. Transient conversion into an active co-chemotaxin

by neutrophils. *J Immunol* **155**, 5369–5374 (1995).

119. Binder, R., Kress, A., Kan, G., Herrmann, K. & Kirschfink, M. Neutrophil priming by cytokines and vitamin D binding protein (Gc-globulin): impact on C5a-mediated chemotaxis, degranulation and respiratory burst. *Mol Immunol* **36**, 885–892 (1999).

120. Piquette, C. A., Robinson-Hill, R. & Webster, R. O. Human monocyte chemotaxis to complement-derived chemotaxins is enhanced by Gc-globulin. *J Leukoc Biol* **55**, 349–354 (1994).

121. Senior, R. M., Griffin, G., Perez, H. & Webster, R. Human C5a and C5a des Arg exhibit chemotactic activity for fibroblasts. *J Immunol* **141**, 3570-3574 (1988).

122. Trujillo, G. *et al.* Cofactor regulation of C5a chemotactic activity in physiological fluids. Requirement for the vitamin D binding protein, thrombospondin-1 and its receptors. *Mol Immunol* **49**, 495–503 (2011).

123. Trujillo, G. & Kew, R. R. Platelet-derived thrombospondin-1 is necessary for the vitamin D-binding protein (Gc-globulin) to function as a chemotactic cofactor for C5a. *J Immunol* **173**, 4130–4136 (2004).

124. Kew, R. R., Sibug, M. A., Liuzzo, J. P. & Webster, R. O. Localization and quantitation of the vitamin D binding protein (Gc-globulin) in human neutrophils. *Blood* **82**, 274–283 (1993).

125. DiMartino, S. J. & Kew, R. R. Initial characterization of the vitamin D binding protein (Gc-globulin) binding site on the neutrophil plasma membrane: evidence for a chondroitin sulfate proteoglycan. *J Immunol* **163**, 2135–2142 (1999).

126. DiMartino, S. J., Shah, A. B., Trujillo, G. & Kew, R. R. Elastase controls the binding of the vitamin D-binding protein (Gc-globulin) to neutrophils: a potential role in the regulation of C5a co-chemotactic activity. *J Immunol* **166**, 2688–2694 (2001).

127. McVoy, L. A. & Kew, R. R. CD44 and annexin A2 mediate the C5a chemotactic cofactor function of the vitamin D binding protein. *J Immunol* **175**, 4754–4760 (2005).

128. Zhang, J., Habiel, D. M., Ramadass, M. & Kew, R. R. Identification of two distinct cell binding sequences in the vitamin D binding protein. *Biochim Biophys Acta* **1803**, 623–629 (2010).

129. Neame, S. J., Uff, C. R., Sheikh, H., Wheatley, S. C. & Isacke, C. M. CD44 exhibits a cell type dependent interaction with triton X-100 insoluble, lipid rich, plasma membrane domains. *Journal of Cell Science* **108 (Pt 9)**, 3127–3135 (1995).

130. Perschl, A., Lesley, J., English, N., Hyman, R. & Trowbridge, I. S. Transmembrane domain of CD44 is required for its detergent insolubility in fibroblasts. *Journal of Cell*

Science **108 (Pt 3)**, 1033–1041 (1995).

131. Lesley, J., Kincade, P. W. & Hyman, R. Antibody-induced activation of the hyaluronan receptor function of CD44 requires multivalent binding by antibody. *Eur. J. Immunol.* **23**, 1902–1909 (1993).

132. Meran, S. *et al.* Hyaluronan facilitates transforming growth factor-β1-dependent proliferation via CD44 and epidermal growth factor receptor interaction. *J Biol Chem* **286**, 17618–17630 (2011).

133. Baaten, B. J. G. *et al.* CD44 regulates survival and memory development in Th1 cells. *Immunity* **32**, 104–115 (2010).

134. Guan, H., Nagarkatti, P. S. & Nagarkatti, M. Role of CD44 in the differentiation of Th1 and Th2 cells: CD44-deficiency enhances the development of Th2 effectors in response to sheep RBC and chicken ovalbumin. *J Immunol* **183**, 172–180 (2009).

135. Schmits, R. *et al.* CD44 regulates hematopoietic progenitor distribution, granuloma formation, and tumorigenicity. *Blood* **90**, 2217–2233 (1997).

136. Kawana, H. *et al.* CD44 suppresses TLR-mediated inflammation. *J Immunol* **180**, 4235–4245 (2008).

137. Ponta, H., Sherman, L. & Herrlich, P. A. CD44: From adhesion molecules to signalling regulators. *Nat Rev Mol Cell Biol* **4**, 33–45 (2003).

138. Yu, W. H. CD44 anchors the assembly of matrilysin/MMP-7 with heparin-binding epidermal growth factor precursor and ErbB4 and regulates female reproductive organ remodeling. *Genes Dev.* **16**, 307–323 (2002).

139. Yu, Q. & Stamenkovic, I. Cell surface-localized matrix metalloproteinase-9 proteolytically activates TGF-beta and promotes tumor invasion and angiogenesis. *Genes Dev.* **14**, 163–176 (2000).

140. Kajita, M. *et al.* Membrane-type 1 matrix metalloproteinase cleaves CD44 and promotes cell migration. *J Cell Biol* **153**, 893–904 (2001).

141. Anderegg, U. *et al.* ADAM10 Is the Constitutive Functional Sheddase of CD44 in Human Melanoma Cells. *J. Invest. Dermatol.* **129**, 1471–1482 (2008).

142. Peterson, R. M., Yu, Q., Stamenkovic, I. & Toole, B. P. Perturbation of hyaluronan interactions by soluble CD44 inhibits growth of murine mammary carcinoma cells in ascites. *Am J Pathol* **156**, 2159–2167 (2000).

143. Yu, Q. Induction of Apoptosis of Metastatic Mammary Carcinoma Cells In Vivo by Disruption of Tumor Cell Surface CD44 Function. *Journal of Experimental Medicine*

186, 1985–1996 (1997).

144. Lammich, S. Presenilin-dependent Intramembrane Proteolysis of CD44 Leads to the Liberation of Its Intracellular Domain and the Secretion of an Abeta -like Peptide. *Journal of Biological Chemistry* **277**, 44754–44759 (2002).

145. Okamoto, I. Proteolytic release of CD44 intracellular domain and its role in the CD44 signaling pathway. *J Cell Biol* **155**, 755–762 (2001).

146. Ward, P. A. The dark side of C5a in sepsis. *Nat Rev Immunol* **4**, 133–142 (2004).

147. Hessian, P., Edgeworth, J. & Hogg, N. MRP-8 and MRP-14, two abundant Ca(2+)-binding proteins of neutrophils and monocytes. *J Leukoc Biol* **53**, 197-204 (1993).

148. Dale, I., Fagerhol, M. K. & Naesgaard, I. Purification and partial characterization of a highly immunogenic human leukocyte protein, the L1 antigen. *Eur J Biochem* **134**, 1–6 (1983).

149. Leukert, N., Sorg, C. & Roth, J. Molecular basis of the complex formation between the two calcium-binding proteins S100A8 (MRP8) and S100A9 (MRP14). *Biol Chem* **386**, 429–434 (2005).

150. Pröpper, C., Huang, X., Roth, J., Sorg, C. & Nacken, W. Analysis of the MRP8-MRP14 protein-protein interaction by the two-hybrid system suggests a prominent role of the C-terminal domain of S100 proteins in dimer formation. *J Biol Chem* **274**, 183–188 (1999).

151. Strupat, K., Rogniaux, H., Van Dorsselaer, A., Roth, J. & Vogl, T. Calcium-induced noncovalently linked tetramers of MRP8 and MRP14 are confirmed by electrospray ionization-mass analysis. *J. Am. Soc. Mass Spectrom.* **11**, 780–788 (2000).

152. Korndörfer, I. P., Brueckner, F. & Skerra, A. The Crystal Structure of the Human (S100A8/S100A9)2 Heterotetramer, Calprotectin, Illustrates how Conformational Changes of Interacting α-Helices Can Determine Specific Association of Two EF-hand Proteins. *Journal of Molecular Biology* **370**, 887–898 (2007).

153. Roth, J. *et al.* MRP8 and MRP14, S-100-like proteins associated with myeloid differentiation, are translocated to plasma membrane and intermediate filaments in a calcium-dependent manner. *Blood* **82**, 1875–1883 (1993).

154. Roth, J. Myeloid-related Protein (MRP) 8and MRP14, Calcium-binding Proteins of the S100 Family, Are Secreted by Activated Monocytes via a Novel, Tubulin-dependent Pathway. *Journal of Biological Chemistry* **272**, 9496–9502 (1997).

155. Vogl, T. *et al.* MRP8 and MRP14 control microtubule reorganization during transendothelial migration of phagocytes. *Blood* **104**, 4260–4268 (2004).

156. Hetland, G., Talgö, G. J. & Fagerhol, M. K. Chemotaxins C5a and fMLP induce release of calprotectin (leucocyte L1 protein) from polymorphonuclear cells in vitro. *MP, Mol Pathol* **51**, 143–148 (1998).

157. Frosch, M. *et al.* Myeloid-related proteins 8 and 14 are specifically secreted during interaction of phagocytes and activated endothelium and are useful markers for monitoring disease activity in pauciarticular-onset juvenile rheumatoid arthritis. *Arthritis Rheum* **43**, 628–637 (2000).

158. Manitz, M. P. *et al.* Loss of S100A9 (MRP14) results in reduced interleukin-8-induced CD11b surface expression, a polarized microfilament system, and diminished responsiveness to chemoattractants in vitro. *Mol Cell Biol* **23**, 1034–1043 (2003).

159. Srikrishna, G. *et al.* Two proteins modulating transendothelial migration of leukocytes recognize novel carboxylated glycans on endothelial cells. *J Immunol* **166**, 4678–4688 (2001).

160. Robinson, M. J., Tessier, P., Poulsom, R. & Hogg, N. The S100 family heterodimer, MRP-8/14, binds with high affinity to heparin and heparan sulfate glycosaminoglycans on endothelial cells. *J Biol Chem* **277**, 3658–3665 (2002).

161. Kerkhoff, C., Sorg, C., Tandon, N. N. & Nacken, W. Interaction of S100A8/S100A9-arachidonic acid complexes with the scavenger receptor CD36 may facilitate fatty acid uptake by endothelial cells. *Biochemistry* **40**, 241–248 (2001).

162. Viemann, D. *et al.* Myeloid-related proteins 8 and 14 induce a specific inflammatory response in human microvascular endothelial cells. *Blood* **105**, 2955–2962 (2005).

163. Ryckman, C., Vandal, K., Rouleau, P., Talbot, M. & Tessier, P. A. Proinflammatory activities of S100: proteins S100A8, S100A9, and S100A8/A9 induce neutrophil chemotaxis and adhesion. *J Immunol* **170**, 3233–3242 (2003).

164. Simard, J. C., Girard, D. & Tessier, P. A. Induction of neutrophil degranulation by S100A9 via a MAPK-dependent mechanism. *J Leukoc Biol* **87**, 905–914 (2010).

165. Newton, R. and Hogg, N. The Human S100 Protein MRP-14 Is a Novel Activator of the ß2 Integrin Mac-1 on Neutrophils. *The Journal of Immunology* **160**, 1427-1435 (1998).

166. Ghavami, S. *et al.* S100A8/A9 at low concentration promotes tumor cell growth via RAGE ligation and MAP kinase-dependent pathway. *J Leukoc Biol* **83**, 1484–1492 (2008).

167. Turovskaya, O. *et al.* RAGE, carboxylated glycans and S100A8/A9 play essential roles in colitis-associated carcinogenesis. *Carcinogenesis* **29**, 2035–2043 (2008).

168. Yonekawa, K. *et al.* Myeloid related proteins activate Toll-like receptor 4 in human

acute coronary syndromes. *Atherosclerosis* **218**, 486-492 (2011).

169. Grevers, L. C. *et al.* S100A8 enhances osteoclastic bone resorption in vitro through activation of Toll-like receptor 4: implications for bone destruction in murine antigen-induced arthritis. *Arthritis Rheum* **63**, 1365–1375 (2011).

170. Doussiere, J., Bouzidi, F. & Vignais, P. V. The S100A8/A9 protein as a partner for the cytosolic factors of NADPH oxidase activation in neutrophils. *Eur J Biochem* **269**, 3246–3255 (2002).

171. Berthier, S. *et al.* Changing the conformation state of cytochrome b558 initiates NADPH oxidase activation: MRP8/MRP14 regulation. *J Biol Chem* **278**, 25499–25508 (2003).

172. Bouzidi, F. & Doussiere, J. Binding of arachidonic acid to myeloid-related proteins (S100A8/A9) enhances phagocytic NADPH oxidase activation☆. *Biochem Biophys Res Commun* **325**, 1060–1065 (2004).

173. Kerkhoff, C. *et al.* The arachidonic acid-binding protein S100A8/A9 promotes NADPH oxidase activation by interaction with p67phox and Rac-2. *FASEB J* **19**, 467–469 (2005).

174. Paclet, M.-H., Berthier, S., Kuhn, L., Garin, J. & Morel, F. Regulation of phagocyte NADPH oxidase activity: identification of two cytochrome b558 activation states. *FASEB J* **21**, 1244–1255 (2007).

175. Berthier, S., Baillet, A., Paclet, M.-H., Gaudin, P. & Morel, F. How Important are S100A8/S100A9 Calcium Binding Proteins for the Activation of Phagocyte NADPH Oxidase, Nox2. (2009).

176. Klempt, M. *et al.* The heterodimer of the Ca2+-binding proteins MRP8 and MRP14 binds to arachidonic acid. *FEBS Lett* **408**, 81–84 (1997).

177. Siegenthaler, G. *et al.* A heterocomplex formed by the calcium-binding proteins MRP8 (S100A8) and MRP14 (S100A9) binds unsaturated fatty acids with high affinity. *J Biol Chem* **272**, 9371–9377 (1997).

178. Rector, C. L. & Murphy, R. C. Determination of Leukotriene A4 stabilization by S100A8/A9 proteins Using Mass spectrometry. *J Lipid Res* **50**, 2064-2071 (2009).

179. Roulin, K. *et al.* The fatty acid-binding heterocomplex FA-p34 formed by S100A8 and S100A9 is the major fatty acid carrier in neutrophils and translocates from the cytosol to the membrane upon stimulation. *Exp Cell Res* **247**, 410–421 (1999).

180. Passey, R. J. *et al.* A null mutation in the inflammation-associated S100 protein S100A8 causes early resorption of the mouse embryo. *J Immunol* **163**, 2209–2216 (1999).

181. Nacken, W. & Kerkhoff, C. The hetero-oligomeric complex of the S100A8/S100A9 protein is extremely protease resistant. *FEBS Lett* **581**, 5127–5130 (2007).

182. Sunahori, K. *et al.* The S100A8/A9 heterodimer amplifies proinflammatory cytokine production by macrophages via activation of nuclear factor kappa B and p38 mitogen-activated protein kinase in rheumatoid arthritis. *Arthritis Res. Ther.* **8**, R69 (2006).

183. Baumann, M. *et al.* MRP8/14 is associated with systemic inflammation in stable coronary atherosclerosis in men. *Eur J Clin Invest* **41**, 1261-1267 (2011).

184. Farris, S. D. *et al.* Mechanisms of urokinase plasminogen activator (uPA)-mediated atherosclerosis: Role of the uPA receptor and S100A8/A9 proteins. *J Biol Chem* **286**, 22665-22677 (2011).

185. Peng, W. H. *et al.* Increased serum myeloid-related protein 8/14 level is associated with atherosclerosis in type 2 diabetic patients. *Cardiovasc Diabetol* **10**, 41 (2011).

186. Altwegg, L. A. *et al.* Myeloid-related protein 8/14 complex is released by monocytes and granulocytes at the site of coronary occlusion: a novel, early, and sensitive marker of acute coronary syndromes. *Eur. Heart J.* **28**, 941–948 (2007).

187. Foell, D. *et al.* Phagocyte-specific S100 proteins are released from affected mucosa and promote immune responses during inflammatory bowel disease. *The Journal of Pathology* **216**, 183–192 (2008).

188. Schmid, K. W. *et al.* Immunohistochemical demonstration of the calcium-binding proteins MRP8 and MRP14 and their heterodimer (27E10 antigen) in Crohn's disease. *Hum. Pathol.* **26**, 334–337 (1995).

189. Ziegler, G. *et al.* Mrp-8 and -14 mediate CNS injury in focal cerebral ischemia. *Biochim Biophys Acta* **1792**, 1198–1204 (2009).

190. Shepherd, C., Goyette, J., Utter, V. & al, E. Inflammatory S100A9 and S100A12 proteins in Alzheimer's disease. *Neurobiology of Aging* **27**, 1554-1563 (2006).

191. Floris, S. *et al.* Monocyte activation and disease activity in multiple sclerosis. A longitudinal analysis of serum MRP8/14 levels. *Journal of neuroimmunology* **148**, 172–177 (2004).

192. Fritz, G., Botelho, H. M., Morozova-Roche, L. A. & Gomes, C. M. Natural and amyloid self-assembly of S100 proteins: structural basis of functional diversity. *FEBS J* **277**, 4578–4590 (2010).

193. Sinha, P. *et al.* Proinflammatory S100 proteins regulate the accumulation of myeloid-derived suppressor cells. *J Immunol* **181**, 4666–4675 (2008).

194. Hermani, A. *et al.* Calcium-binding proteins S100A8 and S100A9 as novel diagnostic markers in human prostate cancer. *Clin. Cancer Res.* **11**, 5146–5152 (2005).

195. Cross, S. S., Hamdy, F. C., Deloulme, J. C. & Rehman, I. Expression of S100 proteins in normal human tissues and common cancers using tissue microarrays: S100A6, S100A8, S100A9 and S100A11 are all overexpressed in common cancers. *Histopathology* **46**, 256–269 (2005).

196. De Vooght, V. *et al.* Oropharyngeal aspiration: an alternative route for challenging in a mouse model of chemical-induced asthma. *Toxicology* **259**, 84–89 (2009).

197. Lakatos, H. F. *et al.* Oropharyngeal aspiration of a silica suspension produces a superior model of silicosis in the mouse when compared to intratracheal instillation. *Exp Lung Res* **32**, 181–199 (2006).

198. Boxio, R., Bossenmeyer-Pourié, C., Steinckwich, N., Dournon, C. & Nüße, O. Mouse bone marrow contains large numbers of functionally competent neutrophils. *J Leukoc Biol* **75**, 604-611 (2004).

199. Zigmond, S. H. & Hirsch, J. G. Leukocyte locomotion and chemotaxis. New methods for evaluation, and demonstration of a cell-derived chemotactic factor. *J Exp Med* **137**, 387–410 (1973).

200. Heit, B. & Kubes, P. Measuring chemotaxis and chemokinesis: the under-agarose cell migration assay. *Sci. STKE* **2003**, PL5 (2003).

201. Johnston, R. B., Jr *et al.* The role of superoxide anion generation in phagocytic bactericidal activity. Studies with normal and chronic granulomatous disease leukocytes. *J Clin Invest* **55**, 1357–1372 (1975).

202. Böyum, A. Separation of leukocytes from blood and bone marrow. Introduction. *Scandinavian journal of clinical and laboratory investigation* (1968).

203. Bhardwaj, R. S. *et al.* The calcium-binding proteins MRP8 and MRP14 form a membrane-associated heterodimer in a subset of monocytes/macrophages present in acute but absent in chronic inflammatory lesions. *Eur. J. Immunol.* **22**, 1891–1897 (1992).

204. Zeituni, A. E., McCaig, W., Scisci, E., Thanassi, D. G. & Cutler, C. W. The native 67-kilodalton minor fimbria of Porphyromonas gingivalis is a novel glycoprotein with DC-SIGN-targeting motifs. *J. Bacteriol.* **192**, 4103–4110 (2010).

205. Shevchenko, A., Wilm, M., Vorm, O. & Mann, M. Mass Spectrometric Sequencing of Proteins from Silver-Stained Polyacrylamide Gels. *Anal. Chem.* **68**, 850–858 (1996).

206. Tanner, S. *et al.* InsPecT: identification of posttranslationally modified peptides from

tandem mass spectra. *Anal. Chem.* **77**, 4626–4639 (2005).

207. Ehrchen, J. M., Sunderkotter, C., Foell, D., Vogl, T. & Roth, J. The endogenous Toll-like receptor 4 agonist S100A8/S100A9 (calprotectin) as innate amplifier of infection, autoimmunity, and cancer. *J Leukoc Biol* **86**, 557–566 (2009).

208. DiMartino, S. J., Trujillo, G., McVoy, L. A., Zhang, J. & Kew, R. R. Upregulation of vitamin D binding protein (Gc-globulin) binding sites during neutrophil activation from a latent reservoir in azurophil granules. *Mol Immunol* **44**, 2370–2377 (2007).

209. Zahn, S., Zwirner, J., Spengler, H.-P. & Götze, O. Chemoattractant receptors for interleukin-8 and C5a: expression on peripheral blood leukocytes and differential regulation on HL-60 and AML-193 cells by vitamin D3 and all-trans rètinoic acid. *Eur. J. Immunol.* **27**, 935–940 (1997).

210. Lominadze, G. *et al.* Myeloid-related protein-14 is a p38 MAPK substrate in human neutrophils. *J Immunol* **174**, 7257–7267 (2005).

211. Lysakova-Devine, T. *et al.* Viral Inhibitory Peptide of TLR4, a Peptide Derived from Vaccinia Protein A46, Specifically Inhibits TLR4 by Directly Targeting MyD88 Adaptor-Like and TRIF-Related Adaptor Molecule. *J Immunol* **185**, 4261–4271 (2010).

212. Devery, J. M., King, N. J. & Geczy, C. L. Acute inflammatory activity of the S100 protein CP-10. Activation of neutrophils in vivo and in vitro. *J Immunol* **152**, 1888–1897 (1994).

213. Lau, W., Devery, J. M. & Geczy, C. L. A chemotactic S100 peptide enhances scavenger receptor and Mac-1 expression and cholesteryl ester accumulation in murine peritoneal macrophages in vivo. *J Clin Invest* **95**, 1957–1965 (1995).

214. Cornish, C. J. *et al.* S100 protein CP-10 stimulates myeloid cell chemotaxis without activation. *J. Cell. Physiol.* **166**, 427–437 (1996).

215. Vandal, K. *et al.* Blockade of S100A8 and S100A9 suppresses neutrophil migration in response to lipopolysaccharide. *J Immunol* **171**, 2602–2609 (2003).

216. Harrison, C. A. *et al.* Oxidation regulates the inflammatory properties of the murine S100 protein S100A8. *J Biol Chem* **274**, 8561–8569 (1999).

217. Föger, N., Marhaba, R. & Zöller, M. Involvement of CD44 in cytoskeleton rearrangement and raft reorganization in T cells. *Journal of Cell Science* **114**, 1169–1178 (2001).

218. Brown, K. L. *et al.* Regulation of hyaluronan binding by F-actin and colocalization of CD44 and phosphorylated ezrin/radixin/moesin (ERM) proteins in myeloid cells. *Exp Cell Res* **303**, 400–414 (2005).

219. Raby, A. C. *et al.* TLR activation enhances C5a-induced pro-inflammatory responses by negatively modulating the second C5a receptor, C5L2. *Eur. J. Immunol.* **41**, 2741–2752 (2011).

220. Mulligan, M. S. *et al.* C5a-dependent up-regulation in vivo of lung vascular P-selectin. *J Immunol* **158**, 1857–1861 (1997).

221. Czermak, B. J. *et al.* In vitro and in vivo dependency of chemokine generation on C5a and TNF-alpha. *J Immunol* **162**, 2321–2325 (1999).

222. Mulligan, M. S. *et al.* Requirement and role of C5a in acute lung inflammatory injury in rats. *J Clin Invest* **98**, 503–512 (1996).

223. Guo, R.-F. & Ward, P. A. Role of C5a in inflammatory responses. *Annu. Rev. Immunol.* **23**, 821–852 (2005).

224. Manthey, H. D., Woodruff, T. M., Taylor, S. M. & Monk, P. N. Complement component 5a (C5a). *Int J Biochem Cell Biol* **41**, 2114–2117 (2009).

225. Foreman, K. E. *et al.* C5a-induced expression of P-selectin in endothelial cells. *J Clin Invest* **94**, 1147–1155 (1994).

226. Albrecht, E. A. *et al.* C5a-induced gene expression in human umbilical vein endothelial cells. *Am J Pathol* **164**, 849–859 (2004).

227. Chervenick, P. A., Boggs, D. R., Marsh, J. C., Cartwright, G. E. & Wintrobe, M. M. Quantitative studies of blood and bone marrow neutrophils in normal mice. *Am J Physiol* **215**, 353–360 (1968).

228. Powelka, A. M. *et al.* Stimulation-Dependent Recycling of Integrin β1 Regulated by ARF6 and Rab11. *Traffic* **5**, 20–36 (2004).

229. Rochon, Kavanagh & Harlan Analysis of integrin (CD11b/CD18) movement during neutrophil adhesion and migration on endothelial cells. *J Microsc* **197**, 15–24 (2000).

230. Yan, M. *et al.* Study on intracellular trafficking of Mac-1 by direct visualization. *Sci. China, C, Life Sci.* **47**, 521–529 (2004).

231. Pierini, L. M., Lawson, M. A., Eddy, R. J., Hendey, B. & Maxfield, F. R. Oriented endocytic recycling of alpha5beta1 in motile neutrophils. *Blood* **95**, 2471–2480 (2000).

232. Naik, N., Giannini, E., Brouchon, L. & Boulay, F. Internalization and recycling of the C5a anaphylatoxin receptor: evidence that the agonist-mediated internalization is modulated by phosphorylation of the C-terminal domain. *Journal of Cell Science* **110 (Pt 19)**, 2381–2390 (1997).

233. Hsu, M. H., Chiang, S. C., Ye, R. D. & Prossnitz, E. R. Phosphorylation of the N-formyl peptide receptor is required for receptor internalization but not chemotaxis. *J Biol Chem* **272**, 29426 (1997).

234. Fan, G. H., Lapierre, L. A., Goldenring, J. R., Sai, J. & Richmond, A. Rab11-family interacting protein 2 and myosin Vb are required for CXCR2 recycling and receptor-mediated chemotaxis. *Mol Biol Cell* **15**, 2456–2469 (2004).

235. Boulay, F. & Rabiet, M. J. The chemoattractant receptors FPR and C5aR: same functions different fates. *Traffic* **6**, 83–86 (2005).

236. Matteoni, R. & Kreis, T. E. Translocation and clustering of endosomes and lysosomes depends on microtubules. *J Cell Biol* **105**, 1253–1265 (1987).

237. Goltz, J. S., Wolkoff, A. W., Novikoff, P. M., Stockert, R. J. & Satir, P. A role for microtubules in sorting endocytic vesicles in rat hepatocytes. *Proc Natl Acad Sci USA* **89**, 7026–7030 (1992).

238. Oda, H. *et al.* Interaction of the microtubule cytoskeleton with endocytic vesicles and cytoplasmic dynein in cultured rat hepatocytes. *J Biol Chem* **270**, 15242–15249 (1995).

239. Rothwell, S. W., Nath, J. & Wright, D. G. Interactions of cytoplasmic granules with microtubules in human neutrophils. *J Cell Biol* **108**, 2313–2326 (1989).

240. Lundgren-Akerlund, E., Olofsson, A. M., Berger, E. & Arfors, K. E. CD11b/CD18-dependent polymorphonuclear leucocyte interaction with matrix proteins in adhesion and migration. *Scand. J. Immunol.* **37**, 569–574 (1993).

241. Sheppard, F. R. *et al.* Structural organization of the neutrophil NADPH oxidase: phosphorylation and translocation during priming and activation. *J Leukoc Biol* **78**, 1025–1042 (2005).

242. Allen, L. A. & Aderem, A. Molecular definition of distinct cytoskeletal structures involved in complement- and Fc receptor-mediated phagocytosis in macrophages. *J Exp Med* **184**, 627–637 (1996).

243. Newman, S., Mikus, L. & Tucci M.A. Differential requirements for cellular cytoskeleton in human macrophage complement receptor- and Fc receptor-mediated phagocytosis. *The Journal of Immunology* **146**, 967-974 (1991).

244. Martin, S., Bradley, J. & Cotter, T. HL-60 cells induced to differentiate towards neutrophils subsequently die via apoptosis. *Clin Exp Immunol* **79**, 448-453 (1990).

245. Naumovski, L. & Cleary, M. L. Bcl2 inhibits apoptosis associated with terminal differentiation of HL-60 myeloid leukemia cells. *Blood* **83**, 2261–2267 (1994).

246. Otake, Y. Retinoid-Induced Apoptosis in HL-60 Cells Is Associated with Nucleolin Down-Regulation and Destabilization of Bcl-2 mRNA. *Mol Pharmacol* **67**, 319–326 (2005).

247. Nagai, Y. *et al.* Toll-like Receptors on Hematopoietic Progenitor Cells Stimulate Innate Immune System Replenishment. *Immunity* **24**, 801–812 (2006).

248. Mita, Y., Dobashi, K., Nakazawa, T. & Mori, M. Induction of Toll-like receptor 4 in granulocytic and monocytic cells differentiated from HL-60 cells. *British journal of haematology* **112**, 1041–1047 (2001).

249. Feng, Y., Zou, L., Si, R., Nagasaka, Y. & Chao, W. Bone marrow MyD88 signaling modulates neutrophil function and ischemic myocardial injury. *Am. J. Physiol., Cell Physiol.* **299**, C760–9 (2010).